uOttawa

L'Université canadienne
Canada's university

FACULTÉ DES ÉTUDES SUPÉRIEURES ET POSTOCTORALES

uOttawa

L'Université canadienne
Canada's university

FACULTY OF GRADUATE AND POSDOCTORAL STUDIES

James Thackeray
AUTEUR DE LA THÈSE / AUTHOR OF THESIS

M.Sc. (Cellular and Molecular Medicine)
GRADE / DEGREE

Department of Cellular and Molecular Medicine
FACULTÉ, ÉCOLE, DÉPARTEMENT / FACULTY, SCHOOL, DEPARTMENT

Examination of Altered Sympathetic Nervous Function in Obesity and Diabetes Mellitus Using (C-11) Meta-Hydroxyephedrine

TITRE DE LA THÈSE / TITLE OF THESIS

Dr. J. DaSilva
DIRECTEUR (DIRECTRICE) DE LA THÈSE / THESIS SUPERVISOR

CO-DIRECTEUR (CO-DIRECTRICE) DE LA THÈSE / THESIS CO-SUPERVISOR

EXAMINATEURS (EXAMINATRICES) DE LA THÈSE / THESIS EXAMINERS

Dr. R. Milne

Dr. J. Van Huysse

Gary W. Slater
Le Doyen de la Faculté des études supérieures et postdoctorales / Dean of the Faculty of Graduate and Postdoctoral Studies

EXAMINATION OF ALTERED SYMPATHETIC NERVOUS FUNCTION IN OBESITY AND DIABETES MELLITUS USING [^{11}C]*META*-HYDROXYEPHEDRINE

BY

JAMES THACKERAY

This thesis is submitted as a partial fulfillment of the Master of Science program in Cellular and Molecular Medicine

Final Draft Submitted 26 September 2006
Ottawa, Ontario, Canada

Your file Votre référence
ISBN: 978-0-494-25836-1
Our file Notre référence
ISBN: 978-0-494-25836-1

EXAMINATION OF ALTERED SYMPATHETIC NERVOUS FUNCTION IN OBESITY AND DIABETES MELLITUS USING [^{11}C]*META*-HYDROXYEPHEDRINE

MSc Thesis 2006, James Thackeray,

Department of Cellular and Molecular Medicine, University of Ottawa

Ottawa, Ontario, Canada

Abnormal sympathetic nervous system (SNS) signaling is a synergistic complication of obesity, diabetes mellitus, and congestive heart failure. *In vivo* biodistribution studies in rats using [^{11}C]*meta*-hydroxyephedrine ([^{11}C]HED) were performed in obese, lean, type I and type II diabetic animals to delineate deviations in sympathetic nervous integrity at the uptake-1 site (NET-1) as compared to healthy controls. Specific, blockable tracer accumulation was observed in myocardium, lung, brown adipose tissue and pancreas. Obese animals exhibit a time-dependent elevation in uptake-1 specific myocardial [^{11}C]HED retention and time-independent depressed tracer accumulation in brown adipose tissue as compared to lean animals. Type II diabetic rats show a time- and hyperglycaemia-dependent reduction of myocardial tracer uptake and a time- and glycaemia-independent increase in brown adipose tissue uptake-1 specific [^{11}C]HED retention. Positron emission tomography using [^{11}C]HED may prove useful in examining alterations in SNS signaling before, during, and subsequent to therapy for obesity and/or DM.

TABLE OF CONTENTS

LIST OF TABLES

LIST OF FIGURES

LIST OF ABBREVIATIONS

%ID/g	percent of injected dose per gram tissue
%ID/g*BW	percent of injected dose per gram tissue normalized for body weight
^{11}C	carbon-11
[^{11}C]HED	[^{11}C]*meta*-hydroxyephedrine
^{13}N	nitrogen-13
^{18}F	fluorine-18
[^{18}F]FDG	[^{18}F]fluorodeoxyglucose
[^{18}F]FMR	6-[^{18}F]fluorometaraminol
Akt	Akt signaling factor (protein kinase B)
Al_2O_3	aluminum oxide
ANS	autonomic nervous system
AR	adrenoceptors
ARC	arcuate nucleus
ATF2	activating transcription factor-2
ATP	adenosine triphosphate
B_{max}	maximal binding density
BMI	body mass index (mass/height^2)
cAMP	3', 5' cyclic adenosine monophosphate
cGMP	3', 5' cyclic guanosine monophosphate
CHF	congestive heart failure
COMT	catechol-*O*-methyltransferase
CT	computed tomography
CVD	cardiovascular disease
DAN	diabetic autonomic neuropathy
DAT	dopamine reuptake transporter
DIO	diet-induced obese rat
DM	diabetes mellitus
DR	diet-resistant (lean) rat
ECD	electrochemical detection
EDTA	ethylenediaminetetraacetic acid

Epi	epinephrine
ERK	extracellular related signal kinase
GABA	gamma aminobutyric acid
GLUT-2	glucose transporter 2
GLUT-4	glucose transporter 4
G protein	guanosine nucleotide binding protein
HCl	hydrochloride, hydrochloric acid
HLB	hydrophilic lipophilic balanced reversed phase sorbent
HPLC	high performance liquid chromatography
HSL	hormone sensitive lipase
K_d	dissociation constant
MAO	monoamine oxidase
MAPK	mitogen activated protein kinase
MAX	mixed-mode anion exchange reversed phase sorbent
MCX	mixed-mode cation exchange reversed phase sorbent
MCR3/4	melanocortin receptors 3 and 4
MIBG	*meta*-iodobenzylguanidine
NE	norepinephrine
NEFA	non-esterified (free) fatty acid
NET-1	norepinephrine reuptake transporter-1, or uptake-1
NO	nitric oxide
NRI	(selective) norepinephrine reuptake inhibitor
NYHA	New York Heart Association (classifications of heart failure)
PET	positron emission tomography
PI-3K	phosphoinositol 3-kinase
PKA	protein kinase A
PKC	protein kinase C
POMC	pro-opiomelanocortin
pSNS	parasympathetic nervous system
SCX	cation exchange analytical column
SNS	sympathetic nervous system

SPECT	single photon emission computed tomography
STZ	streptozocin (streptozotocin)
t-SNARE	t-soluble N-ethylmaleimide-sensitive factor attachment protein receptor
UCP	mitochondrial uncoupling protein
VMAT	vesicular monoamine transporter
V_{max}	maximal velocity
VMH	ventromedial hypothalamus

ACKNOWLEDGMENTS

The results presented in this thesis are the culmination of two years of collaborative work by the PET Biotesting and Radiochemistry divisions of the National Cardiac PET Centre University of Ottawa Heart Institute. The experiments described herein often require the combined effort of several individuals to come to fruition.

Firstly, I would like to acknowledge my supervisor, Dr. Jean DaSilva. His guidance, expertise, and dedication over the last two years are surpassed only by the spirit of fellowship and geniality he fosters in his laboratory. It truly has been and will continue to be an honour and pleasure to work beside him in graduate studies.

Secondly, I would like to express my appreciation to my colleagues in PET Biotesting and Radiochemistry: Miran, Steph, Sam, Paul, Jeff, Michael, Maryam, and Fred, each of whose work and friendship in the last years is well heeded and appreciated. Steph, your organization, camaraderie, and resilient patience have made the last years highly enjoyable. And also Miran, your fraternity, perspective, and unending, unwarranted Croatian wisdom have been invaluable in my success with this and other projects.

Finally, to my family, your interest and support have been sources of inspiration and perseverance. Without you as my foundation, the accomplishments presented herein would be meaningless.

Thank you all for your invaluable contributions to this work. Let's do it all again in four years!

1.0 INTRODUCTION

1.1 Sympathetic Nervous System

An increasing body of evidence indicates that obesity, type II diabetes mellitus (DM), and congestive heart failure (CHF) are similarly associated with impaired signaling of the sympathetic nervous system (SNS) (Brodde, 1993; Brodde and Michel, 1999; Collins and Surwit, 2001; Dulloo, 2002; Hoffman and Lefkowitz, 1995; Link et al., 2003; Yoshitomi et al., 1998). This avenue of research has yet to be fully explored, and represents a potential synergy among several major and growing international health concerns.

1.1.1 General

The autonomic nervous system (ANS) is a primary neural control mechanism for stimulation or inhibition of cardiac and metabolic function (Freeman, 2006; Hoffman and Lefkowitz, 1995). The ANS is comprised of two branches: the sympathetic branch (SNS) and the parasympathetic branch (pSNS). Central sympathetic neurons project from diverse brain areas including the prefrontal cortex locus coeruleus (Talman and Kelkar, 1993), amygdala (al Maskati and Zbrozyna, 1989), and hypothalamus (Swanson et al., 1987) to target organs and organ systems including the heart, vasculature, respiratory system, pancreas, liver, gastrointestinal tract, kidney, and adrenal glands (Figure 1.1) (Freeman, 2006; Niijima, 1986; Noble and Liddle, 2005; Romijn and Fliers, 2005; Schafers et al., 2001; Trampal et al., 2004). In heart, the SNS stimulates contractility, heart rate, and cardiac output, opposed by the pSNS (Freeman, 2006). Upon stimulation, endogenous catecholamines such as norepinephrine (NE) are released from the presynaptic varicosity

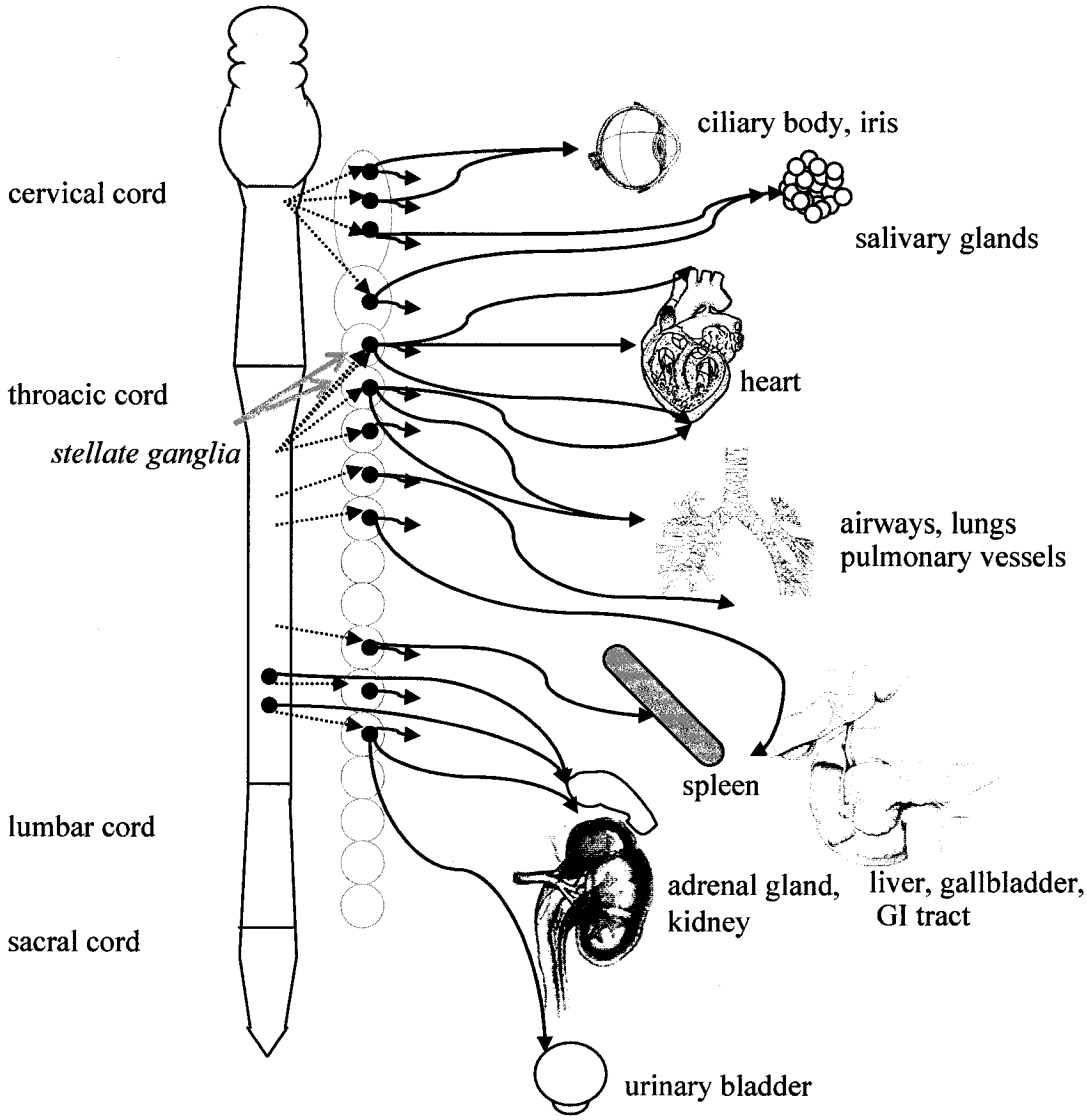

Figure 1.1: Schematic representation of sympathetic nervous innervation of peripheral organs. Synaptic transmission occurs in ganglia from central inputs to peripheral nerves. The stellate ganglia are associated with cardiac and pulmonary sympathetic innervation. Adapted from Hoffman and Lefkowitz (1995).

(bouton) into the synapse where they bind to and stimulate adrenergic receptors (ARs) (Figure 1.2) (Hoffman and Lefkowitz, 1995).

1.1.2 Adrenergic Signaling

ARs are a class of guanine nucleotide binding protein (G protein) coupled receptors. Stimulation of ARs results in the dissociation of the G protein subunits (α, β, γ) from the receptor, and subsequent activation of various signaling cascades and second messenger pathways (Blaak et al., 1993; Brodde et al., 2001; Hagstrom-Toft et al., 1993; Lafontan and Berlan, 1993). The subtype of AR dictates the preferred neurotransmitter and the target. βARs have greatest affinity for NE, and are predominantly located at the membrane surface of target organs. Conversely, αARs are preferentially stimulated by epinephrine (Epi), and are mostly found on vascular endothelial cells (Blaak et al., 1993; Hoffman and Lefkowitz, 1995).

Signaling is terminated by metabolism of the neurotransmitters by monoamine oxidase (MAO) and catechol-*O*-methyltransferase (COMT) or by active reuptake from the synapse via specialized transporters at the bouton membrane (Kopin and Gordon, 1963; Lowe et al., 1975; Raffel et al., 1996). In the case of NE, this reuptake process occurs via the NE reuptake transporter-1 (NET-1), designated the uptake-1 pathway, and represents 50-90% of NE clearance from the synaptic cleft (Figure 1.2) (Eisenhofer et al., 1995). Uptake-2 is an alternative pathway in which NE is actively taken up by the postsynaptic cell, but this process represents only a minor proportion of total synaptic clearance (Tseng et al., 2001). Termination of signaling is also aided by α_2ARs located presynaptically which activate a negative feedback loop to reduce neurotransmitter release (Freeman, 2006; Hoffman and Lefkowitz, 1995; Langer, 1980).

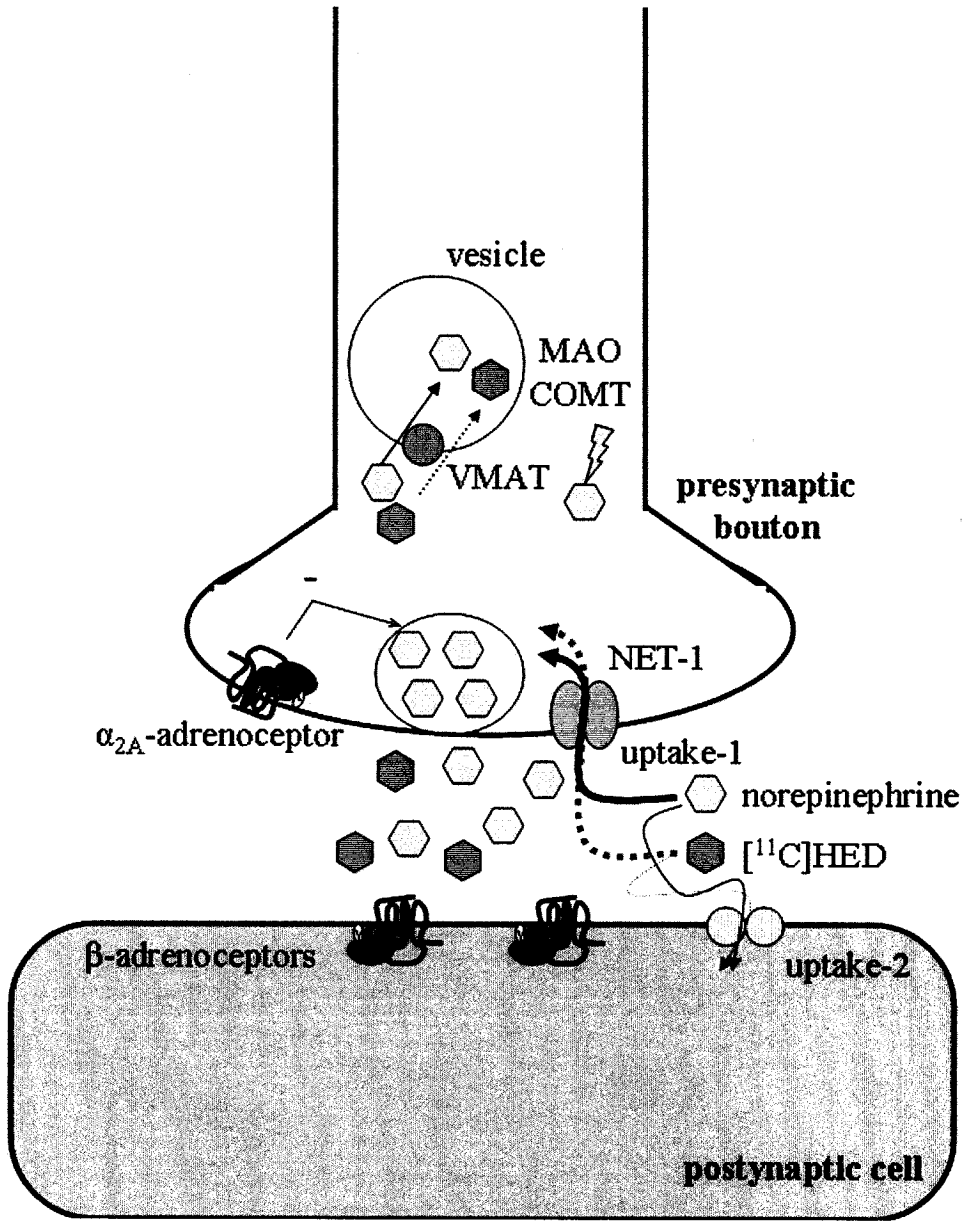

Figure 1.2: Schematic representation of the uptake-1 pathway. NE and [^{11}C]HED are selectively recovered from the synapse by the uptake-1 pathway via NET-1 at the presynaptic bouton. From the bouton, a portion of both NE and [^{11}C]HED is subject either to vesicular packaging via vesicular monoamine transporter (VMAT), re-release into the synapse, or passive diffusion into the synaptic cleft. Some NE is also metabolized by monoamine oxidase (MAO) or catechol-*O*-methyltransferase (COMT). [^{11}C]HED is resistant to both of these enzymes. A minor portion of synaptic NE and [^{11}C]HED is subject to postsynaptic uptake-2 pathway. Adrenoceptors on the postsynpatic cell and presynaptic bouton elicit a variety of effects when stimulated by NE.

1.1.3 Norepinephrine Reuptake Transporter

NET-1 is a 69 kDa Na^+/Cl^- dependent transporter protein, included in a family that comprises the dopamine transporter (DAT), serotonin transporter (SERT), as well as neuronal reuptake transporters for gamma aminobutyric acid (GABA) and glycine (Amara and Pacholczyk, 1991; Blakely et al., 1994; Mandela and Ordway, 2006; Pacholczyk et al., 1991). Each of these transporters consists of twelve transmembrane-spanning domains with intracellular N- and C-termini that include numerous serine, threonine, and tyrosine residues, candidates for phosphorylation (Figure 1.3) (Blakely et al., 1998; Bonisch et al., 1998; Sakai et al., 1997; Torres et al., 2003; Vaughan, 2004). Sequences are highly conserved in the transmembrane domains, suggesting a commonality of transport mechanism (Mandela and Ordway, 2006; Paczkowski and Bryan-Lluka, 2004).

Reuptake of NE is a coordinated electrogenic process wherein the neurotransmitter is cotransported with Na^+ and Cl^- into the neuronal cytoplasm (Mandela and Ordway, 2006; Trendelenburg, 1991). This active transport is enabled by the activity of the Na^+/K^+-ATPase pump, which maintains a Na^+ gradient between the synapse and bouton (Bonisch and Bruss, 1994; Harder and Bonisch, 1985).

Functional lack of NET-1 and subsequent dysregulation of synaptic NE has been linked to several pathologies. Loss of uptake-1 results in a marked decrease in presynaptic and marked increase in synaptic NE levels, reducing regulatory outflow to the periphery because of both depleted NE stores and overstimulation of postsynaptic receptors, thus underscoring the importance of reuptake for the maintenance of normal NE conductance (Xu et al., 2000). NET-1 deficient mice exhibit tachycardia and hypertension, in parallel with twofold elevations in plasma NE concentration, reflecting a loss of sympathetic regulation (Keller et al., 2004). Additionally, chronic blockade of uptake-1 has been shown

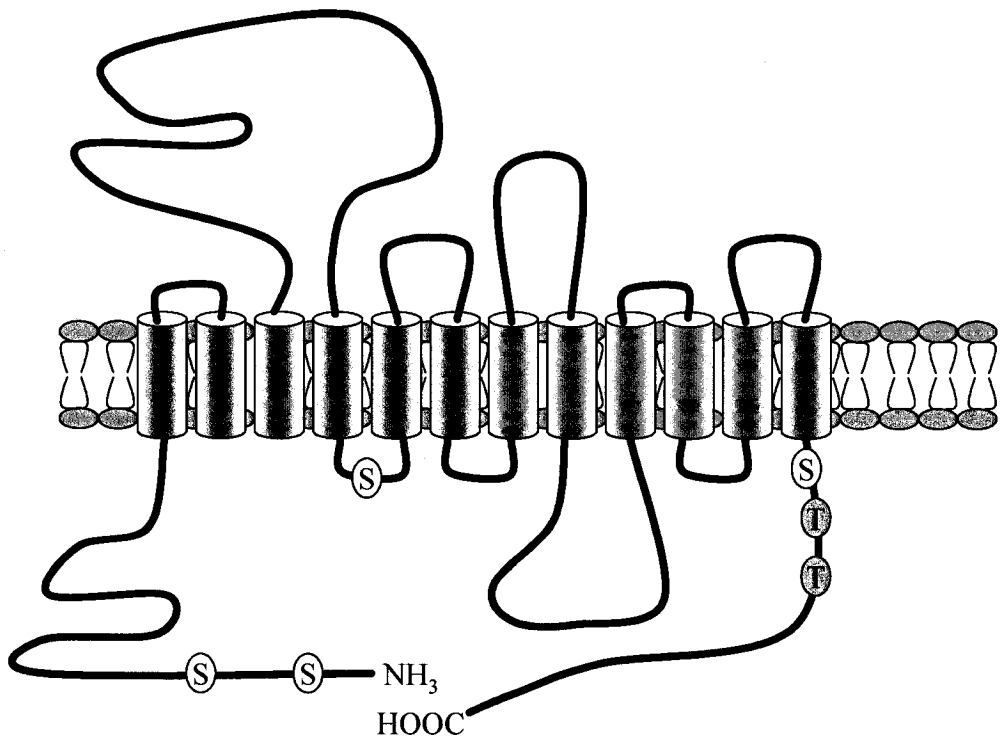

Figure 1.3: Structure of the norepinephrine reuptake transporter. A twelve-transmembrane protein situated at the presynaptic varicosity of sympathetic neurons. Regulation is thought to be partially controlled by phosphorylation of intracellular threonine and serine residues. These amino acids are indicated. Adapted from Vaughan (2004).

to induce orthostatic intolerance, affecting the ability of the baroceptor reflex to compensate for acute changes in blood pressure (Carson et al., 2002). As well as precipitating disease, NET-1 density has also been shown to respond to adverse conditions. For example, altered NET-1 protein expression via post-transcriptional mechanisms has been reported in experimental heart failure (Backs et al., 2001).

There is a high turnover of DAT and GABA transporters at the neuronal surface, reaching rates of 3-5% per minute between the bouton cytoplasm and membrane, an event that is anticipated for NET-1 (Deken et al., 2003; Loder and Melikian, 2003; Mandela and Ordway, 2006). As such, control of NET-1 expression has been widely examined, with several mechanisms, pathways, and physiologic compounds implicated in its regulation.

1.1.4 Regulation of Adrenoceptors and Uptake-1

Overstimulation of ARs, potentially due to elevated release of neurotransmitters, is associated with short term desensitization and internalization of receptors, dampening the basal SNS signal (Brouri et al., 2004; Langer, 1980; Muller et al., 1995; Novak, 1998; Pao and Benovic, 2002; Schafers et al., 1998). Over a longer term, specifically three to five days, transcriptional and/or translational downregulation of ARs is observed, an event that is paralleled by downregulation of NET-1 (Benmansour et al., 2004; Mardon et al., 2003; Muller et al., 1995; Schafers et al., 1998). Binding assay experiments have demonstrated that chronic NE infusion at 1.2 μg/h over five days results in 30-35% reductions in βAR and NET-1 density, as measured with [^{3}H]NE and [^{123}I]*meta*-iodobenzylguanidine (MIBG), respectively (Mardon et al., 2003). In comparison, rats chronically infused with subcutaneous NE also exhibit downregulation of βARs (Seo et al., 1999). NET-1 density was not assessed in the latter study.

Downregulation of NET-1 has also been linked to elevated levels of second messengers such as cyclic adenosine monophosphate (cAMP) and cyclic guanosine monophosphate (cGMP) (Bryan-Lluka et al., 2001; Mandela and Ordway, 2006). Bryan-Lluka and colleagues (2001) demonstrated that administration of the adenylate cyclase activator forskolin elicited a marked decrease in the rate of [^{3}H]NE uptake (V_{max}) and a modest decrease in specific binding of the tritiated NET-1 inhibitor nisoxetine (B_{max}) in rat PC12 cells. Within several hours of exposure, slowed V_{max} is accompanied by reduced NET-1 mRNA and protein expression (Mandela and Ordway, 2006). Other molecules associated with uptake-1 regulation include protein kinase C (PKC) (Apparsundaram et al., 1998; Bonisch et al., 1998), nitric oxide (NO) and related compounds (Kaye et al., 1997), and extracellular calcium (Uchida et al., 1998).

Chronic administration of antidepressants, particularly selective NE reuptake inhibitors (NRI), generally evoke an upregulation of ARs (Hanft and Gross, 1990; Liang et al., 2002; Seo et al., 1999) and reduced expression of uptake-1 protein (Hebert et al., 2001; Liang et al., 2002; Mao et al., 2005). Benmansour and colleagues (2004) reported a marked reduction in [^{3}H]nisoxetine binding in diverse brain regions following 3- and 6-week treatment with the NRI desipramine. The differential pre- and postsynaptic effects relate to the specific inhibition at NET-1 coupled with elevated stimulation at ARs, evoking divergent responses.

Genetic analyses have identified specific regions of the transporter that are required for endocytic regulation of NET-1, including several sequence stretches at the C-terminus (Holton et al., 2005). Deletion of these residues results in an inability to internalize the transporter, altering normal cellular trafficking at the bouton membrane. Phosphorylation is a key mechanism in the regulation of DAT (Huff et al., 1997; Vaughan et al., 1997), and

may play a comparable role in NET-1. There are at least five potential serine or threonine phosphorylation sites within the intracellular component of the NET-1 (Blakely et al., 1994). Extended exposure to the PKC agonist phorbol 12-myristate-13-acetate results in decreased [^{3}H]NE uptake via NET-1 in COS-7 cells transfected with the human variant of NET-1 (Bonisch et al., 1998). This phosphorylation is followed by endocytosis of the transporter, reducing surface expression of NET-1 and subsequently NE transport (Apparsundaram et al., 1998). Mere inhibition of protein phosphatase with okadaic acid was not sufficient to affect the altered NE uptake (Blakely et al., 1994).

NET-1 trafficking is also regulated by synaptic proteins. Microscopy and immunoprecipitation data suggest that neurotransmitter transporters are anchored at the neuronal membrane by large protein complexes including the t-soluble N-ethylmaleimide-sensitive factor attachment protein receptor (t-SNARE) protein syntaxin 1A (Beckman et al., 1998; Geerlings et al., 2000; Haase et al., 2001). In addition to anchoring the transporter at the membrane, syntaxin 1A may also be involved in controlling the intrinsic function of the transporter. Sung and colleagues (2003) transfected CAD cells with human NET-1, and suppressed expression of synaptic syntaxin 1A using antisense oligonucleotides. V_{max} of NET-1 was markedly reduced in syntaxin-suppressed cells (Sung et al., 2003).

The tight regulation of NET-1 indicates that maintenance of the uptake-1 pathway represents an important facet in normal NE signalling.

1.2 OBESITY

1.2.1 General

Obesity is rapidly becoming more prevalent and of greater concern in modernized countries worldwide. Improper diet and sedentary lifestyle have contributed to surging numbers of obese individuals in the last 30 years (Canning et al., 2004; Flegal et al., 2004). Moreover, obesity is an important risk factor in a wide range of other disorders including type II diabetes, heart disease, hypertension, stroke, and premature death (Deedwania and Fonseca, 2005; Kenchaiah et al., 2002; Kostis and Sanders, 2005; U.S. Department of Health and Human Services., 2001).

1.2.2 Obesity and the Sympathetic Nervous System

Recent scientific evidence has suggested a link between SNS signaling and the aetiology of obesity (Bachman et al., 2002; Dulloo, 2002; Ricci and Levin, 2003; Sharma et al., 2001). Dysregulation of basal NE levels resulting in impaired βAR signaling has been postulated to develop partly due to overfeeding. That is, excess energy intake produces elevated SNS activity, leading to alterations in receptor signaling pathways (Landsberg, 1986).

The relationship between the SNS and obesity involves two key metabolic pathways that are regulated by the three major βAR subtypes (β_1AR, β_2AR, β_3AR): (i) lipolysis in white adipose tissue, predominantly mediated by β_1AR, and (ii) non-shivering thermogenesis in brown adipose tissue and skeletal muscle, primarily controlled by β_3AR (Blaak et al., 1993; Collins and Surwit, 2001; Lafontan and Berlan, 1993; Robidoux et al., 2004). In white adipocytes, NE binding by β_1AR stimulates both the protein kinase A (PKA) and extracellular signal-related kinase (ERK) 1 and 2 cascades, resulting in the phosphorylation and subsequent activation of hormone-sensitive lipase (HSL) (Robidoux et al., 2004) (Figure 1.4A). Comparatively, as shown in Figure 1.4B, NE binding by β_3AR in brown

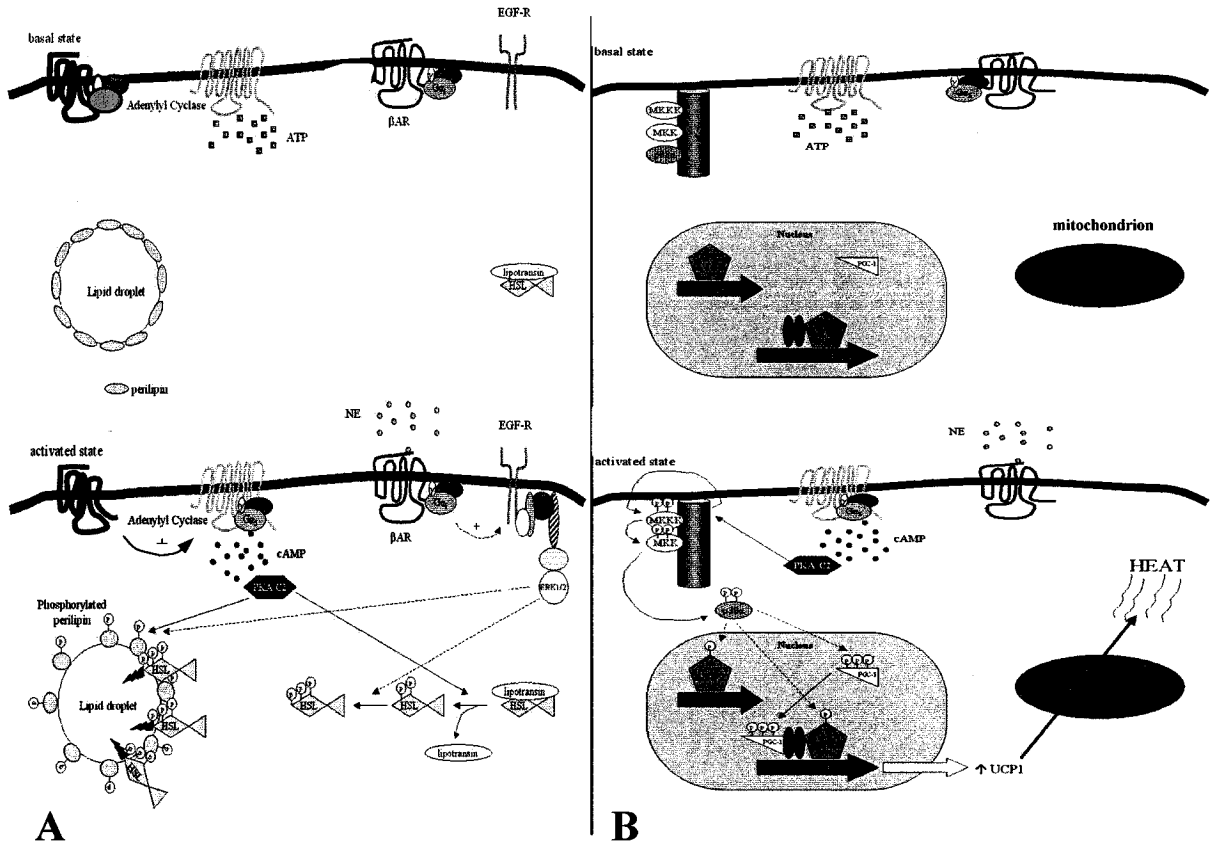

Figure 1.4: Signal transduction of adrenoceptor-induced lipolysis in white adipocytes (**A**). In basal state, perilipin A is bound to the lipid droplet and HSL is coupled to a protective protein, potentially lipotransin. Upon stimulation by NE, G proteins dissociate from the βAR. G_S stimulates adenylyl cyclase to activate PKA-C2, which phosphorylates hormone sensitive lipase (HSL) and perilipin A. G_i activates ERK1/2 cascade, culminating in the phosphorylation of HSL and further phosphorylation of periplipin A, which exposes the lipid droplet to HSL attack. HSL breaks the lipid droplet to triglyceride and NEFA.

Signal transduction of adrenoceptor-induced thermogenesis in brown adipocytes (**B**). In basal state, p38α is anchored with MAP kinases to a scaffold protein on the cellular membrane. Upon stimulation, G_s dissociates from βAR, activating PKA-C2. Through MAPK pathway, p38α is phosphorylated and transmigrates to the nucleus, where it activates the transcription factor ATF2 directly and indirectly through PGC-1. UCP1 expression in mitochondria is upregulated. Adapted from Robidoux *et al.* (2004).

adipocytes leads to sequential stimulation of adenylyl cyclase, PKA, p38 mitogen-activated protein kinase (MAPK), culminating in the nuclear stimulation of activating transcription factor 2 (ATF2), which upregulates expression of uncoupling proteins (UCPs) in mitochondria (Blaak et al., 1993; Harper and Brand, 1993; Robidoux et al., 2004).

A number of studies have addressed how blockade of the SNS signal affects weight gain. Bachman and colleagues (2002) have developed knockout mice that do not express the three known βARs. Even on a standard diet, these β-less mice spontaneously become obese. Similarly, clinical trials in humans using chronic βAR-blockers, inhibiting normal SNS signaling, demonstrate an increased propensity to obesity during therapy (Sharma et al., 2001). The converse is also true, as changes in weight gain profile can also alter the expression of βARs, partially owing to the elevation of various SNS-active blood markers including glucose, insulin, leptin, and NEFAs (Benthem et al., 2000; Feve et al., 1994; Kern et al., 2005; Leibowitz and Wortley, 2004; Liatis et al., 2004; Molon-Noblot et al., 2001; Ren, 2004; Rizk and Dunbar, 2004). A subset of Sprague-Dawley rats, designated diet-induced obese (DIO) due to their tendency to rapidly develop obesity when fed a high fat diet, display an increase in endogenous plasma NE levels as compared to standard chow-fed controls (Levin and Dunn-Meynell, 2000; Levin and Dunn-Meynell, 2002). These differences in baseline NE levels have been postulated to facilitate indentification of rats at risk of developing obesity (Ricci and Levin, 2003).

Levin and colleagues (1983) had previously described the development of diet-induced obesity in Sprague-Dawley rats after three months on high fat diet (Levin et al., 1983). Within the first week of high fat diet consumption, affected rats exhibited 30% elevations in tyrosine hydroxylase and NE, and a substantial 90% increase in NE turnover in intrascapular brown adipose tissue. By the conclusion of the experiment at 3 months, NE

turnover had decreased in heart and other peripheral organs including brown adipose tissue (Levin et al., 1983). As described above, chronically elevated NE evokes downregulation of NET-1 and ARs (Mardon et al., 2003; Seo et al., 1999), adversely affecting normal noradrenergic signal cascades.

1.2.3 Non-Shivering Thermogenesis

The ability of mammals to adjust energy expenditure in response to dietary and temperature fluctuations is termed "adaptive" or "non-shivering" thermogenesis. This process is mediated by a specialized set of mitochondrial proteins, UCPs, that allow the leakage of protons across the inner mitochondrial membrane, dissipating the electrical gradient necessary for ATP generation (Argyropoulos and Harper, 2002; Cannon and Nedergaard, 2004; Harper and Brand, 1993; Harper and Himms-Hagen, 2001). Rather than being used in the generation of ATP, the energy stored in the mitochondrial proton electrochemical gradient is released as heat (Lowell and Bachman, 2003). The activation of βARs on brown adipocytes elicits a two pronged effect: (i) increased rate of UCP1 proton leak, thought to be mediated by lipolysis- and leptin-induced increases in circulating non-esterified fatty acid (NEFA) concentrations, and (ii) upregulation of UCP expression via ATF2 (Hany et al., 2002; Himms-Hagen, 1990; Matthias et al., 2000).

The identification of the relatively thermogenic-tissue-specific atypical or β_3ARs in the early 1990s (Feve et al., 1991) has spurred research into using this receptor as a means of treating obesity. Specific agonists of β_3ARs have been developed and applied in obese animal studies for weight management (Arch and Wilson, 1996). Yoshitomi and colleagues (1998) showed that a 21-day, low-dose regimen of the β_3AR agonist CL316,243 elicited a significant upregulation of UCP1 mRNA in brown adipose tissue of treated rats, though rat weights were not significantly changed on the low-dose treatment. When

administered to dogs over a 12-week period, however, CL316,243 was found to significantly reduce adiposity and body weight (Sasaki et al., 1998). Moreover, post-mortem examination revealed that the visceral and abdominal fat pads of CL316,243-treated dogs were not only smaller than in placebo-treated dogs, but also appeared light brown, suggesting that expansion of brown adipocytes had been promoted within white fat deposits (Sasaki et al., 1998). Measurement of presynaptic activity of the βAR system may be representative of thermogenic activity in obese and lean individuals. Various biological markers also respond to and regulate SNS activity in the periphery, particularly in thermogenic and lipolytic tissues.

1.2.4 Regulatory Factors

There are a number of regulatory factors that exhibit altered expression in obesity and may impact sympathetic outflow. Two of these, glucose and insulin, will be discussed later (Section 1.3.4). Other macromolecules that are differentially expressed in obesity and have been examined extensively in recent years include leptin and NEFAs.

1.2.4.1 Leptin

In addition to genetic predisposition to elevated NE, obese individuals exhibit changes in secretion and responsiveness to the metabolic regulatory hormone leptin. Since its discovery in the mid 1990s (Barinaga, 1995; Barinaga, 1996), leptin has become recognized as an important regulator of body weight, acting via specialized receptors located predominantly in the hypothalamus (Leibowitz and Wortley, 2004). Indeed, one of the most common animal models for studying obesity is the Zucker rat, which features a genetic deletion of the leptin receptor (Coudray et al., 1999; Tschop and Heiman, 2001). Leptin exerts its effects through three distinct pathways: (i) paracrine regulation of triglyceride storage and NEFA release, (ii) hunger and satiety control primarily at the

arcuate nucleus (ARC), and (iii) systemic SNS stimulation, particularly at the ventromedial hypothalamus (VMH) (Leibowitz and Wortley, 2004; Ren, 2004; van Dijk, 2001). The action of leptin at adipocytes leads to increased NEFA circulation, which augments sympathetic signalling in thermogenic tissues (Robidoux et al., 2004; Steinberg and Dyck, 2000). Centrally, at the ARC, binding of leptin inhibits the synthesis of neuropeptide Y and agouti-related protein, potent stimulants of food intake (Leibowitz and Wortley, 2004), signalling a decrease in appetite and the promotion of pSNS activity. Loss of sensitivity to this control mechanism may partially drive the overfeeding observed in obese subjects and the subsequent elevation in SNS activity (Barinaga, 1996; Landsberg, 1986).

Leptin has also been shown to activate thermogenic SNS activity directly and in a dose-dependent manner (Haynes et al., 1997). One of the effectors of this increase is the pro-opiomelanocortin (POMC) neurons within the VMH, which sequentially stimulate the ubiquitous melanocortin receptors 3 and 4 (MCR3/4) in other brain regions (van Dijk, 2001). Stimulation of MCR3/4 increases sympathetic signalling to thermogenic tissues and promotes the upregulation of UCPs (Cettour-Rose and Rohner-Jeanrenaud, 2002; Choi et al., 2003). Moreover, genetically engineered mice that do not express MCR3/4 develop obesity (Choi et al., 2003; O'Rahilly et al., 2004). Satoh and colleagues (1999) demonstrated that microinjection of leptin into the VMH elicited twofold elevations of plasma NE concentrations, three hours post-injection. A similar elevation was observed with intravenous leptin injection, an effect that was severely dampened in VMH-lesioned animals (Satoh et al., 1999).

As plasma levels of leptin are inherently regulated by the degree of adiposity, its secretion is a physiological marker of the obese state and may be used as a measurement for progress of obesity therapy (Ren, 2004). Additionally, excess secretion of leptin in obese

individuals may further augment plasma and synaptic NE levels in peripheral organs, potentially instigating and/or exacerbating the inherent SNS dysfunction in obesity.

1.2.4.2 Non-Esterified Fatty Acids

As discussed above, SNS activity regulates lipolysis. Elevations in NE release consequently result in increased liberation of NEFAs. In disease states characterized by elevated NE such as heart failure, elevations of NEFAs have also been reported (Cohn et al., 1984; Marangou et al., 1988). In addition to correlating with NE levels, NEFA release also appears to activate a positive feedback mechanism to augment NE spillover from central, adrenal medullary, and local sources. Benthem and colleagues (2000) demonstrated that intraportal infusion of NEFAs over a 180 minute period elicited a marked elevation in plasmatic concentration of both NE and Epi. This elevation was accompanied by an early spike in glucose and insulin levels, suggesting that the elevated catecholamines may be an indirect effect of NEFA concentration, though cause and effect are difficult to delineate accurately. Regardless, plasma NEFA levels, regulated by both lipolytic activity and leptin secretion, represent a useful measurement of the progression and persistence of obesity (Richards et al., 2000; Steinberg and Dyck, 2000), and interact in some way with catecholamine release.

1.2.5 Obesity and Heart Disease

There is considerable synergy between obesity and heart disease. Primarily, both disorders are associated with elevations of SNS activity at the detriment of pSNS activity. Bristow and colleagues (1982) demonstrated that NE levels are elevated in end-stage heart failure. Moreover, clinical investigations have shown that reduced vagal (pSNS) function at rest is associated with increased risk for development of hypertension over a three-year period (Liao et al., 1996). The Framingham study has indicated not only that increased body

weight is a major risk factor for the development of hypertension, but also that hypertensive patients have a greater propensity to be obese or overweight (Kannel et al., 1967). Obesity and hypertension are two of the criteria for the metabolic syndrome, a condition that is closely related to insulin resistance (Section 1.3.2). Indeed, obesity is also associated with the development of insulin resistance and hyperinsulinemia (Liatis et al., 2004), further risk factors in the development of heart disease. Elevations of body mass index (BMI) have also been correlated with CHF, with an estimated added risk of 5% for each unit of BMI above the "normal" threshold (Kenchaiah et al., 2002; Poirier et al., 2006).

1.2.6 Therapeutic Intervention

The most commonly physician-recommended treatment of obesity is a combination of a reduced fat intake and exercise (Giacobino, 1999; Mokdad et al., 2001; U.S. Department of Health and Human Services., 2001). The combined effect of this therapy is to reduce energy intake and increase its expenditure, as well as to directly affect SNS activity. Elevated physical activity has been correlated with elevations in basal NE levels, which may overcome the downregulation of βAR and NET-1 that develop due to obesity (Barbier et al., 2000; Enevoldsen et al., 2000; Levin and Dunn-Meynell, 2004). Dietary loss of weight has been shown to improve heart rate variability in obese patients (Liatis et al., 2004), and has also been correlated to decreased mean sympathetic neural activity in microneurography studies (Grassi et al., 1998).

Reduction of adiposity leads to diminished leptin secretion, which in turn decreases the baseline NE levels in obese individuals (Leibowitz and Wortley, 2004). Indeed, research has shown that exercising rats affects facultative, resting, and exercise-induced energy expenditure (Levin and Dunn-Meynell, 2004). Enevoldson and colleagues (2000) showed that Wistar rats on a 15-week swimming program gained weight at a significantly slower

rate than sedentary animals and showed altered levels of leptin and NE. Retroperitoneal, parametrial, and mesenteric fat pads at the conclusion of the experiments weighed less than half of those extracted from controls (Enevoldsen et al., 2000).

Exercise training has also been shown to affect the distribution of myocardial adrenergic and muscarinic receptors. After a progressive 12-week treadmill exercise protocol, rats showed a significant 20% reduction in atrial and 15% reduction in ventricular β_1AR densities compared to sedentary controls, potentially owing to elevated baseline NE over the exercise period (Barbier et al., 2006). Improvements in heart rate variability were also observed following caloric restriction and intermittent fasting (Mager et al., 2006). No change in heart rate variability was detected in exercised rats, which may suggest that these animals exhibit more efficient βAR signaling than sedentary counterparts. Such selective elevations of NE may overcome the sympathetic dysfunction that intensifies the obese state.

1.3 Diabetes Mellitus

1.3.1 General

Diabetes mellitus (DM) represents another major health condition, afflicting more than 2,000,000 Canadians. In the last several years, there has been a considerable increase in DM cases, particularly in adolescents, growing in parallel with increased prevalence of obesity (Deedwania and Fonseca, 2005; Stumvoll et al., 2005).

Normal insulin signaling and glucose transport in cardiac and skeletal muscle depends on insulin receptor binding. Following insulin stimulation, the receptor undergoes autophosphorylation and initiates a series of phosphorylation events involving several signaling molecules including phosphoinositol 3-kinase (PI-3K), Akt/protein kinase B, and

atypical PKC ζ and γ (Taegtmeyer et al., 2002). These kinases are involved in insulin-dependent translocation of glucose transporter 4 (GLUT-4) from the sarcolemma to the myocyte membrane (Calera et al., 1998; Kohn et al., 1996; Pessin and Saltiel, 2000). This process is partially supported by adrenergic activation (Section 1.3.3)

DM is categorized into type I and type II, of which the latter represents approximately 90% of total diagnoses (Shehadeh and Regan, 1995; Stumvoll et al., 2005). Type I DM develops from the loss of pancreatic β-cells, resulting in the absence of insulin secretion, and subsequent inability of peripheral tissues to regulate glucose. The causative factor of β-cell death is as yet unknown, but has been postulated to involve genetic dysregulation and/or autoimmune complications (Cardell, 2006; Daneman, 2006; Tsai et al., 2006). Conversely, type II DM often develops secondary to symptoms of the metabolic syndrome including visceral obesity, hyperglycaemia, hypertriglyceridemia, hypertension, and reduced high-density lipoprotein cholesterol levels (Citrome, 2005; Deedwania and Fonseca, 2005; Haffner et al., 1992; Keenan et al., 2005; Stumvoll et al., 2005). Type II diabetics tend to be overweight or obese and exhibit insulin resistance and consequential hyperinsulinemia (Esler et al., 2001; Quilliot et al., 2005).

Beta cell function is negatively affected by overproduction of insulin (Elder et al., 2005) and overfeeding (Landsberg, 2005). Molon-Noblot and colleagues (2001) demonstrated a marked increase in the occurrence of pancreatic islet lesions in rats without dietary restriction compared to rats on a regulated diet regimen. This so called "diabesity" is a precursor to insulin resistance and the development of both type II DM and the metabolic syndrome (Elder et al., 2005; Keenan et al., 2005).

1.3.2 Insulin Resistance

The vast majority (>90%) of type II diabetic subjects are thought to be resistant to the actions of insulin (Haffner and Miettinen, 1997). Peripheral resistance to insulin develops at the cellular level, wherein insulin receptors lose responsiveness to stimulation (Elder et al., 2005; Goldstein et al., 2002). To compensate for this desensitization, pancreatic β-cells overproduce insulin, leading to β-cell wasting and selective apoptotic cell death (Kostis and Sanders, 2005). As such, an early indication of type II DM is the presence of hyperinsulinemia, which is followed in later stages by hyperglycaemia due to the loss of insulin function. This later stage elevation of glucose levels may further compound the problem, inducing glucotoxicity and liberating pancreatic islet autoimmunogens (Taegtmeyer et al., 2002; Wilkin, 2001). Insulin resistance has become a cornerstone of the metabolic syndrome, as it has been postulated to instigate or exacerbate hypertension, dyslipidemia, hyperglycaemia, and heart disease (Haffner and Miettinen, 1997; Reaven, 2005; Reaven and Chen, 1988; Reaven et al., 1988). Elevated fasting insulin levels are predictive of the development of type II DM and of the presence of multiple metabolic disorders (Haffner et al., 1992). Elder and colleagues (2005) demonstrated that obese adolescents exhibit blood glucose levels similar to their lean counterparts, but that resting insulin levels were markedly elevated, to concentrations comparable with diabetic patients. Insulin resistance is also a hallmark of CHF and coronary heart disease (Bobbio et al., 2003; Haffner and Miettinen, 1997; Kostis and Sanders, 2005; Mokdad et al., 2001; Paolisso et al., 1991). Glycaemic dysregulation has a negative impact on prognosis in heart failure patients (Swan et al., 1997). Elevated glucose and insulin are correlated with higher New York Heart Association (NYHA) functional classes and shorter six-minute walk distances, even in non-diabetic patients (Rosenberg et al., 2005). Left ventricular volumes

at end systole and diastole are also significantly reduced in diabetic CHF patients and non-diabetic patients with hyperglycaemia and hyperinsulinemia (Rosenberg et al., 2005).

1.3.3 Diabetes Mellitus and the Sympathetic Nervous System

Both type I and type II DM have been linked to alterations in SNS signaling, though there remains some controversy whether development of SNS dysfunction is a causative or symptomatic factor.

Insulin signaling is coupled to SNS signaling, markedly affecting normal glucose trafficking in muscle and myocardium. The second messenger systems responsible for this cross-talk have not been fully explored, but are thought to include the insulin receptor- and AR-stimulation responsive molecule PI-3K and the subsequently activated regulatory protein Akt (Morisco et al., 2005; Taegtmeyer et al., 2002). Short term AR stimulation helps to promote translocation of insulin-sensitive GLUT-4 to cell surfaces (Czech and Corvera, 1999; Morisco et al., 2005). Conversely, long term βAR stimulation may inhibit normal phosphorylation of the insulin receptor, preventing GLUT translocation and glucose transport (Morisco et al., 2005). The inconsistency of SNS regulation in DM is well documented in the literature (Ganguly et al., 1987; Ganguly et al., 1986; Kiyono et al., 2001; Schmid et al., 1999; Stevens et al., 1998; Stevens et al., 1999).

There are two major and contradictory alterations in SNS signaling that have been reported in DM: i) decreased vascular resistance in skeletal muscle and resultant increases in blood flow relating to elevated pSNS or depleted SNS activity to endothelium; and ii) a condition designated diabetic autonomic neuropathy (DAN) wherein sympathetic denervation occurs in various peripheral organs, potentially related to elevated basal SNS activity. The latter has predominantly been explored in type I DM.

DM frequently precipitates capillary hyperperfusion and subsequent microangiopathy, the thickening and weakening of vessel walls such that blood and plasma proteins leak out, limiting flow (Tooke, 1995). It has been theorized that increased capillary flow may instigate or contribute to this complication. As vascular tone is mediated in part by the SNS, dysfunctional signaling may be an important factor in this development (Cohen et al., 1990; Schnell et al., 1997). Vervoort and colleagues (1999) demonstrated that arterial NE concentration was reduced and forearm blood flow elevated in type I diabetic patients, with no change in the vasodilating agent NO. Subjects also showed increased responsiveness to infusion of NE, indicating a hypersensitivity of peripheral blood vessel ARs potentially due to a chronic depression of peripheral sympathetic drive. In support of this contention, decreases in plasma NE levels in type I DM compared to both healthy and type II DM patients have been described by several groups (Bell, 2003; Pop-Busui et al., 2004; Schmid et al., 1999; Turpeinen et al., 1996; Yasar et al., 1994).

Microvasculature abnormalities resulting from reductions of NE and SNS drive have been implicated in peripheral and cardiac DAN (Pop-Busui et al., 2004; Schmid et al., 1999). Schmid and colleagues (1999) demonstrated marked reductions in uptake-1 function and neuronal density in right and left ventricles of 6-month-old streptozocin-induced type I DM rats. Indications of neuropathy were more pronounced at 9-months post-induction of diabetes. Clinical studies have related DAN with increased mortality, particularly due to higher susceptibility to sudden cardiac death (Ewing et al., 1980b; O'Brien et al., 1991). Regional alterations in NET-1 density have also been detected using radio-iodinated MIBG in diabetic rats. Scatchard analysis of binding assays with both [^{3}H]desipramine and MIBG revealed a 20% reduction in B_{max} of NET-1 without alterations in binding affinity (Kiyono et al., 2001).

In addition to decreased densities of NET-1, the functionality of the protein may also be altered. Ganguly and colleagues (1987) reported that diabetic animals exhibit a clear increase in the rate of uptake (V_{max}) at both baseline levels and when blocked with cocaine (Ganguly et al., 1987).

NE concentrations may be differentially altered in several organs affected by the SNS. Gallego and colleagues (2003) described elevated NE in the cardiac ventricles in diabetic animals, with decreases in the stellate ganglia (Figure 1.1) and blood serum. Similar observations have demonstrated increased NE in heart, kidney, brain, and spleen in streptozocin-induced diabetic rats compared to controls, an effect that was attenuated by administration of insulin (Ganguly et al., 1987; Ganguly et al., 1986).

There are indications that SNS activity is actually increased in type II DM (Caballero, 2005; Carnethon et al., 2003; Masuo et al., 2005). This contention is consistent with the common copresentation of insulin resistance and obesity in type II DM. Genetic abnormalities in SNS components have been identified in type II DM patients. Masuo and colleagues (2005) have described polymorphisms in β_2AR that appear to contribute to the development of insulin resistance and are positively correlated with elevated plasma insulin and NE levels. Heart rate variability measurements have elucidated a slight elevation in resting heart rate of type II diabetic patients compared to non-diabetic controls, possibly owing in part to altered SNS activity (Carnethon et al., 2003). However, clear distinction of NE levels in type I and type II DM have not been well documented, and appear to fluctuate depending on tissue and measurement methodology (Gallego et al., 2003).

1.3.4 Regulatory Factors

DM is associated with marked changes in several biological macromolecules. These factors have important effects on the SNS which may be involved in the synergy of DM

with obesity and CHF, and may serve to exacerbate the diabetic state. The most well understood markers affected are glucose and insulin. Leptin and NEFAs, also potentially altered in DM, are described above (1.2.4).

1.3.4.1 Glucose

Glucose is a positive regulator of NE release from the SNS. As described previously, overfeeding and subsequent elevations in glucose increase basal plasma NE levels (Landsberg, 1986; Molon-Noblot et al., 2001). Direct arterial infusion of glucose also elicits substantial increases in plasma NE concentrations, particularly in rats prone to development of diet-induced obesity (Levin and Sullivan, 1987; Levin and Sullivan, 1989). However, some clinical studies contradict this contention. Van Gurp and colleagues (2005) demonstrated increased forearm blood flow in sustained hyperglycaemia over a 6 hour period, without alterations in SNS activity, an effect that may result from enhanced NO stimulation. Increased NE levels observed in hearts of diabetic rats can also be attenuated by injection of insulin and subsequent reduction of glucose concentration (Ganguly et al., 1987), providing indirect evidence for a role of glucose in SNS regulation.

Elevations in glucose are often paralleled by elevations in both insulin and NEFAs (Levin and Sullivan, 1989; Reynisdottir et al., 1994) which may be more influential in regulating the SNS than glucose alone. The effects of glucose on NE release may therefore be indirect via insulin.

1.3.4.2 Insulin

Insulin is involved in cross-talk between cardiac metabolic pathways and βAR signaling. Morisco and colleagues (2005) posited that stimulation of βARs in cardiomyocytes impairs insulin signaling, providing a linkage between the SNS and insulin resistance. Specifically, alternative phosphorylation, mediated by the downstream effector protein Akt, desensitizes

the insulin receptor to stimulation and decreases glucose uptake, perpetuating hyperglycaemia and insulin resistance (Morisco et al., 2005). This cross-talk also functions in reverse, as infusion of insulin is associated with increased SNS activity. Prolonged hyperinsulinemia in healthy male subjects evokes marked elevations of heart rate and blood pressure (Kern et al., 2005), consistent with elevated NE stimulation. Moreover, lumbar sympathetic nerve activity increases by 40% following insulin infusion in streptozocin-induced diabetic rats (Rizk and Dunbar, 2004).

In vitro examinations also support the interaction of insulin with NE signaling machinery. Acute treatment of cells with insulin decreases [^{3}H]NE uptake in PC12 cells, indicating a desenstization or downregulation of NET-1 consistent with elevated NE exposure. (Figlewicz et al., 1993a; Figlewicz et al., 1993b). Similarly, infusion of insulin downregulates β_3ARs in 3T3-F442A cells (Feve et al., 1994). Surwit and colleagues (2000) demonstrated that this downregulation was reversible *in vivo* by administering diazoxide, a K^+-ATP channel blocker that suppresses insulin, and consequently relieves insulin resistance and hyperinsulinemia. That is, reduced insulin concentrations restored normal AR expression.

1.3.5 Diabetes Mellitus and Heart Disease

Diagnosis of type I or type II DM confers a two to threefold increase in the risk of developing cardiovascular disease (CVD) (Kostis and Sanders, 2005; Suskin et al., 2000). Indeed, glucose abnormalities including hyperglycaemia and hyperinsulinemia relate to poorer symptomatic status in patients with CHF (Suskin et al., 2000). Swan and colleagues have suggested that insulin resistance is a key diagnostic in CHF, wherein heart failure patients exhibit marked elevations in NE, fasting insulin levels, and substantially decreased insulin sensitivities (Swan et al., 1997; Swan et al., 1994). Moreover, the prevalence of

diabetes is decidedly increased in patients enrolled in major heart failure trials as compared to the general population, particularly in patients of higher NYHA classifications (Kostis and Sanders, 2005)

As discussed previously, one of the primary associations of DM and CVD is DAN. Loss of SNS modulation of heart rate and contractility is correlated with increased risk of cardiac mortality (Ewing et al., 1980a; Ewing et al., 1980b; Stevens et al., 1999). In fact, the 5-year mortality rate of diabetic patients presenting with DAN has been estimated at 16-53%, largely relating to sudden cardiac death (O'Brien et al., 1991).

A second major development in DM that affects cardiac performance is alterations in metabolic activity. In healthy, non-diabetic conditions, the heart primarily generates energy by oxidation of NEFA with small contributions from glycolysis and pyruvate oxidation (Taegtmeyer et al., 1980; Taegtmeyer et al., 2002). Under stress or increased energy demand, a greater contribution is made by glucose fuel sources (Depre et al., 1999a; Depre et al., 1998; Depre et al., 1999b; Goodwin et al., 1998a; Goodwin et al., 1998b). Animal experiments nearly a century ago showed that glucose uptake and respiratory quotient were markedly reduced in diabetic hearts (Starling and Lovatt Evans, 1914). This observation has been more recently compounded with the fact that cardiac dependence on NEFA metabolism for energy is increased in DM (Stanley et al., 1997). That is, the energetics of heart conduction shift further to NEFA oxidation in the diabetic state, rendering the heart less responsive to increased metabolic demand. It has been theorized that with increased levels of NEFA metabolism in the heart, glucose oxidation is inhibited, potentially at the pyruvate dehydrogenase complex via increased mitochondrial acetyl CoA-levels (Randle et al., 1963; Taegtmeyer et al., 2002). Glucose influx to the heart remains constant, and may

alter gene expression of GLUT-4 or glycolytic enzymes, impair glucose tolerance, or even instigate glucotoxicity (Young et al., 2002).

Glucose intolerance has also been associated with alterations in myocardial function. Avendano and colleagues (1999) have reported alterations in heart chamber stiffness and myocardial collagen-linked glycation in alloxan-induced glucose-intolerant dogs. No hemodynamic change was detected in this study, but myocardial dysfunction may result from left ventricular diastolic stiffness in DM patients (Avendano et al., 1999).

1.3.6 Therapeutic Intervention

As with obesity, the most common treatment regimen in type II DM is to manage diet, increase exercise, and promote weight loss (Newman et al., 2004). A diabetes prevention study in Finland demonstrated a reduction of more than 50% of new DM diagnoses following personalized consultations regarding exercise and diet (Tuomilehto et al., 2001). Comparatively, alterations in diet, exercise, or a combination thereof significantly improved diabetes occurrence in the United States (Deedwania and Fonseca, 2005).

Pharmacological treatment regimens of type II DM include several drugs that manage hyperglycaemia, including sulfonylurea derivatives, metformin, acarbose, and troglitazone (Deedwania and Fonseca, 2005; Stumvoll et al., 2005). Sulfonylureas such as tolbutamide stimulate the secretion of insulin (Sartor et al., 1980). Metformin has multiple anti-hyperglycaemic effects, acting on the liver to decrease gluconeogenesis, on striated muscle to increase sensitivity to insulin, and on the kidney to decrease glucose absorption (Bailey and Turner, 1996). Acarbose acts on the gastrointestinal tract to slow carbohydrate digestion and buffer post-prandial glucose levels (Kaiser and Sawicki, 2004). Finally, thiazolidinedione drugs such as troglitazone attempt to enhance insulin sensitivity (Buchanan et al., 2002). By modulating both insulin and glucose levels, these drugs may

exert indirect effects on SNS activity, complimenting primary effects in promoting improvement of the diabetic condition.

1.4 Cardiac Dysfunction, Obesity, and Diabetes Mellitus: Synergies

As discussed above, there are numerous synergies between cardiomyopathies, obesity, and DM. CHF, similar to obesity and DM, is associated with elevated SNS activity and NE release (Bristow et al., 1991; Bristow et al., 1982; Levine et al., 1982). CHF is an end-stage inability of the heart to adequately supply blood to the periphery, often developing in parallel or secondary to primary cardiopathologies including infarction and ischemia. A failing heart attempts to compensate for pathophysiological deficits via several mechanisms including cardiac remodeling, altered contractility, and stimulation of the SNS (Levine et al., 1982; Schafers et al., 1998). CHF and experimental heart failure result in fluctuations in synaptic activities, potentially owing to alterations of NE release into the synapse. Kawai and colleagues (2000) demonstrated a 33-50% reduction in NE uptake activity and greater than 50% decrease in B_{max} of NET-1 following 8 weeks of rapid pacing in rabbits, a disease model of CHF.

It has been well established that insulin resistance and obesity are common compounding factors in the development of CHF (Grassi et al., 2005; Kostis and Sanders, 2005; Poirier et al., 2006). Moreover, treatment of CHF has been correlated with increased incidence of DM. Beta-blocker therapy has been associated with heightened onset of DM, owing to interference with normal glucose tolerance and insulin signaling (Quilliot et al., 2005). However, it is generally accepted that β-blocker administration continues to benefit CHF patients in terms of mortality and hospitalization, even at the detriment of DM symptoms (Bobbio et al., 2003; Haenni and Lithell, 1994; Jacob et al., 1998; Shekelle et al., 2003).

The concurrence of CHF, obesity, and DM appears to derive at least partially from alterations in SNS signaling and NE release. As such, further examination of these synaptic changes may provide useful information in the understanding, treatment, and prevention of these disorders.

1.5 Animal Models

The animal models used in these experiments are designed to mimic the human condition of disease as accurately as possible. Therefore, animals with polygenic or diet-induced origins of disease with intact signaling pathways for SNS-active biomarkers were preferred to single mutations.

1.5.1 Diet Induced Obese and Diet Resistant Rats

As described briefly above (Section 1.2.2), a subset of Sprague-Dawley rats rapidly become obese when fed a high fat diet (DIO). Importantly, a second subset exhibits a transient resistance to increased weight gain (Diet Resistant, DR), providing a direct control group that can be considered "lean" (Levin and Keesey, 1998; Levin and Sullivan, 1987). The animals develop from a polygenic origin, bred specifically within their substrains to preserve genetic traits (Ricci and Levin, 2003). Unlike other obesity models including the ob/ob rat, Zucker fatty rat, or other genetically engineered knock-out mice, these animals exhibit intact signaling systems, including the leptin pathway, important to the study of the SNS (Haynes et al., 1997; Tschop and Heiman, 2001).

Experimental analyses of this animal model have shown synergies with the human obese condition and metabolic syndrome, including elevated insulin levels, abnormal glucose metabolism, and altered plasma NE concentrations as compared to normal Sprague-Dawley animals (Corbett et al., 1986; Farley et al., 2003; Gao et al., 2002; Levin et al., 1989; Levin

et al., 1983; Park et al., 2000). DIO and DR rats each show altered NE concentrations and differential responses to central glucose infusion at the hypothalamic level (Levin and Sullivan, 1987; Levin et al., 1983). These characteristics rendered the DIO rat model of obesity highly preferable for this study.

1.5.2 Streptozocin-Induced Diabetes Mellitus

One of the most common methods for the induction of DM is the injection of streptozocin, a selective alkylating agent that specifically targets pancreatic islet cells (Norton et al., 1996; Schmid et al., 1999). Streptozocin (2-deoxy-2-(3-(methyl-3-nitrosoureido)-D-glucopyranose, also called *streptozotocin*) is a natural toxin produced by *Streptomycetes archromogenes*, and is selectively taken up by pancreatic β-cells via GLUT-2 (Szkudelski, 2001). Its effects on the pancreas are to directly alkylate β-cell DNA, inducing cell death (Delaney et al., 1995; Elsner et al., 2000), and to act as a NO donor, promoting islet destruction via free oxygen radicals (Kroncke et al., 1995; Morgan et al., 1994).

Induction of type I DM follows a relatively high dose *intravenous* injection of streptozocin (>40 mg/kg) (Ganda et al., 1976; Katsumata et al., 1992). High dose administration is very effective in destroying pancreatic β-cell function (Szkudelski, 2001). Induction of type II DM is more contentious, as many methods require long incubation periods to develop hyperinsulinemia, glucose intolerance, and other hallmarks of type II DM. The most reliable induction method requires neonatal intraperitoneal injection of streptozocin, resulting in mild hyperglycaemia and impaired glucose tolerance after approximately 8 weeks (Portha et al., 1979). Alternatively, type II DM can be induced in a shorter timeframe in older rats, a situation that more closely resembles the human manifestation, if slightly more intrusive. Zhang and colleagues have described a method that incorporates consumption of high fat diet for a regulated period followed by moderate dose streptozocin

administered via intraperitoneal injection to reduce bioavailability and slow distribution (Sawant et al., 2004; Srinivasan et al., 2005; Zhang et al., 2003). This approach is theorized to precipitate conditions ideal for development of hyperinsulinemia by β-cell overwork in surviving pancreatic islet cells (Sawant et al., 2004), and was selected for use in this project.

1.6 IMAGING

1.6.1 Positron Emission Tomography

Positron emission tomography (PET) is a non-invasive, dynamic imaging modality that allows for *in vivo* measurement of physiologic parameters.

Radiolabeled ligands or analogues of biological compounds, termed radiotracers, are produced following a series of radiochemical reactions (Finn and Schlyer, 2002; Fowler and Ding, 2002). These radiotracers decay by positron emission (Figure 1.5A). Released positrons discharge energy, displace local electrons and ionize tissue. After dispelling its kinetic energy over a distance, termed "mean positron range", the positron collides with an electron and the resulting positronium undergoes annihilation, transferring the mass of the combined particle to a pair of antiparallel photons of 511 keV each (Herscovitch, 1990; Sedvall, 1991; Thompson, 2002).

A PET scanner consists of a ring of electronic collimators, detectors, and scintillation crystals around an aperture in which the subject is placed (Figure 1.5B). Coincidental detection of antiparallel photons allows for subsequent determination of the location of the annihilation event in three dimensional space. A series of computed calculations provide a functional image of radiotracer distribution (Figure 1.5C) (Koeppe, 2002; Thompson, 2002).

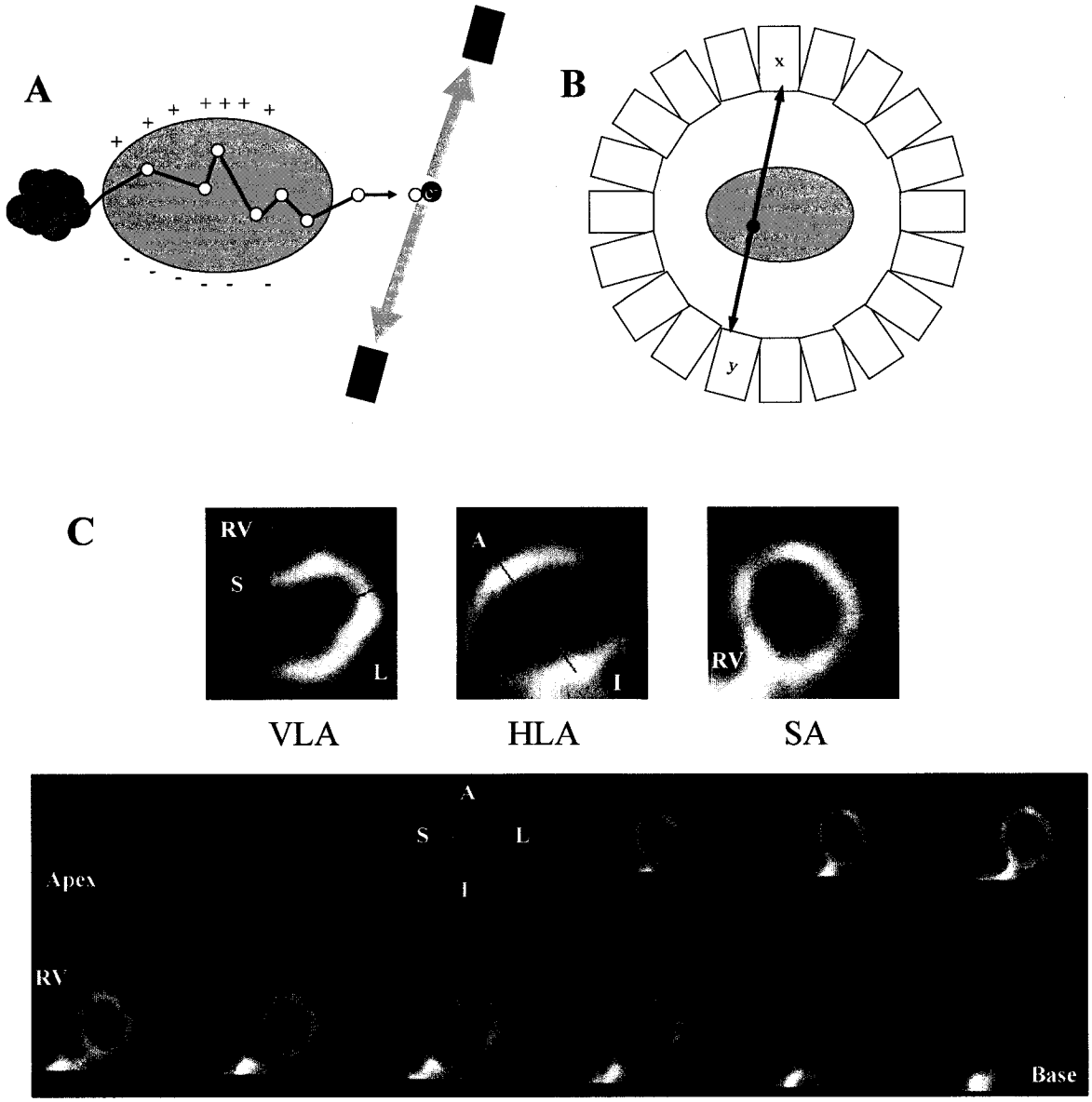

Figure 1.5: Schematic representation of positron emission and annihilation (**A**). Panel B illustrates coincidence detection of annihilation event (solid circle) at x and y by scintillation crystals and electrical collimators (**B**), coupled with computed calculations and corrections render a comprehensive PET image. Adapted from Thompson (2002). Pictured is a cardiac PET image (**C**) of a healthy patient with [^{11}C]HED; vertical long axis (VLA), horizontal long axis (HLA), and serial sections of short axis (SA). Visible are right ventricle (RV) and left ventricle septal (S), lateral (L), anterior (A), and inferior (I) walls. Patient image courtesy of National Cardiac PET Centre, University of Ottawa Heart Institute.

1.6.2 Tracers and Imaging Agents

The uptake-1 pathway can be imaged using PET and radiolabeled analogues of NE (Link et al., 2003; Schwaiger et al., 1990). Several radiotracers have been developed for this purpose, including [^{18}F]fluorometaraminol ([^{18}F]FMR), [^{11}C]*meta*-hydroxyephedrine ([^{11}C]HED), [^{11}C]epinephrine, and [^{11}C]phenylephrine (Del Rosario et al., 1996; Law et al., 1997; Raffel and Wieland, 2001b; Rosenspire et al., 1990; Wieland et al., 1990). Structural comparisons of several NE analogous tracers are shown in Figure 1.6.

Labeling of endogenous neurotransmitters is ineffective, primarily because of susceptibility of Epi and NE derivatives to normal metabolic processes via MAO and COMT (Chakraborty et al., 1993; DeGrado et al., 1993). Metabolic fate is also the primary concern with [^{11}C]phenylephrine (Del Rosario et al., 1996). Additionally, an ideal tracer has little to no postsynaptic activity, rendering the so-called "false neurotransmitter" analogues more advantageous in NET-1 imaging (Raffel and Wieland, 2001).

The NE analogue [^{18}F]FMR has been well investigated, showing high neuronal uptake and low clearance from cardiac neurons (Langer et al., 2000; Wieland et al., 1990). Pharmacological experiments showed specific blockade of [^{18}F]FMR retention following treatment with the NET-1 inhibitor desipramine or the vesicular monoamine transporter (VMAT) inhibitor reserpine (Wieland et al., 1990). Similar reductions in specific tracer uptake were observed following denervation of heart or other peripheral organs, either with phenol-denervation or 6-hydroxydopamine treatment (Wieland et al., 1990). However, low specific activity achieved with ^{18}F-fluorination of radiotracers limited the effectiveness of this radiotracer (Raffel and Wieland, 2001a; Wieland et al., 1990). Recently, higher specific activities have been attained via stereospecific ^{18}F-fluorination

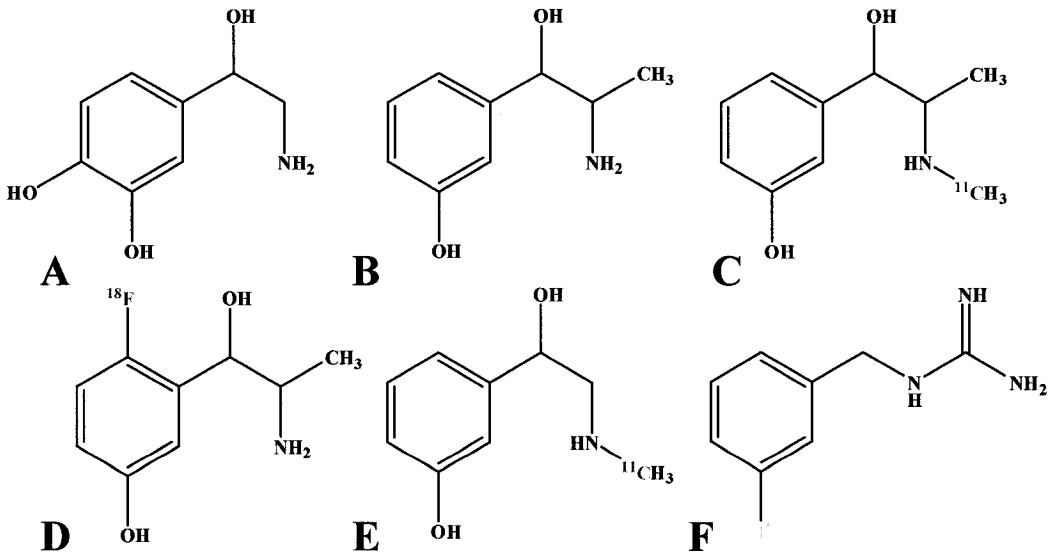

Figure 1.6: Chemical structures of radiotracer analogues of norepinephrine. Pictured are unlabeled norepinephrine (**A**), unlabeled metaraminol (**B**), [^{11}C]*meta*-hydroxyephedrine (**C**), 6-[^{18}F]fluorometaraminol (**D**), [^{11}C]phenylephrine (**E**), and [^{123}I]*meta*-iodobenzylguanidine (**F**).

(Langer et al., 2000) and ^{11}C-methylation of metaraminol (Någren et al., 1996), but due to the reasons described above and the relative simplicity of synthesis, [^{11}C]HED currently remains the preferred presynaptic imaging agent.

Another frequently used presynaptic imaging agent is the single photon emission computed tomography (SPECT) tracer ^{123}I-, ^{125}I-, or ^{131}I-labeled MIBG. Originally developed to image pheochromocytomas, it was soon observed that MIBG exhibited robust uptake in heart tissue (Sisson et al., 1981; Wieland et al., 1981a; Wieland et al., 1981b). However, extraneuronal uptake in hearts of certain mammalian species (Eisenhofer et al., 1992; Graefe et al., 1978; Raffel and Wieland, 2001b) and the shortcomings in spatial resolution and absolute quantification that are characteristic of all gamma-emitting photon radiotracers in SPECT have limited the utility of MIBG. Despite this, it remains heavily used in the laboratory and clinic to assess presynaptic SNS innervation in a wide variety of disorders (Agostini et al., 2000; Merlet et al., 1999; Raffel and Wieland, 2001b; Satoh et al., 1999; Takatsu et al., 2000).

Other targets for imaging of the SNS include βARs and second messenger molecules. βARs have been imaged using several ^{11}C-labeled antagonists and partial agonists including pindolol and carazolol derivatives as well as the more routinely used CGP12177 and 12388 (Hertel et al., 1983; Kopka et al., 2003; Staehelin and Hertel, 1983; Staehelin et al., 1983; van Waarde et al., 2004). Imaging of second messengers is a relatively novel concept. Recently, the phosphodiesterase-4 inhibitor (*R*)-[^{11}C]rolipram has shown potential as an index of intracellular cAMP in brain and myocardial imaging (DaSilva et al., 2002; DaSilva et al., 2001; Lourenco et al., 1999a; Lourenco et al., 1999b; Lourenco et al., 2001; Lourenco et al., 2006).

1.6.2.1 [^{11}C]*meta*-Hydroxyephedrine

One of the most routinely used radiotracers for cardiac imaging of the SNS is [^{11}C]HED. A false neurotransmitter, [^{11}C]HED is subject to the uptake-1 pathway, circulating the radiotracer from the synaptic cleft back into the presynaptic bouton (Raffel and Wieland, 2001b).

[^{11}C]HED can be synthesized in two series and four stereoisomers: the erythro series (*1R,2S*) and (*1S 2R*), and the threo series (*1S,2S*) and (*1R,2R*) (Foley et al., 2002; Van Dort and Tluczek, 2000). Of these stereoisomers, the (*1R,2S*) enantiomer exhibits the greatest selectivity for NET-1 over DAT and SERT with selectivity ratios of 1:10 and 1:71, respectively (Foley et al., 2002). The enantiomer of [^{11}C]HED produced at this facility is predominantly the (*1R,2S*) variation, as the precursor compound metaraminol freebase is stereospecific.

One advantage of [^{11}C]HED over other tracers is its metabolic stability. Its chemical structure renders it resistant to both MAO and COMT (Fuller et al., 1981). Indeed, metabolic analyses have shown that no radioactive metabolites are present in myocardium following [^{11}C]HED injection (Law et al., 1997; Rosenspire et al., 1990). Clinically, [^{11}C]HED has been applied to measure SNS innervation in cardiovascular and other disorders including sudden cardiac death, coronary artery disease, and CHF (Bulow et al., 2003; Nitzsche et al., 1993; Odaka et al., 2001; Uberfuhr et al., 2000), pheochromocytoma (Shulkin et al., 1992; Trampal et al., 2004), diabetes (Stevens et al., 1998; Stevens et al., 1999), and even multi-system atrophy in Parkinson's disease (Berding et al., 2003). Reduced myocardial uptake of [^{11}C]HED generally correlates with poor patient prognoses (Allman et al., 1993). In clinical research, [^{11}C]HED has also been applied in tracking

recovery of myocardial SNS innervation in heart transplant recipients (Bengel et al., 2002; Bengel et al., 2001; Odaka et al., 2001).

The pharmacokinetic properties of [^{11}C]HED have been tested in animal models and isolated organ systems (deGrado et al., 1993; Law et al., 1997; Rosenspire et al., 1990). Retention of [^{11}C]HED is primarily dependent on the functionality and availability of NET-1 (Law et al., 1997; Rosenspire et al., 1990; Ungerer et al., 1993). *Ex vivo* analyses in isolated perfused rat hearts have suggested a correlation between NE concentration and clearance rate of tracer (deGrado et al., 1993), but a complete *in vivo* examination of this phenomenon is incomplete.

Due to the kinetic and structural similarities, the evaluation of comparable tracers such as [^{18}F]FMR has provided additional background regarding the physiological and pharmacological behaviour of [^{11}C]HED. In dogs, [^{18}F]FMR retention is greatly reduced by NET-1 blockade and by inhibitors of vesicular uptake (Wieland et al., 1990), indicating that a substantial proportion of [^{18}F]FMR is packaged into vesicles upon uptake into the bouton. Examination of [^{11}C]phenylephrine, a NE analogue that is susceptible to MAO metabolism, revealed that pretreatment with the MAO A inhibitor clorgyline increased [^{11}C]phenylephrine retention in heart (Del Rosario et al., 1996). While these findings have bearing on the overall behaviour of [^{11}C]HED *in vivo*, a full analysis of the impact of elevated NE or altered vesicular packaging has not been performed.

1.6.3 Extra Cardiac Imaging

1.6.3.1 Pancreatic Imaging

Several pancreatic imaging agents have been developed with limited success. Extra-pancreatic uptake of tracer in the gastrointestinal tract, creating poor signal-to-noise ratios, has been a substantial obstacle for the development of radiotracers for pancreatic imaging

(Sweet et al., 2004). Another challenge for successful pancreatic β-cell imaging is the requirement for the candidate tracer to bind with higher affinity to endocrine cells than exocrine cells. Some of the PET radioligands that have been investigated include pSNS imaging agents such as 4-[^{18}F]fluorobenzyltrozamicol (Clark et al., 2004) and labeled derivatives of the sulfonylurea drugs glibenclamide and tolbutamide (Sweet et al., 2004). However, development of candidate tracers for pancreatic imaging remains in its infancy. Localization of the pancreas may be possible using fused PET/Computed Tomography (CT) technology, isolating the pancreas with CT in order to delineate PET tracer uptake in subsequent calculations. It is of interest to note that the University of Ottawa Heart Institute National Cardiac PET Centre is in the process of purchasing a PET/CT human camera in the 2006 fiscal year.

1.6.3.2 Brown Adipose Tissue Imaging

Until recently, brown adipose tissue was considered to compose only a small proportion of adipose deposits in adult humans (Collins and Surwit, 2001). However, recent use of the metabolic tracer [^{18}F]fluorodeoxyglucose ([^{18}F]FDG) in full body scans has revealed anomalous tracer uptake in areas of supraclavicular or "USA" fat (Cohade et al., 2003; Haney et al., 1999; Tatsumi et al., 2004), suggesting that brown adipose tissue can be localized in large mammals. In rats, brown adipose tissue exhibits high [^{18}F]FDG uptake, especially with exposure to cold temperatures or SNS stimulation (Tatsumi et al., 2004). The isolation of brown adipose tissue in humans represents an opportunity for future PET studies tracking therapeutic interventions. Use of [^{11}C]HED and [^{18}F]FDG in a sequential PET imaging protocol may facilitate the delineation of brown adipose tissue deposits for image reconstruction. The advent of fused PET/CT technology may also assist in the localization of brown adipose deposits in subjects.

1.7 Research Objectives and Hypotheses

1.7.1 Research Objectives

The *long term* goal of this project is to examine *in vivo* sympathetic nervous integrity in myocardium and thermogenic tissues in health and disease states with altered NE signaling including obesity and type II DM.

The primary objectives of this project were:

i) to enhance the understanding of the relationship between SNS signaling at the NET-1 site in the development and progression of obesity and DM, particularly with regard to myocardium, brown adipose tissue, and pancreas

ii) to define background data necessary for the development of imaging procedures with [^{11}C]HED and PET to assess progression of disease state and/or effectiveness of therapy in obesity and type II DM

1.7.2 Primary Hypotheses

The primary hypotheses of this project were:

i) specific, blockable retention of [^{11}C]HED will be detected in tissues with rich SNS innervation, particularly myocardium, brown adipose tissue, and pancreas

ii) less efficient SNS signaling in obese and type II DM animals will result in elevated baseline NE concentrations and/or depleted NET-1 densities in myocardium, brown adipose tissue, and pancreas

iii) more efficient SNS signaling in lean animals will result in decreased baseline NE concentrations and/or enhanced NET-1 densities in myocardium, brown adipose tissue, and pancreas

iv) the alterations in NE concentration and/or NET-1 densities in myocardium, brown adipose tissue, and pancreas can be effectively quantified using [^{11}C]HED

1.7.3 Specific Aims

The specific aims of this project were:

i) to establish time course of [^{11}C]HED uptake in select tissues *in vivo* in rat

ii) to examine the effect of acute blockade of NET-1 sites on tracer retention

iii) to evaluate response of [^{11}C]HED accumulation to increased synaptic competition with NE analogues

iv) to investigate the effect of decreased volume of distribution on [^{11}C]HED kinetics by blocking vesicular storage

v) to assess [^{11}C]HED retention following acute and chronic elevation and depression of synaptic NE via MAO inhibition and modulation of α_2ARs

vi) to confirm physiological differences between DIO and DR rats in terms of weight gain and food consumption

vii) to ascertain differences in NET-1 density and/or synaptic NE concentration exhibited by DIO and DR rats as compared to normal controls at short, intermediate, and long term time points

viii) to delineate differences in NET-1 density and/or synaptic NE concentration exhibited in type I and type II DM as compared to normal, age-matched controls at short and intermediate time points*

* in the scope of this project, *in vivo* work only defines the presence of variation in NET-1 density, synaptic NE concentration, or both; future work will address the individual factors involved using autoradiography and quantitiative HPLC to delineate variations in NET-1 and NE respectively

1.7.4 Expected Results

The expected results of this project were:

i) [^{11}C]HED will exhibit high uptake and long retention in tissues with rich adrenergic innervation, particularly heart, brown adipose tissue, and pancreas

ii) inhibition of uptake-1 will eliminate specific neuronal retention of [^{11}C]HED and markedly reduce tracer accumulation in these tissues

iii) vesicular blockade with reserpine will either increase or decrease specific [^{11}C]HED retention due to depressed synaptic NE levels and blockade of the vesicular distribution volume, respectively

iv) elevation of synaptic NE or analogous compounds will selectively reduce [^{11}C]HED neuronal accumulation due to increased competition for limited reuptake sites; depression of synaptic NE will selectively increase [^{11}C]HED retention due to reduced competition

v) obese and lean rats will exhibit marked differences in weight gain profiles due to factors beyond food consumption alone

vi) tracer uptake in brown adipose tissue and pancreas will be decreased in obese and elevated in lean rats as compared to controls due to differential regulation of SNS signaling in these animals; myocardial tracer retention may be less affected due to lesser dependence on central NE spillover for NE supply

vii) [^{11}C]HED retention may be either increased or decreased in brown adipose tissue and pancreas in type I and type II DM, owing to differential NE levels in these tissues in disease states; myocardial retention is most likely to decrease, as NE concentration should be increased in this region

1.7.5 Potential for Future PET Studies in Humans

If hypotheses are correct, [^{11}C]HED retention indices may be indicative of altered NE concentrations in the absence of dysregulated NET-1 densities. Moreover, protocols using [^{11}C]HED may be useful in predicting the development of heart complications in obese and diabetic patients that do not yet present indications of CVD.

If pancreatic and brown adipose tissue retention of tracer can be effectively isolated from background, the procedures could be equally useful in examining the alterations of SNS signaling in these tissues before, during, and subsequent to therapy for obesity and/or DM.

2.0 MATERIALS AND METHODS

2.1 RADIOCHEMICAL SYNTHESIS OF [^{11}C]*META*-HYDROXYEPHEDRINE

(*1R,2S*)-Metaraminol freebase was prepared from (*1R,2S*)-metaraminol bitartrate (Sigma-Aldrich) as described previously (Rosenspire et al., 1990). Briefly, alkaline metaraminol bitartrate in saturated sodium bicarbonate solution is extracted multiple times with ethyl acetate, dried, and filtered.

[^{11}C]HED is synthesized by *N*-[^{11}C]-methylation of metaraminol freebase with [^{11}C]methyl iodide (Figure 2.1). Briefly, the target material* is bombarded with 11 MeV of protons accelerated by a cyclotron (CTI), producing $^{11}CO_2$ via the $^{14}N(p,\alpha)^{11}C$ radiochemical reaction. $^{11}CO_2$ is then reduced with lithium aluminum hydride in the presence of tetrahydrofuran and hydoriodic acid to yield $^{11}CH_3$. *N*-[^{11}C]Methylation of metaraminol freebase is then carried out in the presence of dimethylformamide at 90°C. [^{11}C]HED is purified by semi-preparative high performance liquid chromatography (HPLC) using a 250 x 10 mm Luna 10 μm C-18 column (Phenomenex) in 5/95 acetonitrile (MeCN) / 0.1 M ammonium formate (HNH_3COOH) at a flow rate of 7 mL/min. The [^{11}C]HED peak (retention time approximately 7.0 minutes) is collected, solvent removed via rotary evaporation, and the product reformulated in saline and sterilized by filtration prior to injection. Products were further tested for quality control with analytical HPLC using a 250 x 4.6 mm Partisil SCX 10 μm cation exchange column in 10/90 MeCN / 0.1 M HNH_3COOH at 2.5 mL/min (retention time is approximately 3.0 minutes). Specific activities obtained range between 200-1500 mCi/μmol (7.4-55.5 Bq/μmol).

---

* Specifically, a gas mixture of nitrogen with 1% oxygen. Moisture and carbon dioxide absorbers are connected to the gas tank delivery line prior to the target to avoid contamination.

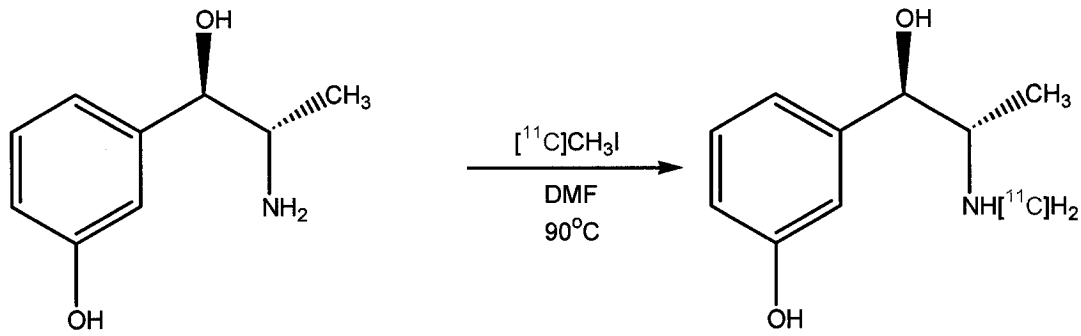

Figure 2.1: Synthesis of (*1R,2S*)-[^{11}C]HED by *N*-[^{11}C]methylation of metaraminol freebase by [^{11}C]methyl iodide.

In cases where specific activity was inadequate (<200 mCi/μmol), experiments were postponed or conducted using only animals pretreated with desipramine, for which specific uptake of [^{11}C]HED is effectively blocked, and specific activity is not a concern. Total synthesis time for [^{11}C]HED is approximately thirty-five minutes.

2.2 Animals

2.2.1 General

Animal experiments were conducted in accordance with the recommendations of the Canadian Council on Animal Care and with approval from the Animal Care Committee of the University of Ottawa. Adult male Sprague-Dawley, Diet-Induced Obese, and Diet Resistant rats were obtained from Charles River Canada (Montreal, QC) and housed singly or in pairs in a temperature-controlled animal facility under a 12 h light/dark cycle with food and water *ad libitum*.

2.2.2 Food Composition

Animals used in general pharmacological experiments as well as type I diabetic animals were maintained on standard chow diet (Harlan Teklad). This diet energy balance consists of 9% fat, 67% carbohydrate, 19% protein, and 5% fibre. Food consumption was not monitored for chow-fed animals.

DIO and DR rats as well as Sprague-Dawley rats used in type II diabetes experiments were fed a high fat diet (Research Diets D12266B). Kilocalories of the diet are composed of 32% fat, 51% carbohydrate, 17% protein. A comparable control diet (Research Diets D12489B) with similar constituents to the high fat diet but a caloric makeup similar to standard chow, specifically 11% fat, 72% carbohydrate, 17% protein, was also assessed.

In applicable studies, particularly those for obesity and diabetes experiments, body weight and food consumption were monitored twice weekly. Cumulative weight gain was monitored from initiation of high fat diet until the day of the experiment. Food consumption was divided to render a daily intake, and expressed as a percentage of total body weight (Equation 1).

$$\textit{Equation 1:}\quad \frac{(\text{food remaining } t_x - \text{food provided } t_{x-n})/\ n}{\text{Body weight } t_x}$$

where t_x = date of measurement; t_{x-n} = date food provided; n = number of days between

In studies for which plasma was collected for insulin analysis (Section 2.6), animals were fasted overnight prior to the biodistribution experiment. Biodistribution time line for obesity studies is shown in Figure 2.2.

2.2.3 Induction of Diabetes

Type I DM was induced in chow-fed Sprague-Dawley rats via intravenous injection of high dose streptozocin (Sigma, 65 mg/kg). Induction of type II DM used a lower dose of strepoztocin (45 mg/kg) administered after 14 days of high fat diet consumption in Sprague-Dawley rats. The action of streptozocin is described above (Section 1.5.2).

Streptozocin was dissolved as described elsewhere (Zhang et al., 2003). Briefly, a solution of 0.1 M tribasic sodium citrate buffer was prepared in sterile water and adjusted to a pH of 4.0 by addition of 50 µL of 0.1 N hydrochloric acid (HCl) to accommodate for the high basicity of streptozocin. The drug was then dissolved in the desired concentration, resulting in a final pH of 5.5-6.0. Osmolality was adjusted by addition of 0.9% sodium chloride (Astra Zeneca) to 370 mOsm.

Blood glucose measurements were used as a primary endpoint for determination of diabetic status. Animals exhibiting and maintaining blood glucose concentrations greater than 11

mmol/L between 7 and 28 days following streptozocin treatment were classified as hyperglycaemic and diabetic, whereas animals exhibiting blood glucose concentration less than 11 mmol/L in this timeframe were considered as euglycaemic streptozocin-treated animals (Srinivasan et al., 2005; Zhang et al., 2003).

2.2.4 Blood Glucose Monitoring

Blood glucose measurements were acquired for diabetes studies. Briefly, a hind limb of the animal was shaved to the knee and sterilized with an alcohol swab. A bead of blood was then obtained by piercing the pedal vein using a 23-gauge needle. The blood droplet was collected using a blood glucose monitor (AccuChek Inform, Roche), and the output reading was recorded. Measurements were taken at regulated intervals prior to and after diabetes induction (Figure 2.2).

2.3 Biodistribution

Biodistribution studies were performed as previously described (Lourenco et al., 2001; Lourenco et al., 2006). Briefly, 1.4-2.0 mCi (200-1500 mCi/μmol) (51.8-74 MBq, 7.4-55.5 GBq/μmol) of [^{11}C]HED was injected as a 0.1-0.3 mL bolus into the lateral tail vein of each conscious, restrained rat. Tail veins were vasodilated using an infrared heat lamp to facilitate injection. In each individual experiment, all animals received approximately the same mass dose of [^{11}C]HED (0.24-1.26 μg). Animals were sacrificed by decapitation at a defined time point following tracer injection. Time course evaluation included sacrifice times of 15, 30, 45, 60, and 90 minutes following tracer injection. Documented pharmacological studies favour a 30 minute post-tracer time point, and initial time course evaluation supported this incubation period (Law et al., 1997; Rosenspire et al., 1990). Subsequent experiments were conducted using 30 minute sacrifice time.

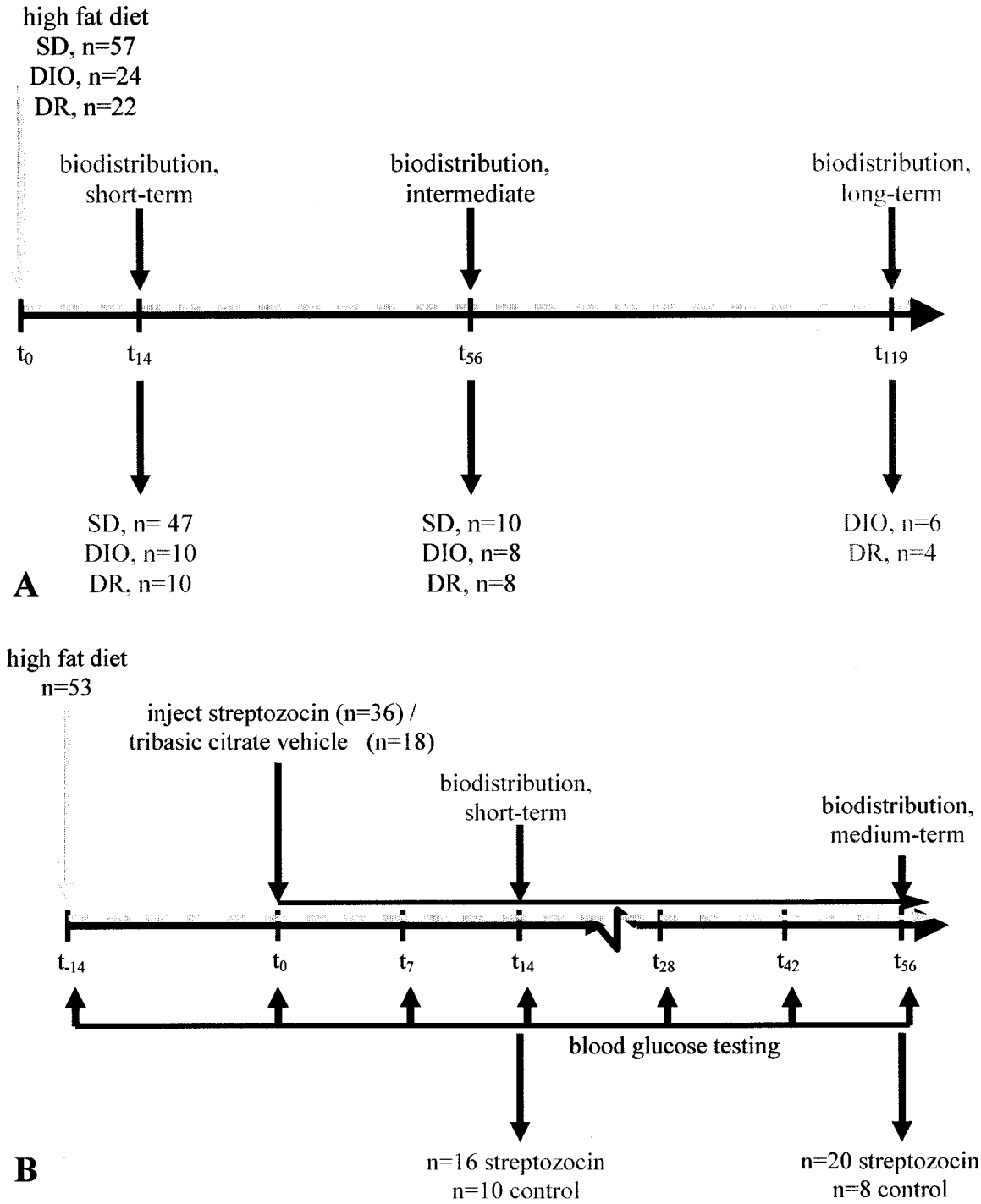

Figure 2.2: Timeline of obesity (**A**) and type II diabetes mellitus (**B**) experiments. Time on high fat diet, time of treatment, and blood sampling points are indicated. Endpoints for biodistribution experiments were at 14, 56, and 119 days following high fat diet or streptozocin, as shown.

Myocardial tissue (right and left atria, right and left ventricular free walls, and intraventricular septum), one kidney, and pieces of intrascapular brown adipose tissue, peritoneal white adipose tissue, quadriceps femoris, lung, and liver were rapidly excised. Samples of trunk blood were collected in heparin or ethylenediaminetetraacetic acid (EDTA) tubes to prevent coagulation*, and 2 mL samples were taken. Standard 1% dilutions of [^{11}C]HED injection volume were counted in triplicate. Tissue and blood samples were placed in pre-weighed gamma-counter tubes (VWR), and counted for radioactivity in a gamma counter (Packard). Post-weights were obtained immediately following radioactivity counting.

Residual radioactivity in syringes and tails was measured and subtracted to obtain the true injected dose. This dose was then time-corrected for decay and used in calculations to determine the percent injected dose per gram of tissue (%ID/g). The resulting value was multiplied by rat body weight (%ID/g*BW) to normalize for differences in body mass and allow meaningful comparisons across groups.

Following counting, blood samples were centrifuged using a benchtop centrifuge (Jouan, CR3i) at 4000 rpm for 5 minutes to separate plasma. Plasma samples were stored at -80°C for subsequent NE and insulin determination.

Due to circadian rhythm-driven fluctuations in plasmatic NE levels, experiments were conducted at consistent times of the day (Martinez-Merlos et al., 2004). All biodistribution experiments were completed between 09:00 and 11:30, at the start of the inactive phase of the nocturnal rat circadian rhythm, at which point NE levels are declining, but consistent between experiments.

---

* Heparin interferes with the radio-immune assay for insulin, necessitating use of EDTA tubes.

2.4 Analysis of Diet, Fasting

Due to the diverse nature of diets used within this project, a pilot analysis was conducted to determine whether diet composition affected retention of [^{11}C]HED. Sprague-Dawley rats were divided into two groups and fed either high fat diet or comparable control diet for 14 days. These groups were then further subdivided into a fasting overnight and a fed overnight group prior to the biodistribution experiment.

2.5 Drug Treatments

All drugs used in these studies were obtained from Sigma-Aldrich (St. Louis, MO). Biological half lives and literature searches were used to inform dosage, administration time, and washout period. Unless otherwise indicated, drugs were dissolved in sterile isotonic 0.9% sodium chloride solution (Astra Zeneca).

2.5.1 Blockade of Uptake-1

The effect of blocking the uptake-1 pathway on [^{11}C]HED retention was assessed using the NET-1 inhibitors desipramine HCl (10 mg/kg) (Rosenspire et al., 1990) and nisoxetine HCl (10 mg/kg) (Tejani-Butt et al., 1990). Both drugs were administered by intraperitoneal injection 30 minutes prior to tracer.

Pretreatment with desipramine is considered to effectively block all presynaptic uptake of [^{11}C]HED (Law et al., 1997; Rosenspire et al., 1990). Therefore, all tracer retention following this drug treatment represents non-specific accumulation. In subsequent chronic experiments, uptake-1-specific [^{11}C]HED retention was determined indirectly by administration of desipramine as a blocking agent.

2.5.2 Synaptic Competition for Reuptake

The impact of increased synaptic competition for uptake-1 sites on [^{11}C]HED kinetics was tested using the precursor compound and NE analogue metaraminol bitartrate, administered as an intravenous co-injection with tracer (1.3 mg/kg) (Law et al., 1997). Endogenous NE was increased by inhibiting the catabolic enzyme MAO with tranylcypromine HCl. A dose-response curve was generated for 0.5, 1.0, 2.0, 5.0, and 10.0 mg/kg, given ip 1 hour prior to tracer injection (Keck et al., 1991). Subchronic elevation of NE was also tested by administering tranylcypromine over a 14 day period (7.5 mg/kg/day*7 days, 10.0 mg/kg /day *7 days, 24 hour washout) (Takahashi et al., 1999). Subchronically treated rats were tested for uptake-1 specific retention as described above.

2.5.3 Vesicular Blockade

The component of total [^{11}C]HED retention dependent on vesicular packaging was evaluated by administering the VMAT blocker reserpine (5 mg/kg, 24 hours prior) (Raasch et al., 2004). Reserpine was dissolved in a 90/10 solution of sterile water and glacial acetic acid. Final pH was buffered to 5.5 using sodium biocarbonate. As an irreversible inhibitor, reserpine also depletes synaptic NE by blocking vesicular packaging and exposing catecholamines to the metabolic pathways of MAO and COMT.

2.5.4 Alpha Adrenoceptor Agonism and Antagonism

The effect of decreased synaptic competition for reuptake on [^{11}C]HED retention was tested by administration of the α_2AR agonist clonidine HCl. Selective stimulation of the presynaptic α_2AR is required for decreased NE efflux from the varicosity. A dose-response curve was generated for 0.05, 0.1, 0.5, and 1.0 mg/kg, administered ip 3 hours prior to tracer (Garcia-Sevilla and Zubieta, 1986; Rocchini et al., 2004). Low doses of clonidine

are considered more efficacious in attaining selective presynaptic α_2 agonism (Urano et al., 2004).

An alternative method to increase synaptic NE was tested for comparison with tranylcypromine data, using the α_2AR inhibitor yohimbine HCl given at 10.0 mg/kg, 15 minutes prior to tracer (Pacak et al., 1992). Yohimbine was dissolved in a 75/20/5 solution of acidified saline,* propylene glycol, and ethanol.

2.6 Insulin Measurements

Insulin was measured using a commercially available radio-immune assay (Linco Research, St. Charles, MO). Procedural analysis was conducted as described elsewhere (Satoh et al., 2005). Briefly, a fixed concentration of ^{125}I-labeled insulin is mixed with assay buffer,† guinea pig anit-rat insulin antibody, and the analyte plasma sample over a three day procedure. Precipitating reagent and centrifugation are used to obtain a firm pellet consisting of antibody and bound insulin. An inverse correlation between labeled reference insulin binding and unlabeled analyte insulin binding to the antibody within the pellet indicates the concentration of native insulin in the sample. That is, low radioactivity indicates high analyte insulin. Calculations were performed to determine the concentrations of insulin in each analyte sample.

---

* Specifically, 9 µL 0.1 N HCl per 1000 µL of saline.

† 0.05 M Phosphosaline, pH 7.4 with 0.025 M EDTA, 0.08% Na^+Azide, 1% RIA Grade bovie serum albumin

2.7 Data Analysis

Data are expressed as %ID/g*BW and further analysed on the basis of percent changes compared to normal and/or vehicle treated, age-matched controls. Percent change as compared to controls is determined using Equation 2:

$$\textit{Equation 2: } \frac{(\%ID/g*BW_{group}) - (\%ID/g*BW_{control})*100\%}{(\%ID/g*BW_{control})}$$

where $\%ID/g*BW_{group}$ indicates the tracer retention values in the variable group being tested and $\%ID/g*BW_{control}$ represents the same measurement in untreated controls

Uptake-1 specific retention of HED is calculated using Equation 3:

$$\textit{Equation 3: } (\%ID/g*BW_{total}) - (\%ID/g*BW_{desipramine})$$

*where $\%ID/g*BW_{total}$ indicates the total tracer retention value in tested group without pretreatment and $\%ID/g*BW_{desipramine}$ indicates the non-specific tracer retention as assessed by blocking specific retention of [^{11}C]HED using desipramine**

Percent change in specific retention is derived using a combination of Equation 2 and Equation 3. That is, non-specific tracer accumulation is subtracted from both treated and control animals, allowing for calculation of the percent change in specific retention without complication from non-specific retention.

$$\textit{Equation 4 } \frac{(\%ID/g*BW^{SR}_{group}) - (\%ID/g*BW^{SR}_{control})}{(\%ID/g*BW^{SR}_{control})}$$

where SR = Specific Retention (from Equation 3)

Statistical analyses are carried out using one-way analysis of variance (ANOVA) with Bonferroni's post hoc analysis. Significance level is set at $p<0.05$.

In animal characteristic comparisons, paired T-tests were used to delineate statistical variability in weight gain, food consumption, and blood marker levels. Significance level is set at $p<0.05$.

---

* As previously noted, this calculation assumes that desipramine provides a complete blockade of specific tracer retention.

3.0 RESULTS

3.1 PHARMACOLOGY

3.1.1 Time Course Evaluation

Time course evaluation of [^{11}C]HED at 15-90 minutes (Figure 3.1) revealed high uptake in myocardial tissue (0.42-0.52 %ID/g*BW, 30 minutes). The highest retention occurred at 30 minutes, slightly elevated from 15 minutes, and slowly declining to 90 minutes. High retention values were also observed in brown adipose tissue, lung, and pancreas (0.20±0.09, 0.16±0.05, 0.13±0.03 %ID/g*BW, respectively). These tissues showed a fairly consistent declination in tracer accumulation over the course of 90 minutes.

Liver and kidney tracer retention increased slightly over the time course, with liver [^{11}C]HED accumulation surpassing cardiac levels at 45 minutes post-tracer administration. Maximal liver tracer retention was 0.41±0.05 %ID/g*BW. Tracer presence in blood was consistently low, never exceeding 0.02 %ID/g*BW during the 90 minute timeframe. Low retention was also detected in white adipose tissue and skeletal muscle at 30 minutes. Tracer uptake in hypothalamus, brainstem, and cerebellum were negligible as [^{11}C]HED is impermeable to the blood brain barrier.

Due to consistently high uptake in tissues of interest, half-life of ^{11}C (20.4 min), and previously documented pharmacological studies at the 30 minute incubation time, this time point was selected for future work (Law et al., 1997; Rosenspire et al., 1990).

3.1.2 Blockade of Uptake-1

Pretreatment of rats with the NET-1 blocker desipramine elicited a marked reduction in

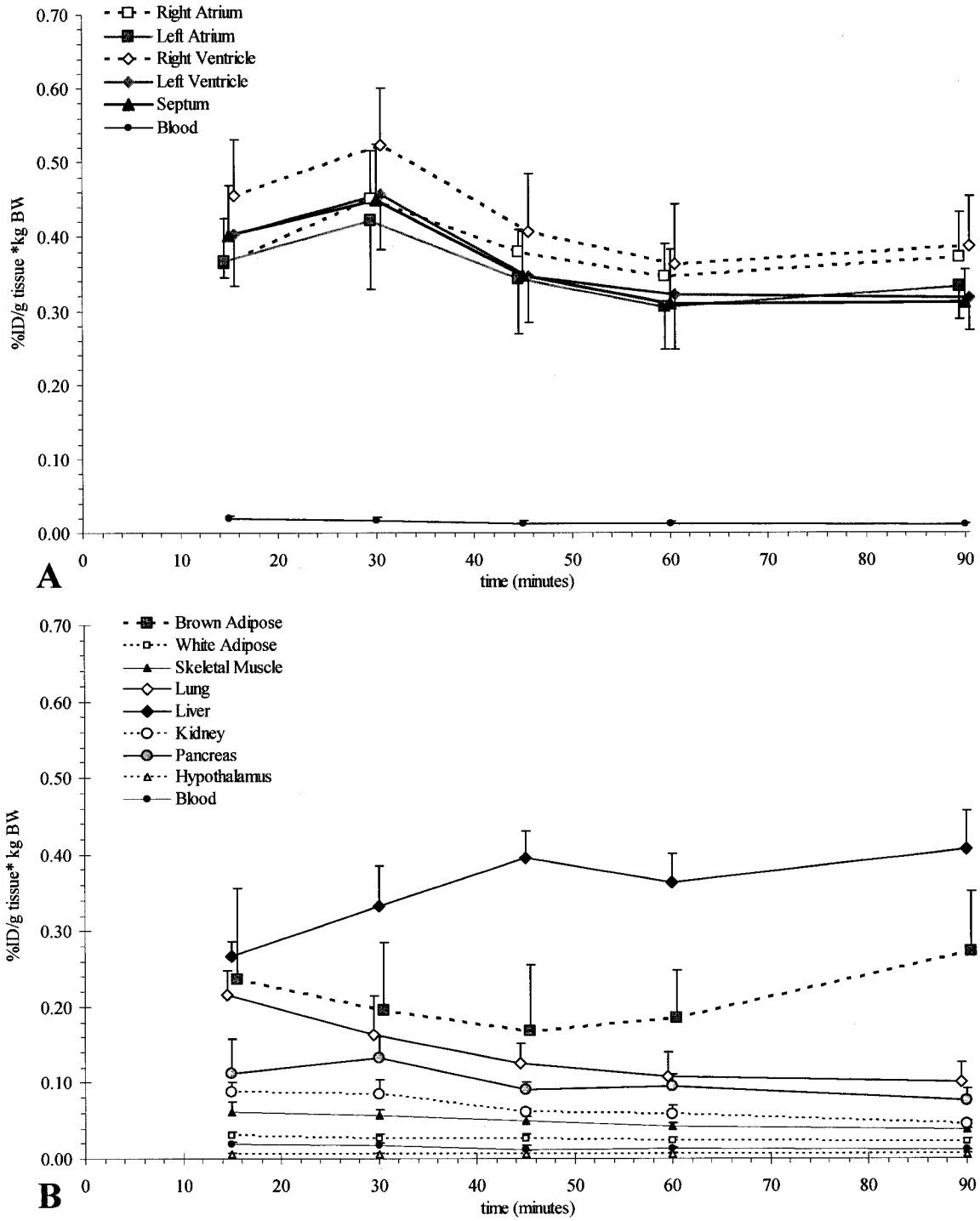

Figure 3.1: Time course evaluation of [^{11}C]HED in selected tissues. Panel **A** shows myocardial tracer accumulation at 15, 30, 45, 60, and 90 minutes post-tracer injection. Panel **B** describes tracer uptake in other peripheral tissues at these same time points.

retention of [^{11}C]HED in myocardium and select peripheral tissues (Figure 3.2). Total tracer accumulation was significantly reduced to 0.04-0.05 %ID/g*BW in myocardial tissues (Table 3.1). Additionally, total [^{11}C]HED retention was markedly reduced following desipramine treatment in brown adipose tissue, white adipose tissues, lung, and pancreas. Tracer accumulation was significantly increased in liver, kidney and blood. No change in total [^{11}C]HED retention was apparent in skeletal muscle. Similar results were observed following pretreatment with the comparable NET-1 inhibitor nisoxetine (Figure 3.2).

3.1.3 Direct Synaptic Competition for Reuptake

Administration of the precursor compound and NE analogue metaraminol significantly reduced myocardial retention of [^{11}C]HED to a level comparable to desipramine treatment (Figure 3.2, Table 3.1). Brown adipose tissue, lung, and pancreatic accumulation of [^{11}C]HED was also appreciably decreased compared to controls. Tracer accumulation in blood was slightly augmented, similar to NET-1 blockade. No change in [^{11}C]HED retention was apparent in liver, kidney, or skeletal muscle.

3.1.4 Blockade of Vesicular Storage

Inhibition of VMAT with reserpine produced a decrease in total [^{11}C]HED retention (Figure 3.3). Differential effects in atria and ventricles were apparent, as total tracer retention was reduced by approximately 50% more in ventricles than in atria, (Table 3.1). Moderate decreases in tracer accumulation (40-50%) were also observed in brown adipose tissue and pancreas, though the former did not reach statistical significance. [^{11}C]HED retention in liver was markedly increased by 41.8% increase compared to controls. No

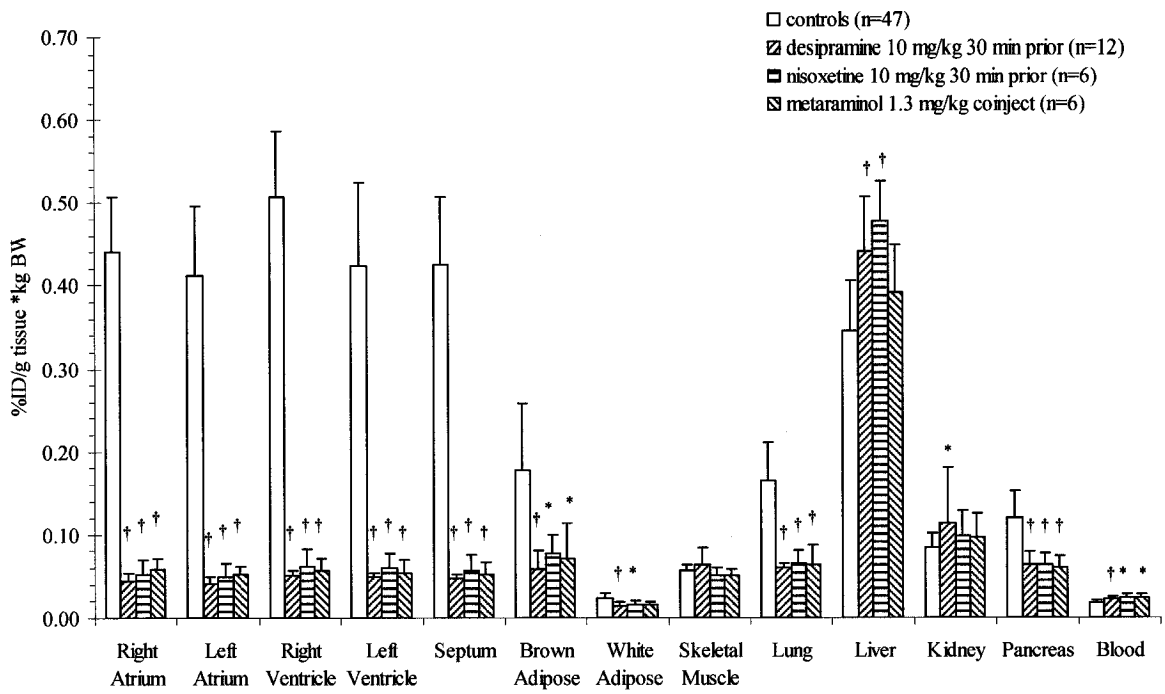

Figure 3.2: Effect of interference with normal uptake-1 function on the total retention of [^{11}C]HED in selected tissues. Blockade with desipramine (10 mg/kg) or nisoxetine (10 mg/kg) or increased synaptic competition with metaraminol (1.3 mg/kg). * $p<0.05$, † $p<0.0001$, one-way ANOVA with Bonferroni post hoc compared to controls.

Table 3.1: Change in total [^{11}C]HED retention in selected tissues following various pharmacological treatments.

Treatment	*percent change in total [^{11}C]HED retention to controls*					
	Left Ventricle	Brown Adipose	Pancreas	Lung	Skeletal Muscle	Blood
Desipramine 10 mg/kg 30 min prior	-89±11	-67±25	-47±12	-64±7	+12±4	+31±5
Nisoxetine 10 mg/kg 30 min prior	-86±27	-56±16	-48±12	-60±14	-12±2	+36±8
Metaraminol 1.3 mg/kg Coinjection	-87±26	-60±36	-50±11	-62±23	-11±2	+36±9
Reserpine 5 mg/kg 24 h prior	-74±5	-40±16	-49±5	-3.5±0.7	-10±1	-2.5±0.4

Percent change to controls is calculated as (treated-controls)/controls*100%.
Statistical significance of these results is indicated in figures only, as the values obtained here are indirect calculations not result values.

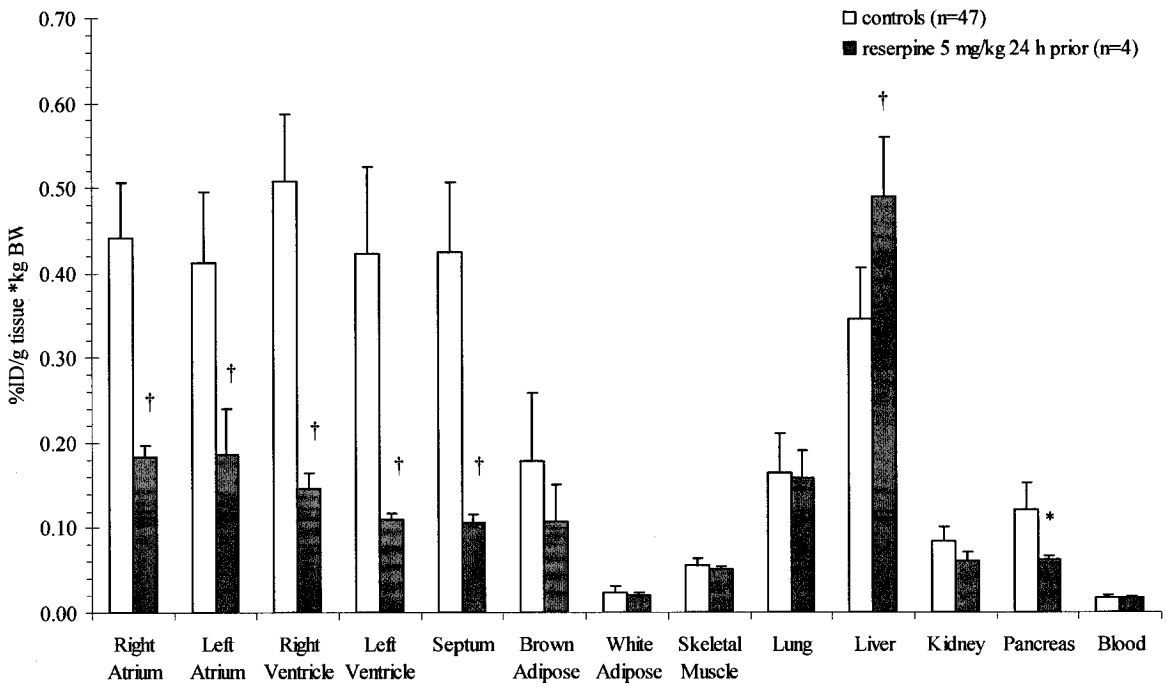

Figure 3.3: Effect of vesicular blockade on total [^{11}C]HED retention. Biodistribution following reserpine (5 mg/kg 24 h prior) pretreatment. * $p<0.001$, † $p<0.0001$, one-way ANOVA with Bonferroni post hoc compared to controls.

significant change in tracer retention was detected in white adipose tissue, lung, kidney, skeletal muscle, or blood.

3.1.5 Competition with Endogenous Norepinephrine

3.1.5.1 Acute Effects

Acute elevation of synaptic NE using tranylcypromine evoked a dose-dependent reduction of total [^{11}C]HED accumulation in tissues that exhibit uptake-1-specific retention (Figure 3.4 Table 3.2). In left ventricle, tracer retention was reduced by 29-82% to controls following treatments of 0.5-10.0 mg/kg of tranylcypromine. All myocardial regions exhibited a similar dose-response to elevated synaptic NE. This inverse relationship was also apparent in NET-1-rich regions such as brown adipose tissue, white adipose tissue, lung, and pancreas.

A dose-dependent increase in tracer retention was observed in liver tissue, with a maximal accumulation of 0.48±0.06 %ID/g*BW at 10.0 mg/kg tranylcypromine. No significant changes in [^{11}C]HED uptake were detected in kidney or skeletal muscle. A minor increase in blood retention was observed at the highest dose.

3.1.5.2 Subchronic Effects

The effect of subchronic administration of tranylcypromine on total [^{11}C]HED accumulation was localized primarily at the ventricular myocardium (Figure 3.5). Right and left ventricular free wall and intraventricular septum [^{11}C]HED retention was reduced by 18-26% compared to vehicle-treated controls. No significant changes in total tracer accumulation were detected in atria or other peripheral tissues.

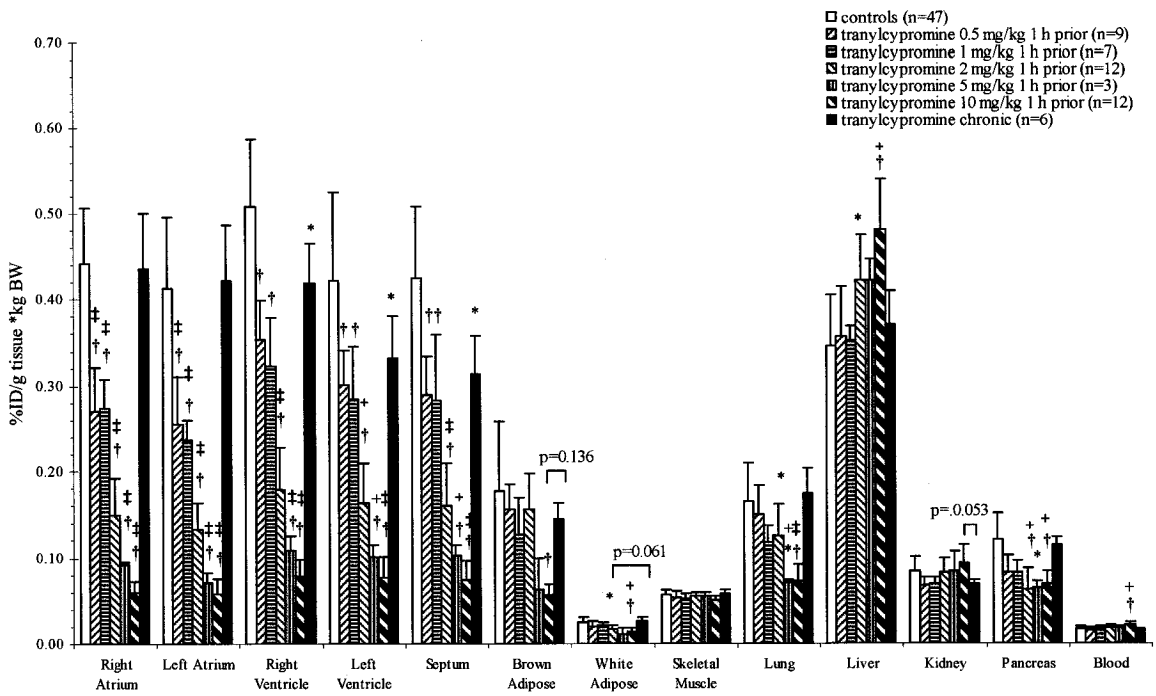

Figure 3.4: Effect of acutely elevated synaptic norepinephrine on total [^{11}C]HED retention via monoamine oxidase inhibition with tranylcypromine (0.5-10 mg/kg 1 h prior). Acute treatment is compared to subchronic treatment (7.5 mg/kg/day*7 days, 10 mg/kg/day*7 days, 24 h washout). * $p<0.05$, † $p<0.0001$, one-way ANOVA with Bonferroni post hoc compared to controls. + $p<0.05$, ‡ $p<0.0001$, one-way ANOVA with Bonferroni post hoc compared to chronic tranylcypromine treatment.

Table 3.2: Change in total [^{11}C]HED retention in selected tissues following various doses of tranylcypromine.

Dose	*percent change in total [^{11}C]HED retention to controls*					
	Left Ventricle	Brown Adipose	Pancreas	Lung	Skeletal Muscle	Blood
0.5 mg/kg	-29±4	-13±2	-31±7	-9±2	-5±0.6	-7±1
1.0 mg/kg	-33±7	-28±9	-32±5	-28±5	-9±1	-4±0.6
2.0 mg/kg	-31±17	-13±3	-48±19	-24±7	-2±0.1	+6±1
5.0 mg/kg	-76±11	-64±37	-46±5	-57±3	-4±0.4	+8±0.5
10.0 mg/kg	-82±27	-68±16	-43±9	-56±15	-12±1	+27±4
Subchronic	-22±3	-18±2	-5±0.4	+6±1	+3±0.3	-4±0.3

Subchronic treatment was 7.5mg/kg/day*7 days, 10 mg/kg/day*7 days with 24 hour washout period.
Percent change to controls is calculated as (treated-controls)/controls*100%.
Statistical significance of these results is indicated in figures only, as the values obtained here are indirect calculations not result values.

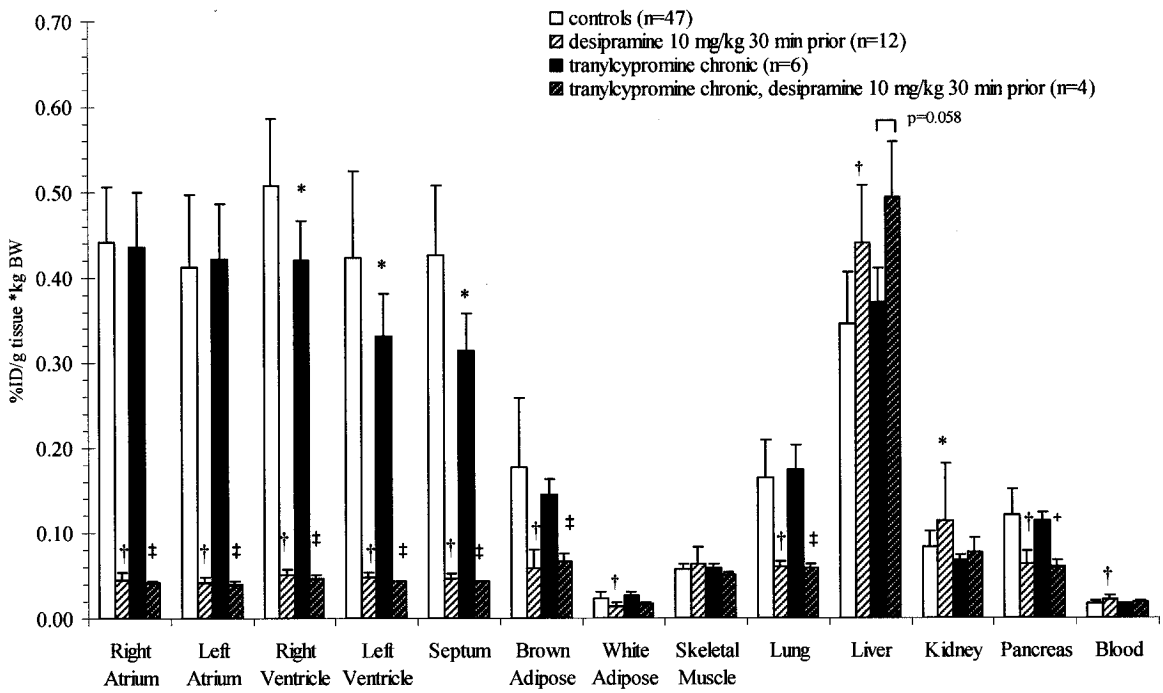

Figure 3.5: Effect of chronically elevated synaptic norepinephrine on total and non-specific retention of [^{11}C]HED via monoamine oxidase inhibition with tranylcypromine. Shown here, subchronic administration of tranylcypromine (7.5 mg/kg/day*7 days, 10 mg/kg/day*7 days, 24 h washout) with and without acute pretreatment with desipramine (10 mg/kg) to delineate non-uptake-1 specific retention. * $p<0.05$, † $p<0.0001$, one-way ANOVA with Bonferroni post hoc compared to controls. + $p<0.05$, ‡ $p<0.0001$, one-way ANOVA with Bonferroni post hoc compared to chronic tranylcypromine treatment.

Alterations in uptake-1 specific [^{11}C]HED retention were calculated by acute administration of desipramine in subchronically tranylcypromine-treated rats (Table 3.3). Desipramine pretreatment reduced total cardiac [^{11}C]HED retention by 86.4-90.4% versus subchronic tranylcypromine alone. Uptake-1 specific [^{11}C]HED retention was significantly reduced by 18.4-28.2% in ventricular tissues compared to untreated controls. Decreases in tracer accumulation were also detected in brown adipose tissue (-33.9) and pancreas (-3.8), but these reductions were not statistically significant in total tracer retention.

Tracer uptake in subchronically-treated animals significantly differed from most acute doses in myocardium (Figure 3.4), and from high acute doses in white adipose tissue, lung, liver, pancreas and blood.

3.1.6 Alpha Adrenoceptor Agonism and Antagonism

3.1.6.1 Acute Agonism

Administration of clonidine at 0.05 to 1.0 mg/kg elicited a varied response in total [^{11}C]HED retention in myocardium and peripheral tissues (Figure 3.6). In myocardium, total tracer accumulation following low dose (0.05 mg/kg) clonidine was significantly reduced by 17-35% in atria and right ventricle; no change was observed in left ventricle or intraventricular septum. A marked increase of 82% in tracer accumulation was elicited in kidney. No change in [^{11}C]HED retention was detected in other peripheral tissues following treatment with 0.05 mg/kg clonidine hydrochloride.

At moderate dose (0.5 mg/kg), a trend of increased total tracer accumulation was seen in right and left ventricle, intraventricular septum, brown adipose tissue, lung, and kidney. Increases ranged from modest (+2.4% in right ventricle) to marked (+91.2% in kidney). Left ventricular tracer retention was elevated to 0.49 %ID/g*BW, an increase of 15.8% to

Table 3.3: Change in uptake-1 specific retention of [^{11}C]HED following 14 days of treatment with tranylcypromine.

	percent change in uptake-1 specific [^{11}C]HED retention to controls						
	Right Atrium	Left Atrium	Right Ventricle	Left Ventricle	Septum	Brown Adipose	Pancreas
Tranylcypromine 7.5mg/kg/d*7, 10 mg/kg/d*7	-0.7	+2.7	-18.4	-22.8	-28.2	-33.9	-61.4

Uptake-1 specific retention is defined as total retention - non-specific retention.
Percent change is calculated as $(SR_{treated} - SR_{control})/SR_{control}$ *100%, where SR= specific retention.
Statistical significance of these results is indicated in figures only, as the values obtained here are indirect calculations not result values.

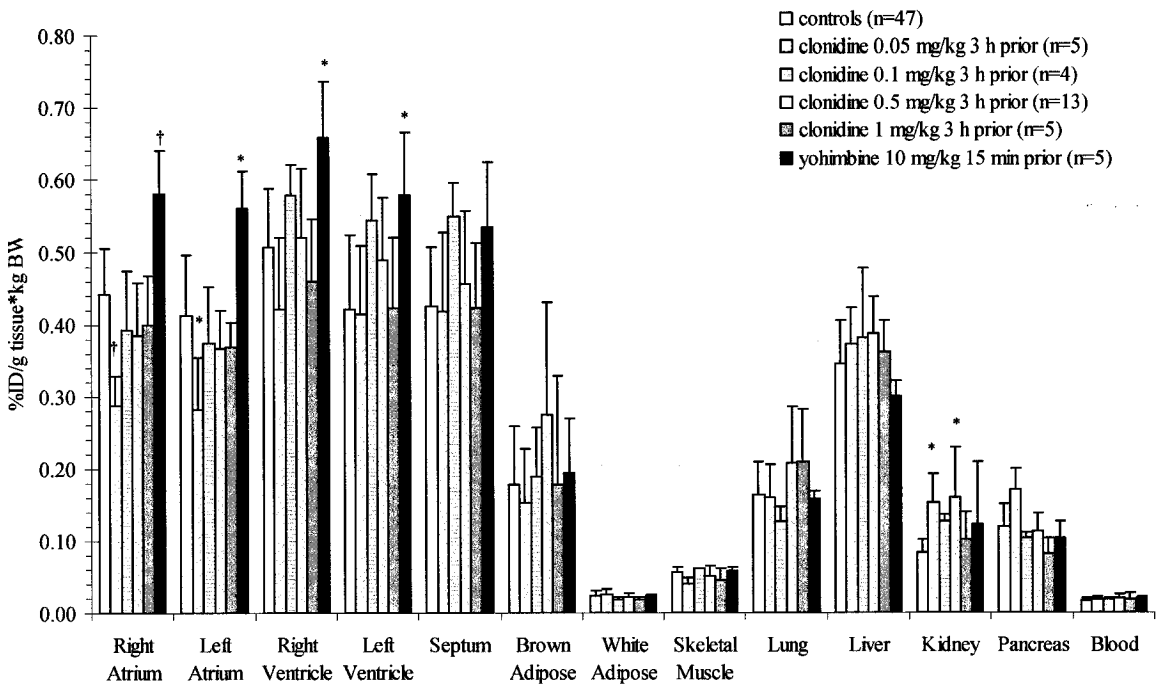

Figure 3.6: Effect of acute modulation of alpha-2 adrenoceptors with the agonist clonidine and the antagonist yohimbine on total [^{11}C]HED retention. Acute pretreatment with clonidine (0.05-1.0 mg/kg, 3 h prior) and yohimbine (10 mg/kg 15 min prior). * $p<0.05$, † $p<0.0001$, one-way ANOVA with Bonferroni post hoc.

controls, but this increase was not statistically significant. The increase in brown adipose tissue tracer uptake was relatively high, though quite varied at +53.8±30.9% as compared to untreated controls.

High dose clonidine (1.0 mg/kg) elicited no clear change in myocardial [^{11}C]HED retention. Only pancreas showed a slight reduction of 31.7% to controls (p=0.133).

3.1.6.2 Acute Antagonism

Yohimbine had a marked effect on myocardial retention of [^{11}C]HED, but did not significantly affect total tracer accumulation in periphery (Figure 3.6). A significant increase in tracer retention was apparent throughout myocardium, elevating cardiac distribution by 25.8-36.8%. Tracer accumulation in brown adipose tissue, white adipose tissue, skeletal muscle, lung, liver, kidney, pancreas, and blood was unchanged compared to untreated controls.

3.2 Obesity

3.2.1 Effect of Diet

A study was conducted to determine the effect of divergent diets on [^{11}C]HED kinetics and distribution. There were no significant differences in total tracer retention between chow diet, high fat diet, or the comparable control diet (Figure 3.7A). Animals fed the comparable control diet showed a modest decrease in tracer distribution to ventricular tissues: 8.8-19.9% reduction compared to chow diet, but this reduction was not statistically significant.

The effect of fasting rats overnight prior to the biodistribution study was also examined (Figure 3.7B). Fasting appears to have minimal impact on total tracer retention, with a

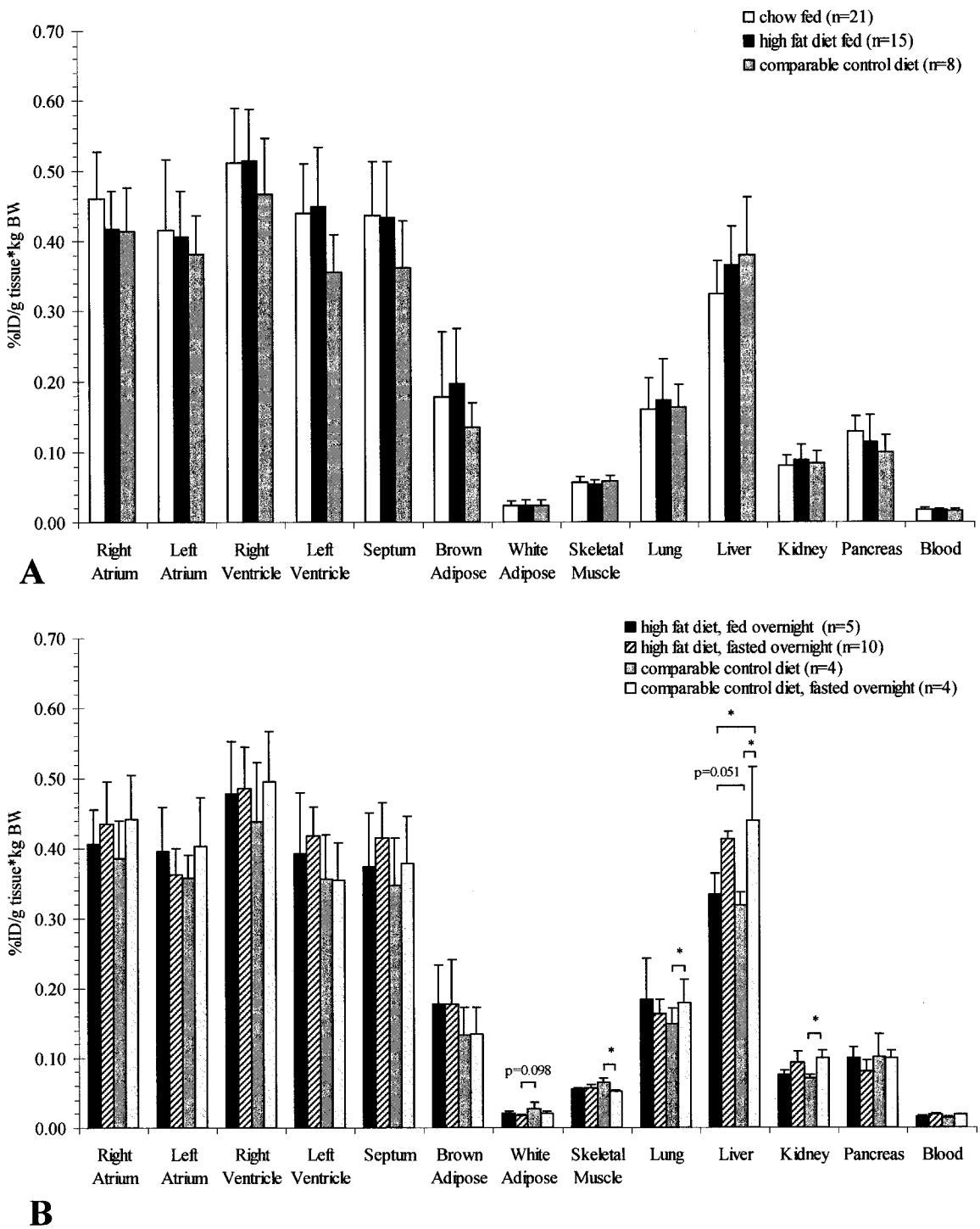

Figure 3.7: Comparison of the effects of standard chow, high fat diet (Research Diets), and comparable control diet on total [^{11}C]HED retention (**A**) and the effect of fasting rats prior to tracer injection (**B**). * $p<0.05$, one-way ANOVA with Bonferroni post hoc.

greater effect in comparable control diet compared to high fat diet. Increased tracer retention was apparent in the liver and kidney of rats fasted overnight compared to rats fed overnight. A significant increase in [^{11}C]HED retention was observed in lung, as was a reduction in skeletal muscle on comparable control diet. Importantly, no changes in total tracer accumulation were observed in tissues of interest, specifically myocardium, brown adipose tissue, and pancreas.

3.2.2 Animal Characteristics

3.2.2.1 Weights and Weight Gain Profiles

On arrival at 5 weeks of age, there was no noticeable difference in weights between DIO DR rats (134±15 and 129±11 g, respectively). A significant difference in weight gain profiles was appreciable within the first 7 days of high fat diet consumption (Figure 3.8A). The divergence of the two strains increases consistently during the first 8 weeks of high fat diet. At day 56, the difference in weight gain begins to stabilize, though cumulative weight gain remains significantly different up to 17 weeks on high fat diet.

Weekly weight gain for DIO, DR, and control Sprague-Dawley rats is detailed in Table 3.4. Weight gain over 119 days in Sprague-Dawley rats is currently being investigated.*

3.2.2.2 Food Intake

Food intake in DIO and DR rats is relatively similar throughout the 119 day protocol (Figure 3.8B). When food intake is considered as a percentage of body weight, there is no statistically significant deviation between the two strains eating habits.

During the initial weeks, DIO rats consumed 11.9±0.7% of their body weight in high fat diet, compared to 11.1±0.4% for DR rats. As the animals grow, the percentage of body

* Experiment scheduled for October 2006.

Table 3.4: Weights of DIO, DR, and Sprague-Dawley rats at various time points.

Group	*weights at various age points (grams)*					
	Arrival	Endpoint A	T_{28}	Endpoint B	T_{84}	Endpoint C
	T_0	T_{14}		T_{56}		T_{119}
Controls	174±5	224±27	305±37	405±37	N/A	N/A
DIO	134±15	241±21	322±36	449±54	536±39	594±35
DR	129±11	224±14	290±15	389±23	469±40	522±57

Feeding of high fat diet commences upon arrival (T_0).
Endpoints A (short-term, 14 days), B (intermediate term, 56 days), and C (long term, 119 days) indicate times of biodistribution and sacrifice.

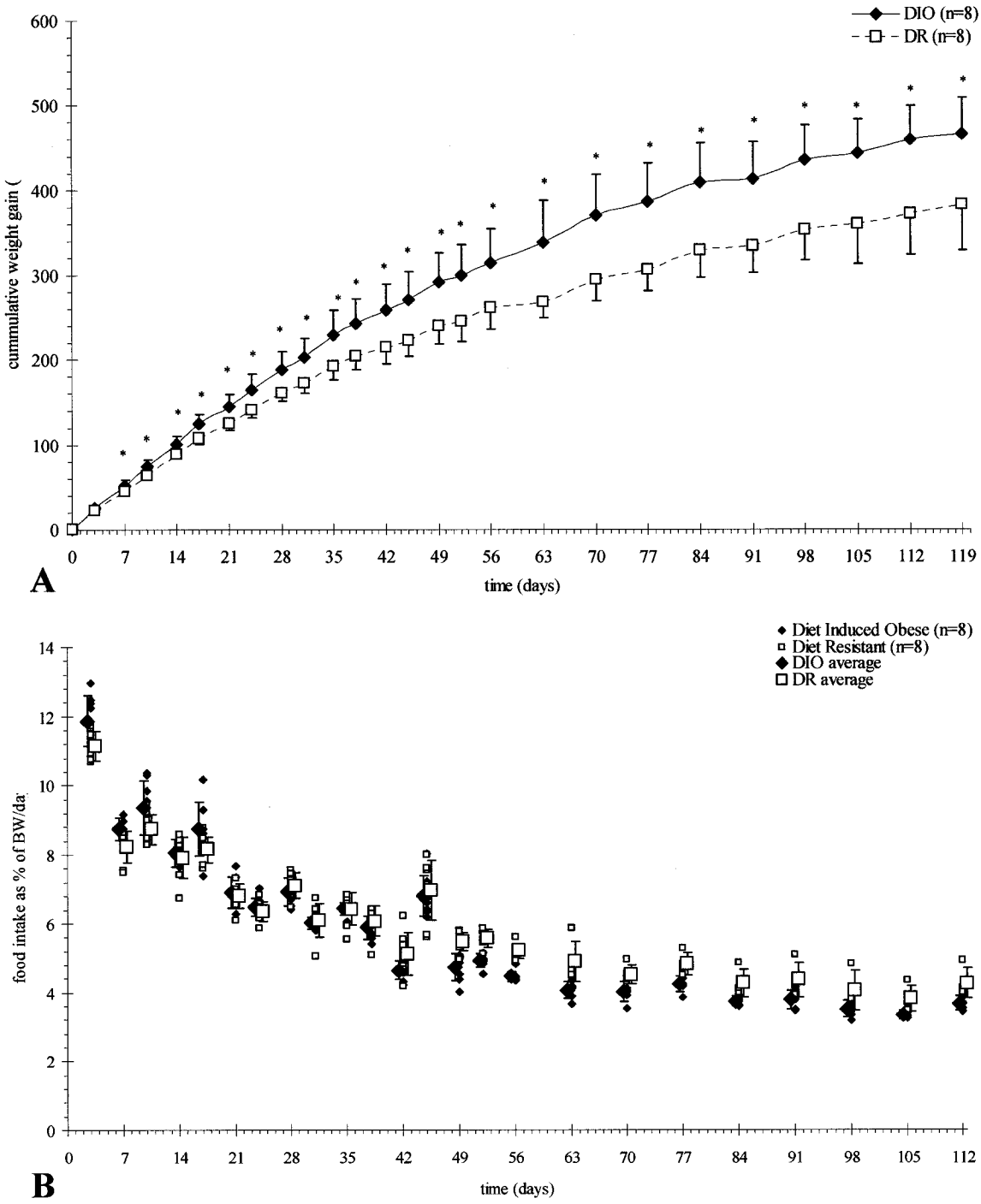

Figure 3.8: Weight gain (**A**) and food intake (**B**) of diet induced obese, diet resistant and Sprague-Dawley rats over an eight week period. Cumulative weight gain is calculated to start of high fat diet consumption. Food intake is presented as a percentage of body weight. * $p<0.05$, two-tailed T-test.

weight consumed is drastically reduced, following a hyperbolic curve to an asymptote at approximately 4% of body weight. At day 14, DIO and DR rats consumed 8.1±0.4% and 7.9±0.6% of body weight, respectively. By the sixth week on high fat diet, DR rats tended to have slightly increased food consumption as compared to DIO animals, a pattern that remained consistent for the remainder of the experimental time frame. The percentages were relatively similar, however, as seen at 56 days (4.5±0.1 and 5.2±0.2) and 112 days (3.7±0.2 and 4.3±0.5). As such, the differences in weight gain between DIO and DR rats are not merely a result of increased food consumption in the former.

3.2.2.3 Insulin Levels

Measurement of plasma insulin was completed in a sample group of DIO, DR and normal Sprague-Dawley rats at 14 and 56 days. Variability of fasting insulin levels was high for each sample. No clear deviation in plasma insulin concentration was detected between DIO and DR after 14 days of high fat diet consumption (0.28±0.18 and 0.33±0.16 ng/mL). Insulin levels were greatly increased after 56 days of high fat diet consumption in normal and DIO, and to a lesser extent in DR (1.19±0.69, 1.49±0.82, and 0.63±0.38 ng/mL, respectively). Insulin levels of individual rats are shown in Table 3.5.

3.2.3 Biodistribution of [^{11}C]HED in DIO and DR Rats

3.2.3.1 Short Term (14 Days)

At 14 days of high fat diet consumption, there is no significant change in [^{11}C]HED retention between DIO, DR, and control Sprague-Dawley rats (Figure 3.9A). Myocardial tracer accumulation was relatively unchanged in DIO and slightly but not significantly reduced in DR (-22.5% in left ventricle) versus controls.

Brown adipose tissue uptake of [^{11}C]HED is slightly greater in DR rats as compared to DIO

Table 3.5: Fasting plasma insulin in DIO, DR, and Sprague-Dawley control rats at 14 and 56 days following high fat diet consumption.

Group	*plasma insulin (ng/mL)*
CTL, 14 days (n=7)	0.57±0.31
DIO, 14 days (n=8)	0.24±0.15
DR, 14 days (n=8)	0.28±0.14
CTL, 56 days (n=10)	1.51±0.92
DIO, 56 days (n=4)	1.49±0.82
DR, 56 days (n=5)	0.62±0.38

Average fasting insulin levels ± standard deviations in rats following biodistribution experiments.
No significant variance was found using two-tailed T-test.

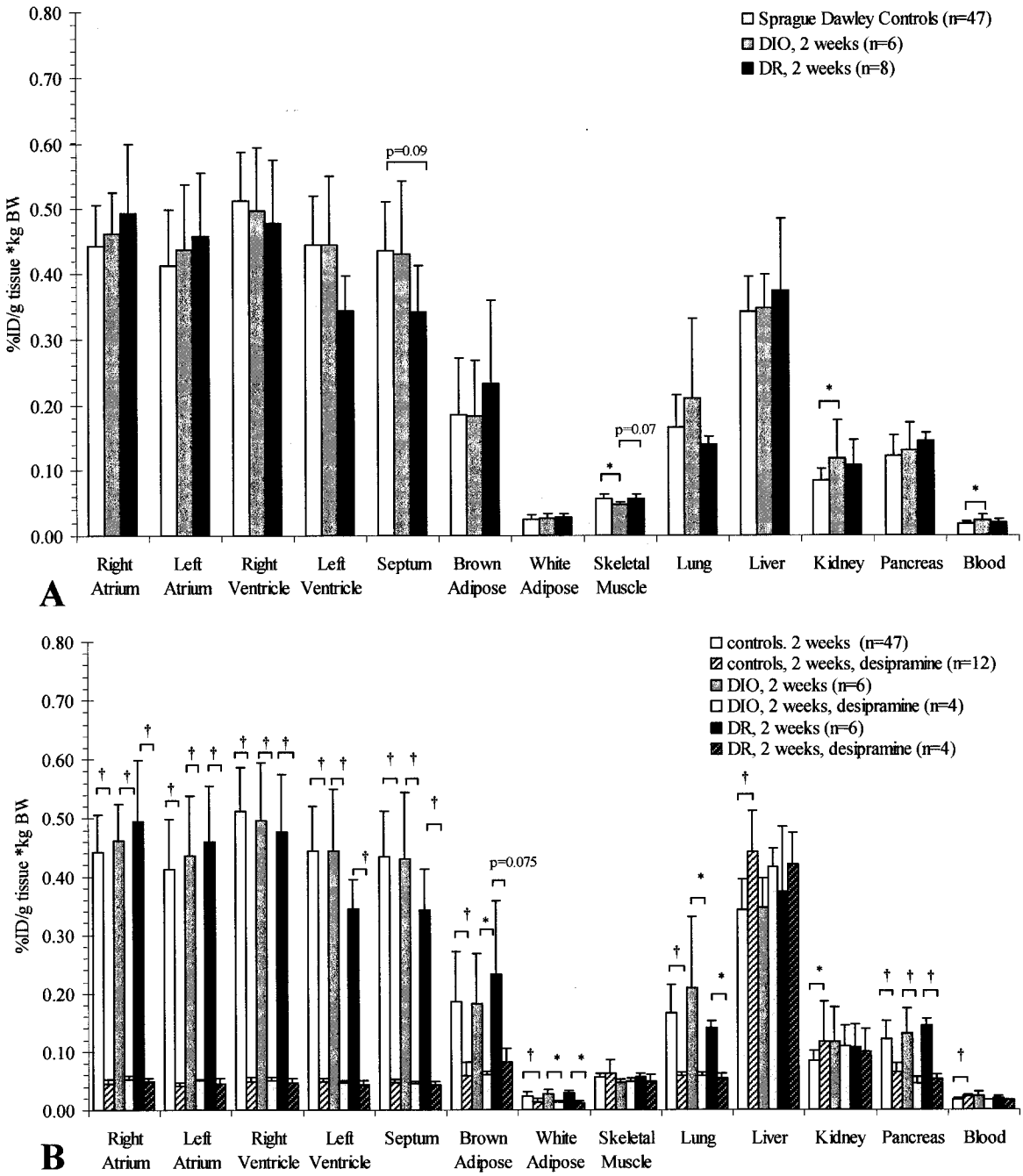

Figure 3.9: Biodistribution of [^{11}C]HED in diet-induced obese, diet resistant rats, and Sprague-Dawley rats two weeks after commencing high fat diet (**A**). Pretreatment with desipramine (10 mg/kg 30 min prior) is used to delineate changes in uptake-1 specific retention (**B**). * $p<0.05$, † $p<0.0001$, one-way ANOVA with Bonferroni post hoc, as indicated.

and Sprague-Dawley rats, but does not reach statistical significance. Pancreatic tracer accumulation was similar between all three rat strains. There was a significant increase in tracer retention in kidney and blood of DIO rats as compared to Sprague-Dawley controls. Pretreatment of DIO and DR rats with desipramine showed no changes in non-specific [^{11}C]HED accumulation (Figure 3.9B). Blocked retention values in myocardium were comparable in DIO and DR rats (0.04-0.05 %ID/g*BW, all tissues). Variation in uptake-1 specific [^{11}C]HED retention among strains were directly comparable to alterations in total tracer accumulation (Table 3.6, 3.7).

3.2.3.2 Intermediate Term (56 Days)

By 56 days, a significant variation in tracer distribution was apparent between DIO and DR rats, with normal Sprague-Dawley rats exhibiting retention levels at an intermediate level between the two substrains (Figure 3.10A). While no change in [^{11}C]HED retention was observed in atrial tissues, ventricles displayed a tendency for increased tracer accumulation in DIO and decreased accumulation in DR compared to controls (Table 3.6, 3.7).

Conversely, tracer accumulation was significantly decreased in DIO and non-signficantly increased in DR compared to Sprague-Dawley controls in brown adipose tissue. A similar reduction in DIO total tracer retention appears in skeletal muscle. There was no difference in [^{11}C]HED accumulation in white adipose tissue, liver, kidney, pancreas, or blood between the three strains.

Similar to 14 day data, non-specific [^{11}C]HED retention is unchanged in DIO, DR, and Sprague-Dawley normal rats pretreated with desipramine (Figure 3.10B). NET-1 blockade results in slightly higher non-specific retention than seen at 14 days, but the reduction in tracer retention remains consistently high (85-95% in myocardium) and highly significant. Differences in uptake-1 specific binding are shown in Tables 3.6 and 3.7.

Table 3.6: Difference in uptake-1 specific retention of [^{11}C]HED in DIO and DR rats at 2 and 8 weeks after initiation of high fat diet compared to age-matched Sprague-Dawley controls.

Group	*% change in uptake-1 specific [^{11}C]HED retention to age-matched controls*						
	Right Atrium	Left Atrium	Right Ventricle	Left Ventricle	Septum	Brown Adipose	Pancreas
DIO, 2 weeks	+2.5	+3.9	-3.5	+0.3	-0.6	-4.7	+49.2
DR, 2 weeks	+11.8	+11.5	-6.9	-24.1	-22.8	+18.4	+60.2
DIO, 8 weeks	+3.5	+8.6	+7.0	+21.2	+25.0	-85.1	+45.9
DR, 8 weeks	-2.4	-10.2	-22.6	-17.0	-16.0	-7.6	-7.4

Uptake-1 specific retention is defined as total retention – non-specific retention (pretreated with desipramine 10 mg/kg 30 min prior).

Percent change is calculated as $(SR_{(DIO \text{ or } DR)} - SR_{SD})/SR_{SD} * 100\%$, where SR=specific retention

Statistical significance of these results is indicated in figures only, as the values obtained here are indirect calculations not result values.

Table 3.7: Percent difference in uptake-1 specific retention of [^{11}C]HED in DIO versus DR at 2, 8, and 17 weeks after initiation of high fat diet.

Age Group	*% difference in uptake-1 specific [^{11}C]HED retention between DIO vs. DR*						
	Right Atrium	Left Atrium	Right Ventricle	Left Ventricle	Septum	Brown Adipose	Pancreas
2 weeks	-8.3	-6.8	+3.7	+32.1	+28.6	-19.5	-6.8
8 weeks	+6.1	+21.0	+38.3	+46.1	+48.9	-83.9	+57.6
17 weeks	+26.5	+34.4	+49.6	+77.5	+64.3	-61.1	+59.8

Uptake-1 specific retention is defined as total retention – non-specific retention (pretreated with desipramine 10 mg/kg 30 min prior).
Percent difference is calculated as $(SR_{DIO} - SR_{DR})/SR_{DR} *100\%$, where SR=specific retention. Positive values indicate higher retention in DIO than DR; negative values indicate lower retention in DIO than DR.
Statistical significance of these results is indicated in figures only, as the values obtained here are indirect calculations not result values.

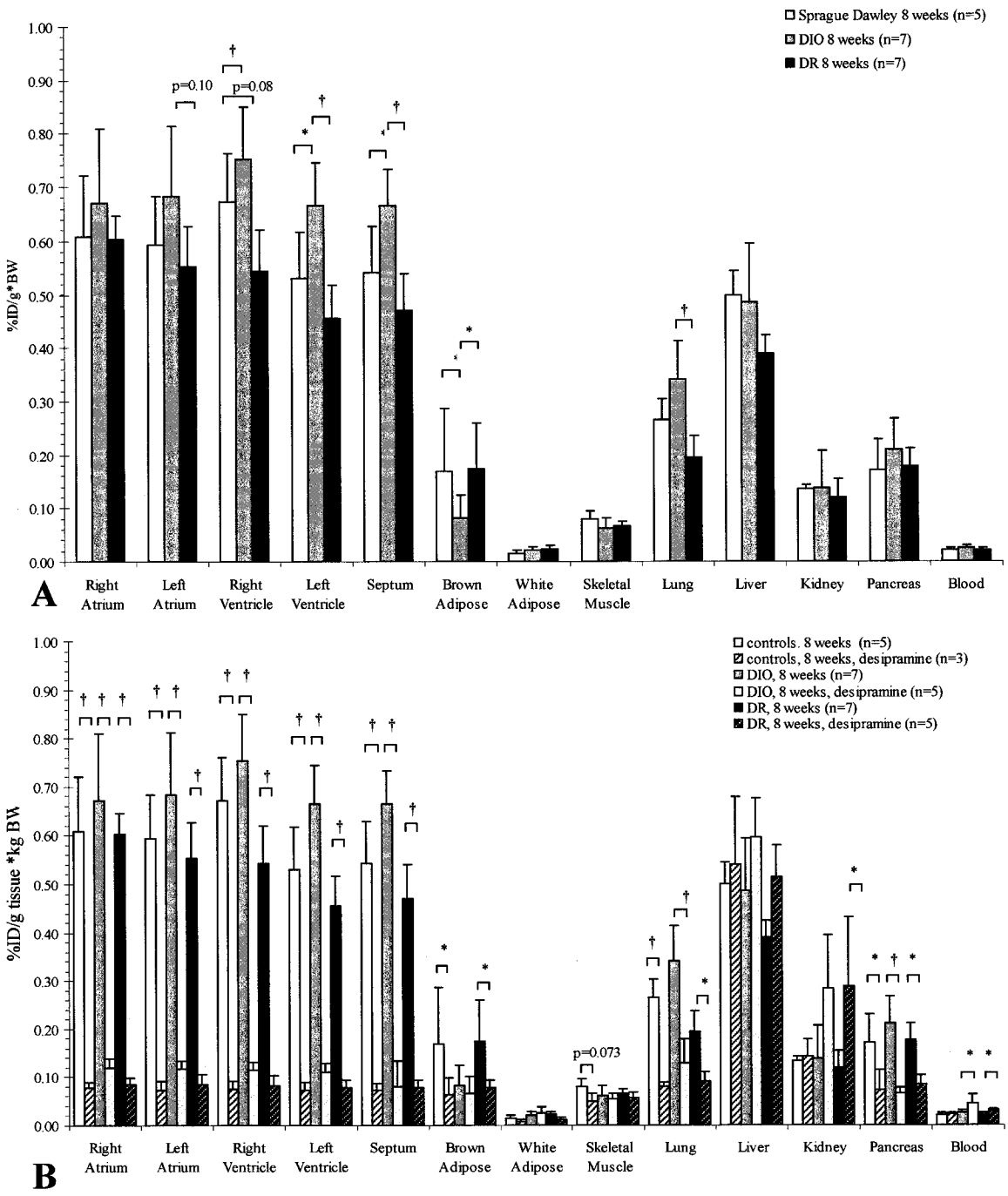

Figure 3.10: Biodistribution of [^{11}C]HED in diet-induced obese, diet resistant rats, and Sprague-Dawley rats eight weeks after commencing high fat diet (**A**). Pretreatment with desipramine (10 mg/kg 30 min prior) is used to delineate changes in uptake-1 specific retention (**B**). * $p<0.05$, † $p<0.0001$, one-way ANOVA with Bonferroni post hoc, as indicated..

3.2.3.3 Long Term (119 Days)

The deviation in biodistribution of [^{11}C]HED widens at 119 days on high fat diet (Figure 3.11). There is significant difference in myocardial tracer accumulation between DIO and DR ventricles and a differential trend in atria. Lung retention continues to follow the same pattern as myocardium, as does pancreatic [^{11}C]HED uptake, though the elevation in DIO pancreata is not statistically significant to DR.

Brown adipose tissue tracer retention is comparable to levels observed at the intermediate time point. No differences were detected in brown adipose tissue, white adipose tissue, skeletal muscle, liver, kidney, or blood. Differences in tracer retention in tissues of interest between DIO and DR rats are described in Table 3.7.

A single DIO rat was pretreated with desipramine, showing clear blockage of tracer uptake as seen at other time points (data not shown). Uptake-1 specific retention data will be completed in the immediate future.* As mentioned above, no Sprague-Dawley normals have been maintained for the full 119 days on high fat diet. However, tracer distribution is expected to fall between DIO and DR levels, as seen at the 56 day time point.

3.3 Diabetes Mellitus

3.3.1 Animal Characteristics

3.3.1.1 High Dose Streptozocin

Immediately following intravenous injection of streptozocin (65 mg/kg, iv), animals exhibited a lack of weight gain over the two week evaluation period (Figure 3.12). Initial weights of streptozocin-treated and control rats were 195±9 and 200±13 g, respectively. One day after streptozocin treatment, type I diabetic animals lost an average of 10.5±0.4%

* Experiment scheduled for October 2006.

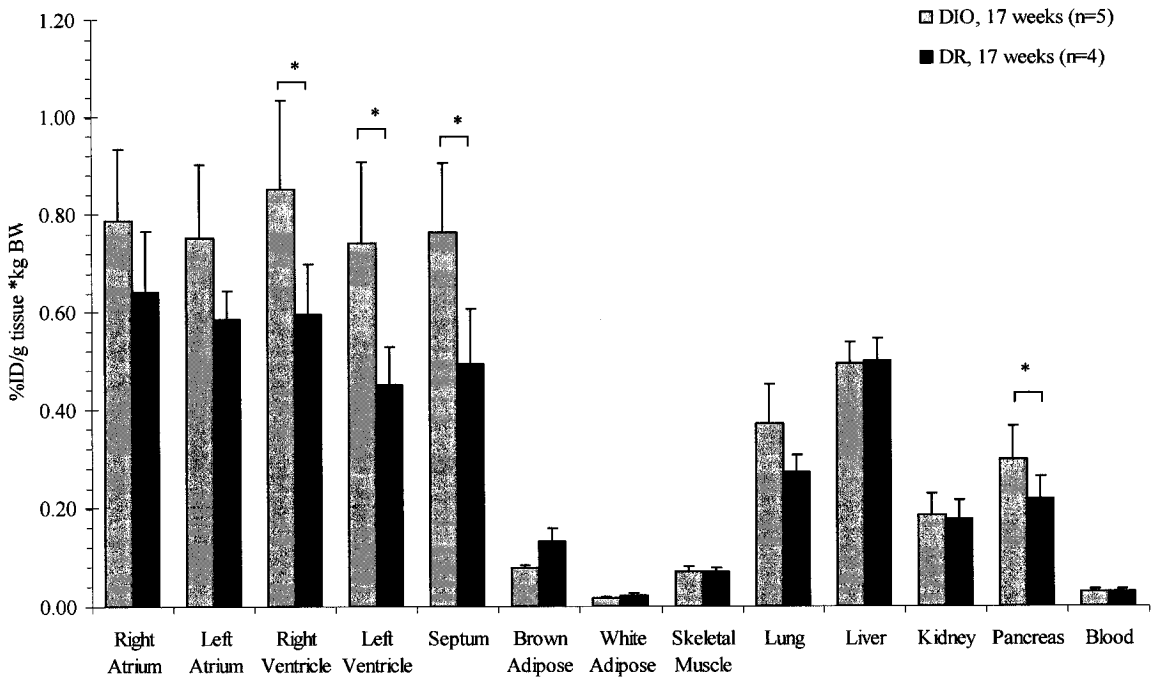

Figure 3.11: Biodistribution of [^{11}C]HED in diet-induced obese and diet resistant rats, seventeen weeks after commencing high fat diet. * $p<0.05$, † $p<0.0001$, one-way ANOVA with Bonferroni post hoc, comparisons indicated.

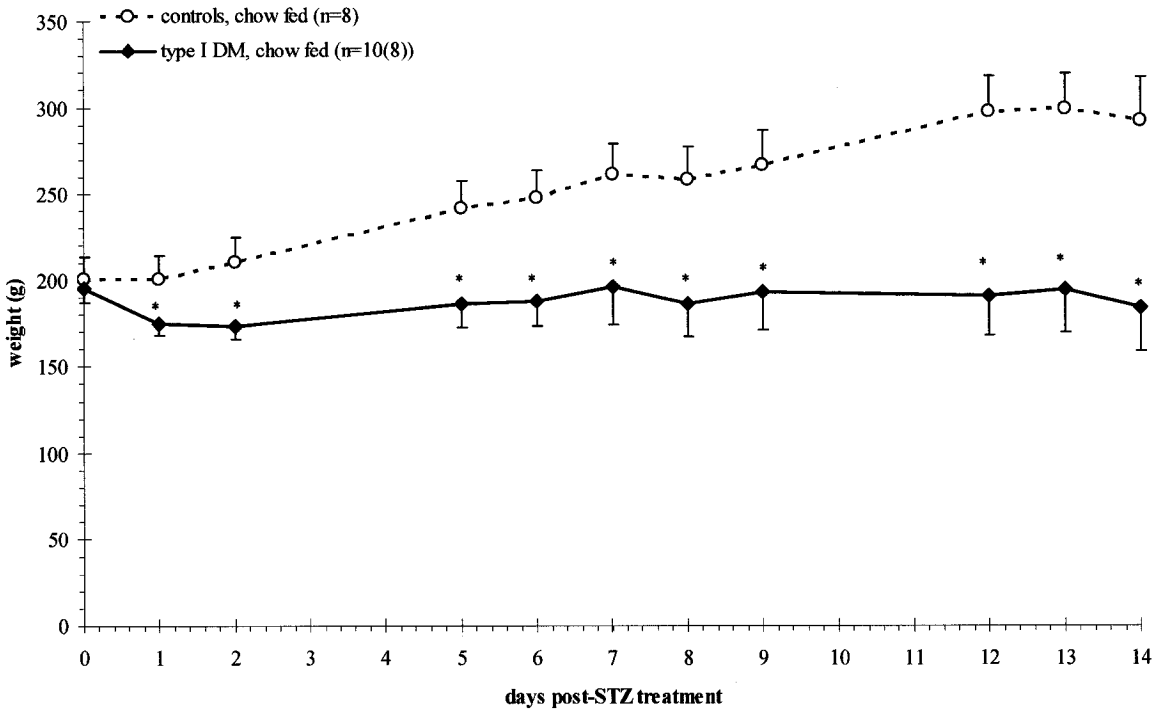

Figure 3.12: Comparison of weight following induction of type I diabetes mellitus compared to vehicle treated controls. * $p < 0.05$ two-tailed T-test, compared to controls.

of total body weight. By the second day post-injection, diabetic animals had stabilized, but never again gained weight during the experimental protocol. Comparatively, control animals gained an average of 98±14 g over the same time course.

Blood glucose concentrations were markedly elevated in type I diabetic animals (Table 3.8). Fasting blood glucose was taken following the experiment, and remained elevated.

There was a 20% mortality rate in type I DM group, partially owing to dehydration due to polydipsia and polyuria. Comparable mortality has been reported (Szkudelski, 2001). After the fourth day, all animals in the experimental group were injected with a subcutaneous bolus of saline to prevent further mortality, an intervention that was successful in preventing further deaths.

3.3.1.2 Moderate Dose Streptozocin

Intraperitoneal injection of 45 mg/kg streptozocin had a less dramatic effect on weight gain patterns in treated animals compared to controls (Figure 3.13). Immediately following streptozocin injection, rats that became hyperglycaemic exhibited a slight and transient stunting of weight gain as compared to controls. Treated animals that maintained normal blood glucose levels did not show altered weight gain patterns. The differences in weight gain between hyperglycaemic, streptozocin-treated, euglycaemic, streptozocin-treated and tribasic citrate treated controls were not remarkable in the short term (185±27, 214±20, 224±23 g, respectively). The difference in weight gain was more pronounced at later time points (278±37, 378±33, and 405±34 g, at 56 days, respectively).

Blood glucose levels of streptozocin-treated animals showed a bifurcation immediately following treatment (Figure 3.14). Of 36 total treated animals, 18 elicited clear elevations in blood glucose concentration at 7 days post-injection. The remaining 18 treated animals

Table 3.8: Blood glucose levels of type I and II diabetic rats at various time points.

Group	*blood glucose level (mmol/L)*					
	Pre high fat diet T_{-14}[a]	Baseline T_0[a]	Interval T_7[a]	Endpoint A T_{14}[b]	Interval T_{28}[a]	Endpoint B T_{56}[c]
Controls	6.3±0.5	6.5±1.2	6.1±0.6	3.7±1.6	6.3±0.6	6.1±0.9
Type I diabetic	N/A	6.1±1.0	25.1±4.2	16.9±4.6	N/A	N/A
Type II diabetic, total	6.2±0.5	6.3±0.6	17.8±6.9	4.9±2.5	13.2±7.3	15.1±10.3
Type II diabetic, hyperglycaemic	6.3±0.4	6.2±0.5	21.5±5.1	6.5±2.3	19.2±5.4	23.6±8.2
Type II diabetic, euglycaemic	6.1±0.2	6.4±0.7	11.8±5.0	3.0±0.3	7.2±1.3	6.7±1.1

High fat diet initiated at T_{-14} and streptozocin injection at T_0.
Endpoints A and B represent biodistribution and sacrifice times (14 and 56 days).

a. at -14, 0, 7, 28, and 56 days, blood glucose was obtained without fasting
b. at 14 days, fasting blood glucose was taken from trunk blood following biodistribution experiment
c. at 56 days, fed blood glucose was taken from pedal vein prior to the biodistribution experiment

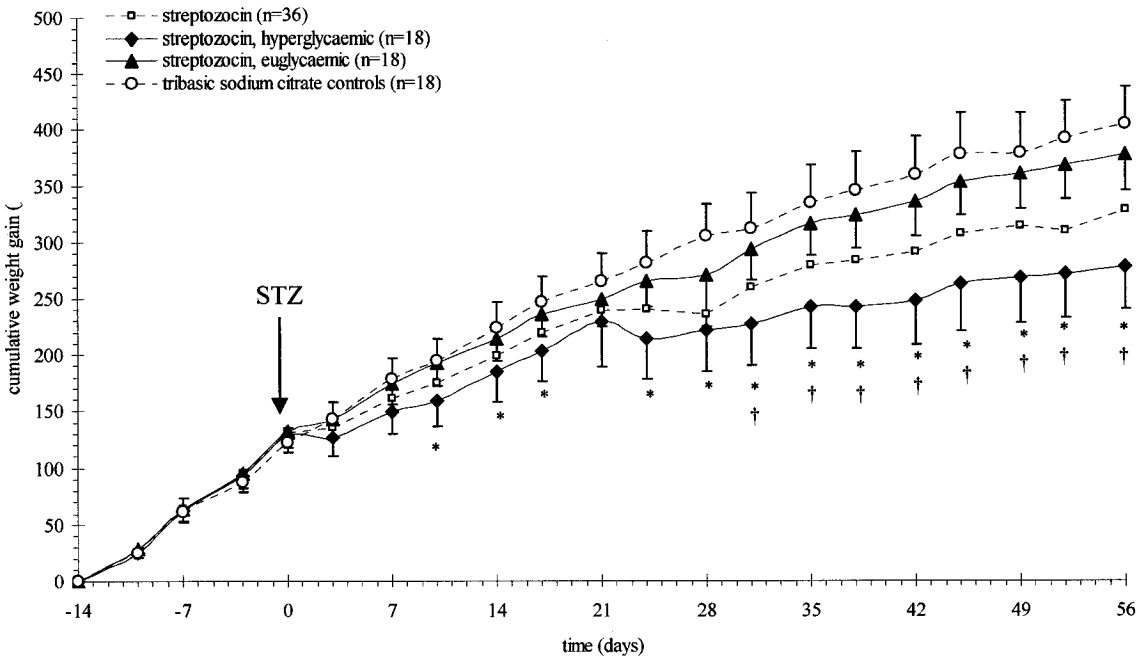

Figure 3.13: Comparison of weight following induction of type II diabetes mellitus with streptozocin compared to vehicle treated controls. Treated animals were divided according to glycaemic state. * $p<0.05$, two-tailed T-test to controls; † $p<0.05$, two-tailed T-test to euglycaemic streptozocin-treated rats.

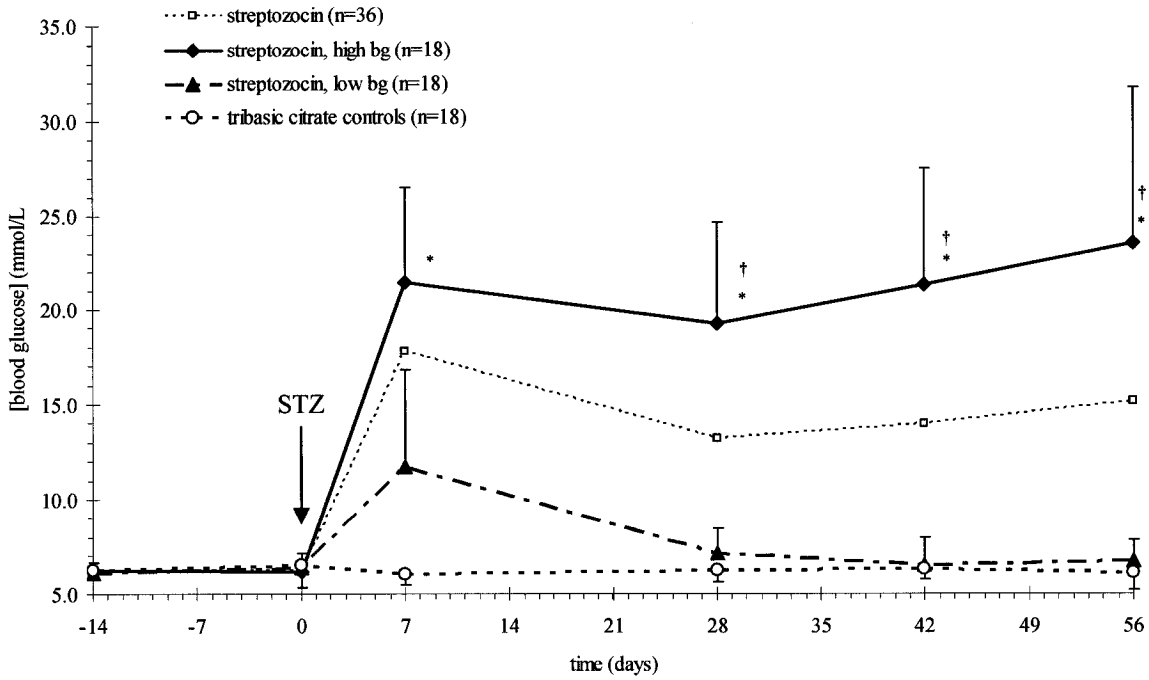

Figure 3.14: Average blood glucose levels following streptozocin (45 mg/kg ip) or citrate administration. Hyperglycaemia was defined as blood glucose concentration >11 mmol/L. Biodistribution procedures were carried out at 10 or 56 days following streptozocin treatment. * $p<0.05$, two-tailed T-test to controls; † $p<0.05$, two-tailed T-test to euglycaemic, streptozocin-treated animals.

had lower blood glucose levels, and receded to the baseline level of control rats 28 days after receiving streptozocin. This success rate is in keeping with documented rates (Szkudelski, 2001; Zhang et al., 2003). As such, it was necessary to subdivide treated rats into hyperglycaemic (blood glucose concentration ≥11 mmol/L) and euglycaemic (<11 mmol/L) groups. Hyperglycaemic animals exhibited consistently high fed blood glucose levels after injection with streptozocin.

Plasma insulin levels were measured in high- and moderate-dose streptozocin rats and controls at 14 and 56 days post-treatment (Table 3.9). Variability in concentrations was substantial. As expected, insulin was essentially absent in type I diabetic rats, with insulin levels of 0.057±0.010 ng/mL, a significant reduction compared to chow-fed controls. In type II diabetic models, an alternative pattern was observed. At 24 days high fat diet and 10 days post-streptozocin treatment, average insulin concentrations in hyperglycaemic streptozocin-treated, euglycaemic streptozocin-treated, and control rats were 0.756±0.518, 0.164±0.080, and 0.654±0.412, ng/mL, respectively. Significantly lower insulin concentration was apparent in euglycaemic animals. Concentrations were augmented at the 56-day time point in control and euglycaemic treated animals but were significantly lower in hyperglycaemic treated animals (0.701±0.707, 0.626±0.567, and 0.216±0.183 ng/mL).

3.3.2 Biodistribution of [^{11}C]HED in Diabetic Rats

3.3.2.1 Short Term Type I Diabetes Mellitus (14 Days)

Biodistribution of [^{11}C]HED at 30 minutes post-injection was minimally affected in type I diabetic rats, exhibiting highly similar total retention in myocardium and most peripheral tissues (Figure 3.15).

A slight decrease of 28% in tracer accumulation in type I DM rats compared to controls was apparent in brown adipose tissue, but this reduction was not statistically significant.

Table 3.9: Fasting plasma insulin in Sprague-Dawley, high dose (65 mg/kg, iv), and moderate dose (45 mg/kg ip) streptozocin-treated rats at 14 and 56 days post-treatment.

Group	*plasma insulin (ng/mL)*
Controls, chow-fed 14 days (n=8)	0.16±0.12
Type I diabetic, 14 days (n=8)	0.06±0.01*
Controls, high fat fed 10 days (n=6)	0.65±0.41
Type II diabetic, hyperglycaemic, 10 days (n=8)	0.76±0.52
Type II diabetic, euglycaemic, 10 days (n=7)	0.16±0.08*
Controls, high fat fed 56 days (n=11)	0.70±0.71
Type II diabetic, hyperglycaemic, 56 days (n=9)	0.22±0.18*
Type II diabetic, euglycaemic, 56 days (n=11)	0.63±0.57

Average fasting insulin levels ± standard deviation in rats following biodistribution experiments.
* $p<0.05$, two-tailed T-test

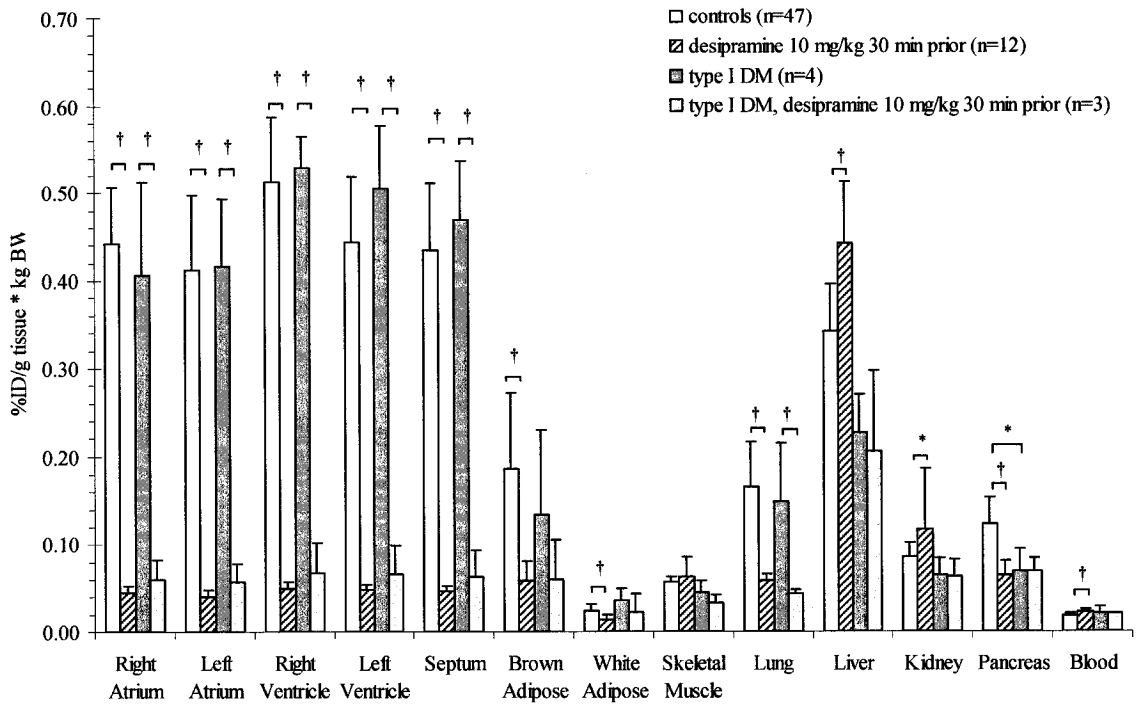

Figure 3.15: Biodistribution of [^{11}C]HED in high dose streptozocin-treated rats (65 mg/kg iv), two weeks following induction of diabetes. Pretreatment with desipramine (10 mg/kg 30 min prior) was used to delineate uptake-1 specific retention of [^{11}C]HED (B). * $p<0.05$, † $p<0.0001$, one-way ANOVA with Bonferroni post hoc.

Pancreatic tissue retention of [^{11}C]HED was significantly reduced by 43.3% in type I DM compared to age matched controls. A similar trend was observed in liver. No difference in tracer retention was detected in white adipose tissue, skeletal muscle, lung, kidney, or blood.

Pretreatment with desipramine indicated no change in non-specific tracer retention (Figure 3.15, Table 3.10). There were significant reductions in type I DM tracer retention in all tissues that exhibit uptake-1 specific retention following desipramine administration. Specific retention data is described in Table 3.10.

3.3.2.2 Short Term Type II Diabetes Mellitus (10-14 Days)

At 10 days post-streptozocin injection, treated animals were classified as hyperglycaemic (blood glucose level ≥11 mmol/L) or euglycaemic (blood glucose level <11 mmol/L). Slight, non-significant differences in tracer retention were observed in myocardium between the two treated groups and the control group, but biodistribution of [^{11}C]HED was unchanged in most tissues with the exception of brown adipose tissue (Figure 3.16A, Table 3.10).

Myocardial tracer retention was slightly but not significantly increased by 8-14% in hyperglycaemic animals. Comparatively, euglycaemic rats exhibited total tracer accumulation in myocardium at levels directly comparable to controls.

In both hyperglycaemic and euglycaemic streptozocin-treated animals, there was a stark and significant increase of [^{11}C]HED retention in brown adipose tissue. Total tracer accumulation was elevated by 160.5 and 129.6% compared to controls in hyperglycaemic and euglycaemic rats respectively.

Table 3.10: Percent change in uptake-1 specific [^{11}C]HED retention in type II diabetic rats at 14 and 56 days following induction of diabetes with streptozocin. Type I animals are included for comparison.

Group	*% change in uptake-1 specific [^{11}C]HED retention to age-matched controls*						
	Right Atrium	Left Atrium	Right Ventricle	Left Ventricle	Septum	Brown Adipose	Pancreas
Type I, 14 days, hyperglycaemic	-13.0	-3.5	0	+10.9	+4.6	-42.1	-99.9
Type II, 10 days, hyperglycaemic	+10.4	+6.5	+14.7	+15.5	+13.6	+239.1	+78.5
Type II, 10 days, euglycaemic	+1.2	+10.4	-6.6	-12.5	-11.4	+194.6	+70.2
Type II, 56 days, hyperglycaemic	-53.9	-52.9	-44.6	-41.2	-45.3	+290.6	+14.6
Type II, 56 days, euglycaemic	-8.6	-14.5	-6.3	-6.0	-6.5	+283.1	-13.8

Uptake-1 specific retention is defined as total retention – non-specific retention (pretreated with desipramine 10 mg/kg 30 min prior).
Percent change is calculated as $(SR_{diabetic} - SR_{control})/SR_{control} * 100\%$, where SR=specific retention.
Statistical significance of these results is indicated in figures only, as the values obtained here are indirect calculations not result values.

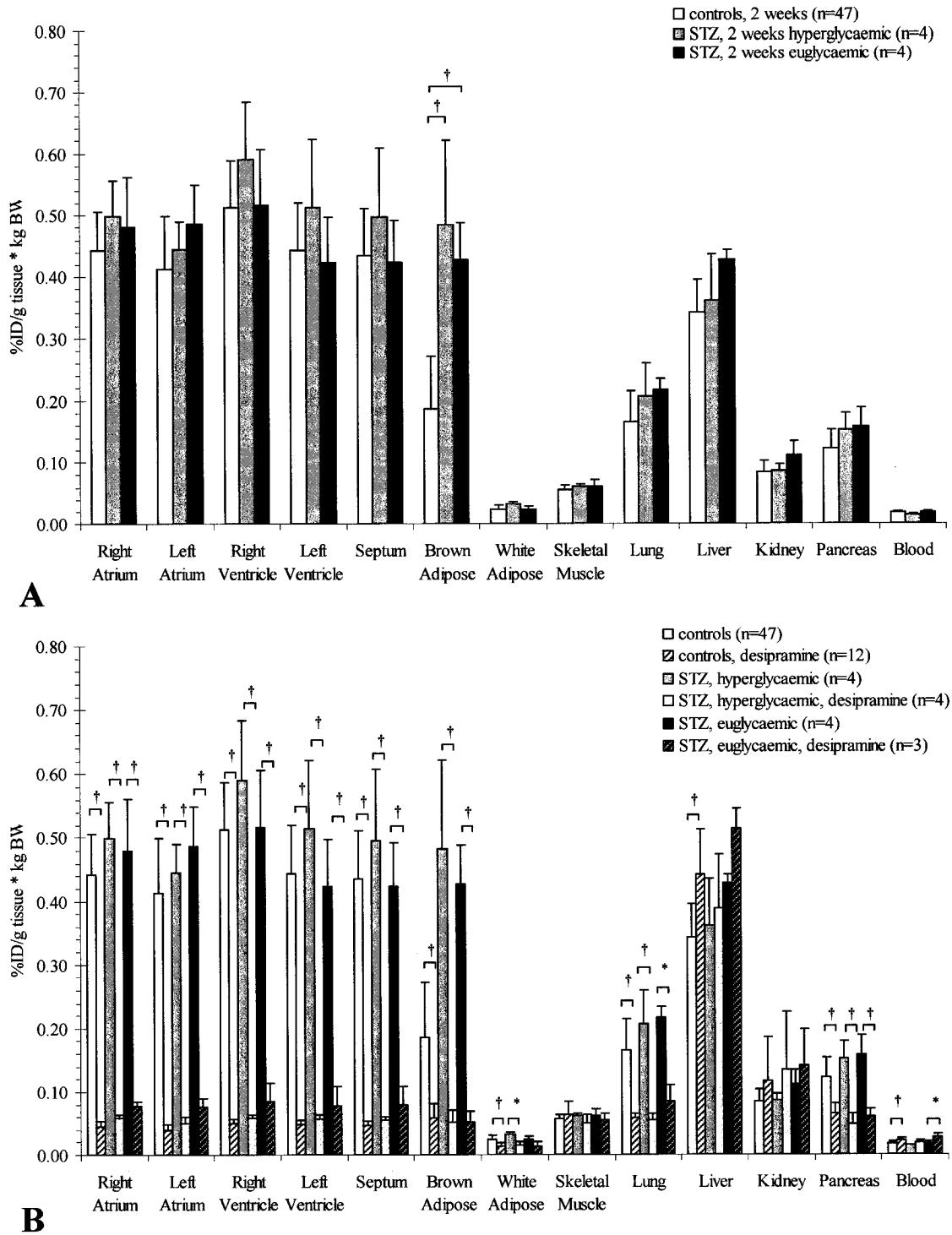

Figure 3.16: Biodistribution of [^{11}C]HED in hyperglycaemic and euglycaemic moderate-dose streptozocin-treated rats (45 mg/kg), two weeks following treatment (A). Pretreatment with desipramine (10 mg/kg 30 min prior) was used to delineate changes in uptake-1 specific retention of [^{11}C]HED (B). * $p<0.05$, † $p<0.001$, one-way ANOVA with Bonferroni post hoc.

There is a trend of increase in white adipose tissue in hyperglycaemic animals, and a slight augmentation of liver [^{11}C]HED retention in euglycaemic animals. However, no clear difference in total tracer retention was found in other peripheral tissues.

Pretreatment with desipramine revealed that non-specific retention of [^{11}C]HED was unchanged in streptozocin-treated animals compared to controls in all tissues (Figure 3.16B). Total tracer retention was significantly diminished in all cardiac regions, brown adipose tissue, white adipose tissue, lung, and pancreas, as seen in control animals. Uptake-1 specific retention in brown adipose tissue was even more markedly increased than total retention in streptozocin-treated animals (Table 3.10).

3.3.2.3 Intermediate Term Type II Diabetes Mellitus (56-63 Days)

Abrupt differences in tracer retention were observed in intermediate term streptozocin-treated animals (Figure 3.17A). As with short term moderate dose streptozocin animals, hyperglycaemic and euglycaemic subgroups were used to distinguish symptoms of type II DM in treated rats.

Myocardial retention of [^{11}C]HED was substantially and significantly decreased by 23.6-31.9% in hyperglycaemic rats versus controls. Conversely, no change was detected in euglycaemic streptozocin-treated animals, which varied from control animals by only 1.1-7.3%.

As was observed in short term animals, both subgroups of streptozocin-treated animals exhibited large increases in total brown adipose tissue tracer accumulation (169% and 165%). A similar increase in tracer accumulation was observed in white adipose tissue of hyperglycaemic streptozocin-treated animals, showing a 126% increase to controls.

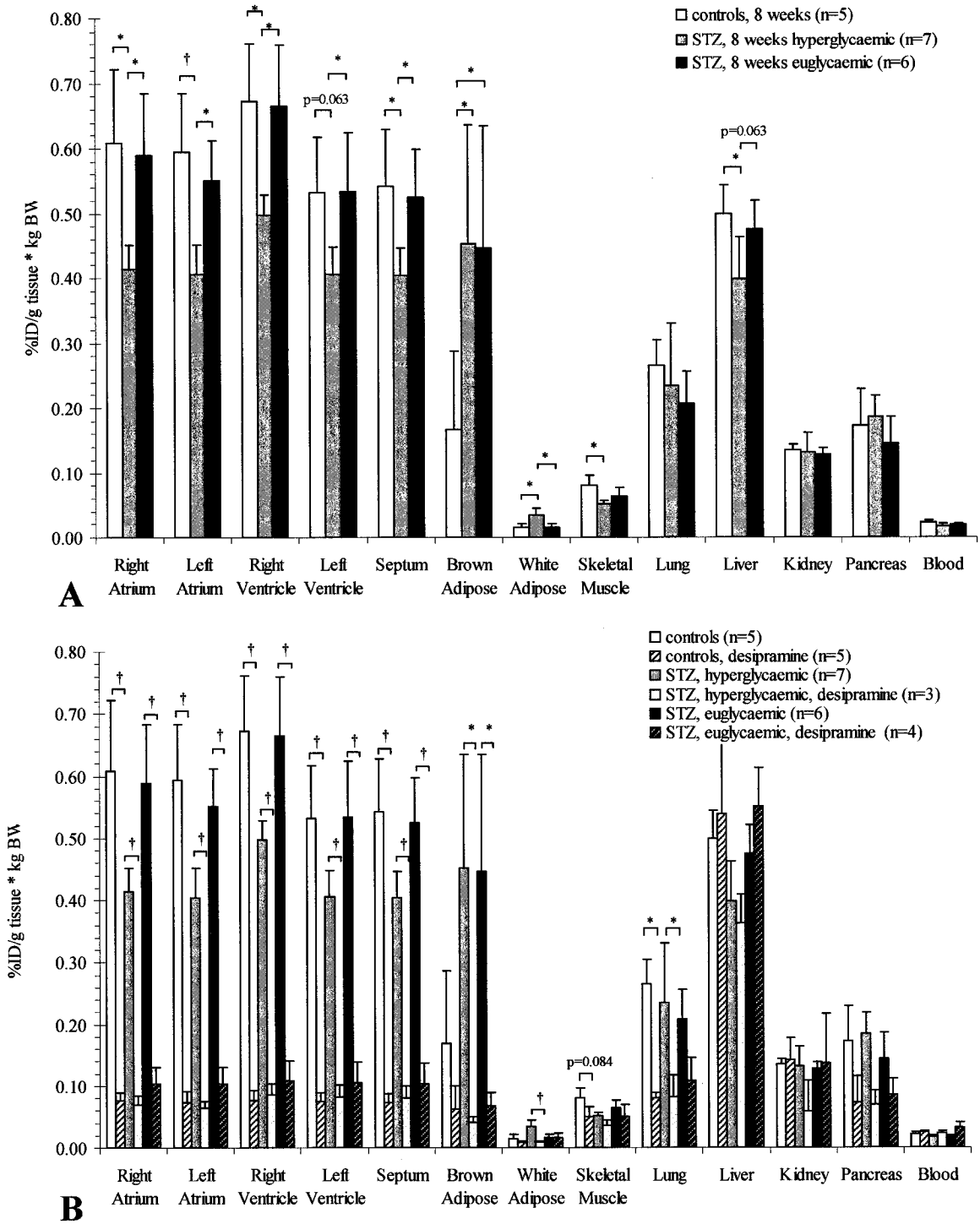

Figure 3.17: Biodistribution of [^{11}C]HED in hyperglycaemic and euglycaemic moderate-dose streptozocin-treated rats (45 mg/kg ip), eight weeks following treatment (**A**). Pretreatment with desipramine (10 mg/kg 30 min prior) was used to delineate changes in uptake-1 specific retention of [^{11}C]HED (**B**). * $p<0.05$, † $p<0.001$, one-way ANOVA with Bonferroni post hoc.

Slight and significant reductions of [^{11}C]HED retention in hyperglycaemic streptozocin-treated animals were observed in skeletal muscle, liver, and blood. No additional differences were detected for the euglycaemic treated subgroup.

Additionally, no difference in non-specific tracer retention was detected between type II diabetic and control animals following acute treatment with desipramine hydrochloride (Figure 3.17B). As in short term animals, the stark change in brown adipose tissue [^{11}C]HED accumulation was amplified when considering uptake-1 specific retention. Full specific retention data is provided in Table 3.10.

4.0 DISCUSSION

4.1 PHARMACOLOGY

4.1.1 General

The pharmacological portion of our project sought to expand the understanding of [^{11}C]HED behaviour *in vivo*, and to determine the presence of uptake-1 specific retention of the tracer in tissues not previously examined, particularly brown adipose tissue and pancreas. Studies with [^{11}C]HED have demonstrated high, persistent tracer accumulation in tissues with rich adrenergic innervation such as heart, lung, adrenal glands, and spleen (Law et al., 1997; Rosenspire et al., 1990). Uptake-1 B_{max} values in human myocardium have been measured at 28-80 fmol/mg protein (Ungerer et al., 1998). This high concentration of NET-1 is proportional to B_{max} values for postsynaptic βAR, as estimated in PET studies using [^{11}C]CGP12177 and [^{11}C]CGP12388 (12.7±3.2 and 9.7±1.8 pmol/mL, respectively) (Delforge et al., 2002; Doze et al., 2002). Conceivably, postsynaptic βAR density is reflective of presynaptic nervous integrity, as they are similarly regulated (Mandela and Ordway, 2006; Pao and Benovic, 2002). A direct correlation between [^{11}C]HED and [^{11}C]CGP12177 retention has been established (Link et al., 2003). The substantial retention of [^{11}C]HED in the heart is also representative of the importance of NE reuptake in this organ. Indeed, more than 80% of NE utilized by the myocardium is synthesized locally within sympathetic nerves supplying the organ (Kopin and Gordon, 1963).

We have shown high retention of [^{11}C]HED in brown adipose tissue, registering at approximately half of cardiac %ID/g*BW values at 30 minutes post tracer injection Postsynaptic measurements of βAR density support this contention as Zucker obese rats

showed uptake of [^{3}H]CGP12177 in crude brown adipose tissue membrane to be between one third and one half of cardiac levels (Raasmaja and York, 1988). Wide variation in tracer uptake is noted in brown adipose tissue as well, with considerably high standard deviation values. The amount of intrascapular brown adipose tissue available for excision in each animal was inconsistent, introducing a potential source of error. Additionally, unlike the focused tight synapses observed in cardiac tissue, SNS innervation to expansive tissues such as adipocytes and skeletal myocytes is more dispersed, increasing variability of uptake-1 availability (Birkenfeld et al., 2002; Esler, 1993), and [^{11}C]HED retention. Little uptake of [^{11}C]HED was observed in white adipose tissue, with levels of radioactivity similar to that seen in blood, suggesting less dense innervation in this tissue compared to brown adipocytes. This contention is logical, as a combination of thermogenesis and lipolysis mediated by βARs is expected in brown adipocytes, as compared to lipolysis alone in white adipocytes.

The pancreas is also known to exhibit extensive SNS and pSNS innervation, partially controlling regulation of insulin and glucagon secretion (Noble and Liddle, 2005). It is therefore unsurprising that considerable tracer uptake is observed in this tissue.

Accumulation of [^{11}C]HED over time in liver and kidney likely result from the metabolic fate of the tracer. Distribution of radiotracers to organs of metabolism and excretion generally increases at later time points following administration (Law et al., 1997; Lourenco et al., 2001; Lourenco et al., 2006; Rosenspire et al., 1990). Lack of brain distribution of [^{11}C]HED was expected, as, like endogenous NE, the ephedrine molecule is very hydrophylic, rendering it impermeable to the blood brain barrier, and effectively blocking meaningful uptake in brain.

Of additional importance is the low presence of tracer in blood, which has been noted in previous studies (Bengel et al., 2002; Bengel et al., 2001; Law et al., 1997; Link et al., 2003; Rosenspire et al., 1990; Schafers et al., 1998). Low concentrations of [^{11}C]HED in blood and plasma add significance to observed variations in tissue tracer retention. That is, accumulation of [^{11}C]HED in various tissues is minimally affected by perfusion and delivery considerations.

Long retention time with little clearance in all tissues rich in NET-1 implies a low k_4 kinetic constant, supporting the distribution model for [^{11}C]HED proposed by DeGrado and colleagues (1993). The prolonged maintenance of high tracer accumulation may also relate to an additional compartment of distribution (Section 4.1.4).

4.1.2 Blockade of NET-1

The stark reduction in [^{11}C]HED retention following NET-1 inhibition confirms previous data (deGrado et al., 1993; Law et al., 1997; Rosenspire et al., 1990). Desipramine and nisoxetine have been demonstrated as highly selective for the uptake-1 transporter, with K_d values of 2.8 and 0.7 nM, respectively (Malizia et al., 2000; Tejani-Butt et al., 1990). In addition to partitioning in cell membranes, plasma proteins, and other non-specific binding sources, non-specific [^{11}C]HED uptake can be partially attributed to extraneuronal uptake-2 retention, which may be differential in variable tissues. In characterizing the novel NET-1 selective [^{11}C]-phenethylguanidine radiotracers, Raffel and colleagues (2005) have described blocking the uptake-2 pathway using corticosterone.

The ability to functionally block tracer accumulation in heart, brown adipose tissue, pancreas, white adipose tissue, and lung indicates that these tissues exhibit uptake-1 specific retention of [^{11}C]HED. Imaging of lung is not feasible, however, owing to low *in vivo* tissue density (0.26 g/cm^3) compared to heart (1.05 g/cm^3) (Lourenco et al., 2006),

complicating acquisition of clear, high-contrast images. This consideration does not interfere with biodistribution data, however. Conversely, no NET-1 derived tracer accumulation was observed *in vivo* in skeletal muscle, potentially owing in part to the dispersed nature of the SNS and sparse levels of NET-1 in this tissue. Indeed, the majority of NE signaling to skeletal muscle is supplied by general spillover from other peripheral organs to the plasma and the adrenal glands, not local nervous supply (Esler et al., 1990). This observation is supported by the lack of specific binding of radiolabeled CGP12177 in skeletal muscle (van Waarde et al., 1992; Van Waarde et al., 1992), indicating wide dispersal of postsynaptic signaling sites.

4.1.3 Direct Synaptic Competition

As another false neurotransmitter, metaraminol competes for limited presynaptic reuptake sites with both endogenous NE and [^{11}C]HED. Our results support the work of Law and colleagues (1997) who generated a dose response curve to both metaraminol and unlabeled HED. As observed with desipramine and nisoxetine, uptake-1 specific retention was delineated by substantial decreases of tracer retention in myocardium, brown adipose tissue, pancreas, white adipose tissue, and lung. Lack of a change in total tracer retention compared to NET-1 blockade in peripheral tissues that do not exhibit specific tracer retention (i.e. skeletal muscle) indicates that non-specific accumulation of [^{11}C]HED is likely independent of any extraneuronal transport mechanism, since there is no competition effect observed with the elevated NE elicited by desipramine or nisoxetine. This observation relegates the uptake-2 pathway to a minor component of non-specific [^{11}C]HED retention.

4.1.4 Blockade of Vesicular Storage

Reserpine reduced tracer retention by about two thirds of uptake obtained with desipramine, indicating a lesser effect on uptake-1 specific retention. This result suggests that vesicular packaging is an important factor instilling long retention time on [^{11}C]HED, imposing an additional kinetic constant on the distribution model. This contention is supported by the work of Raffel and Wieland (2001), who demonstrated that perfused rat hearts extracted from animals pretreated with reserpine exhibit substantially faster clearance of [^{11}C]HED than those from untreated animals. Studies with [^{18}F]FMR in dogs have shown reductions in tracer accumulation following reserpine treatment of 75-80%, reductions more comparable with NET-1 blockade than with our reserpine results (Wieland et al., 1990).

The pharmacological action of reserpine is two-pronged, particularly following a lengthy incubation time (i.e. 24 h prior to tracer). Irreversible inhibition of VMAT not only prevents specific trafficking of NE and its analogues to the vesicles, but also serves to deplete synaptic NE by preventing docking of the vesicle and release of its contents at the bouton (LaBuda and Fuchs, 2002). Decreased synaptic NE would promote increased tracer uptake due to lessened competition at uptake-1 sites. Considering this, total [^{11}C]HED retention in reserpine-treated animals may be augmented compared to normal synaptic circumstances, suggesting a smaller role for vesicular distribution than is actually warranted. That is, the aggregate effect of blocked vesicular uptake of [^{11}C]HED and depleted synaptic NE is to render falsely high [^{11}C]HED retention values. Experiments with a shorter lag time to tracer may delineate the pure acute effects of reserpine on [^{11}C]HED, which would be expected to more closely resemble [^{18}F]FMR results.

4.1.5 Competition with Endogenous Norepinephrine

4.1.5.1 Acute Effects

While it has been long-established that [^{11}C]HED accumulation is reduced following downregulation or blockade of NET-1 (Link et al., 2003; Tseng et al., 2001), the effect of acute elevation of synaptic NE in the absence of NET-1 downregulation has not been described *in vivo*. DeGrado and colleagues reported that in isolated, perfused rat hearts, infusion of NE accelerated [^{11}C]HED washout without affecting initial uptake kinetics. [^{18}F]FMR uptake has been shown to increase in response to reduced NE levels in phenol-treated canine heart, though these studies are complicated by the fairly rapid denervation of cardiac tissue following phenol exposure (Wieland et al., 1990).

An early generation antidepressant, tranylcypromine is known to elicit elevations of all catecholamines including NE in brain and peripheral tissues (Giralt and Garcia-Sevilla, 1989). Routledge and Marsden (1987) described a 64% elevation in hypothalamic NE following an intraperitoneal injection of 10 mg/kg tranylcypromine to rats. Tranylcypromine has also been associated with cardiovascular effects reminiscent of SNS stimulation. Two hours following acute tranylcypromine treatment, systolic and diastolic blood pressure was mildly increased (Balon et al., 1990; Keck et al., 1991). Elevated NE would be expected to elicit dose-dependent reductions in [^{11}C]HED uptake comparable to scaled doses of metaraminol or unlabelled HED (Law et al., 1997), owing to the similar mechanism of competition.

Previous experiments have examined the effects of a comparable drug, the MAO A selective inhibitor clorgyline on the analogous tracer [^{11}C]phenylephrine. Findings indicated that clorgyline administration increased cardiac accumulation of

[^{11}C]phenylephrine (Del Rosario et al., 1996). This result may be explained by both the predominant localization of MAO isoforms and the metabolic susceptibility of phenylephrine to MAO breakdown. While the majority of MAO in rat heart is extraneuronal (Lowe et al., 1975), MAO A is thought to predominate within the neuron, whereas MAO B is concentrated in the synaptic cleft, partially anchored extracellularly to the presynaptic membrane (Del Rosario et al., 1996; Fowler et al., 2004; Greenshaw et al., 1988; Rawlow et al., 1980). The MAO A selective inhibitor clorgyline therefore does not evoke the synaptic effect on NE elicited by non-selective tranylcypromine. Lack of MAO A breakdown of phenylephrine in the neuron confers greater retention of tracer, rendering its kinetics more similar to MAO resistant [^{11}C]HED (Del Rosario et al., 1996). Conceivably, administration of clorgyline prior to [^{11}C]HED injection would elicit a less dramatic alteration of tracer uptake than is observed with tranylcypromine, as functional synaptic MAO B would prevent NE elevation. This could be further compared with effects of administration of the selective MAO B inhibitor deprenyl.

The results support a gradual increase in synaptic NE proportional to elevated tranylcypromine dosage, leading to increased uptake-1 competition and reduced [^{11}C]HED retention. NE levels may be as important a factor in determining [^{11}C]HED accumulation as NET-1 density. Ungerer and colleagues (2000) have demonstrated a positive correlation ($r=0.65$) between uptake-1 expression and [^{11}C]HED uptake. This correlation may be strengthened by accounting for NE concentrations in the synapse.

4.1.5.2 Subchronic Effects

Subchronic administration of tranylcypromine was expected to induce alterations in NET-1 expression owing to chronic elevations of synaptic NE. Continuous infusion of NE via osmotic subcutaneous minipumps has been shown to substantially decrease AR and NET

densities in brain and myocardium (Mardon et al., 2003; Seo et al., 1999). Similarly, repeated administration of tranylcypromine has been associated with increased baseline NE levels and downregulation of postsynaptic receptors. Giralt and Garcia Sevilla (1989) reported decreased B_{max} values for α_2AR in several brain regions following a 14 day regimen of tranylcypromine.

Our results indicate that altered specific tracer uptake is focused primarily at the myocardial ventricles. Lack of changes in atria may reflect differential distribution of NET-1 or variable regulation of the uptake-1 pathway. Atrial uptake-1 densities and NE content are generally twofold higher than those of the ventricles (Pissarek et al., 2002; Shore et al., 1958). As such, atria may exhibit a more efficient means of accommodating for fluctuation in NE levels without transporter downregulation. In other peripheral tissues, elevation of NE may not be as focused, owing to the dispersed nature of SNS boutons and predominant contribution of NE plasma spillover and adrenal supply over local synthesis (Birkenfeld et al., 2002; Esler et al., 1990). Longer term treatment would be expected to overcome these compensatory measures and generate a more homogenous reduction of tracer uptake in heart and other tissues that exhibit uptake-1 specific retention.

The decrease in tracer retention observed in ventricles following subchronic tranylcypromine treatment was significantly different from moderate dose acute treatments, indicating that the effect observed does not merely result from acute stimulation. Importantly, long-term treatments are associated with compensatory mechanisms, reducing the overall effect of the drug and imparting tolerance to acute administration (O'Brien, 1995; Sydow et al., 2004).

4.1.5.3 Measurement of Norepinephrine

These results would benefit from a quantitative examination of NE concentration within ventricular, adipose, and pancreatic tissue. A novel method for NE extraction, detection, and quantification using high performance liquid chromatography is being developed for this purpose (Appendix B).

4.1.6 Alpha Adrenoceptor Modulation

Distribution of αARs is relatively ubiquitous in peripheral organ systems, signaling primarily in the vasculature to promote vasoconstriction (Angus and Cocks, 1984; Brodde et al., 2001; Fagerholm et al., 2004). One isoform of αARs, the α_{2A}AR, is predominantly localized at the presynaptic neuronal membrane, and has been thought to play a role in normal NE signal transduction, controlling a negative feedback loop to reduce NE release in the presence of excess neurotransmitter (Angus et al., 1984; Baker et al., 1984; Brede et al., 2002; Du and Riemersma, 1992; Zugck et al., 2003). Indeed, knockout of the α_{2A}AR in mice has been shown to not only have a marked effect on plasma and urine catecholamine levels due to increased spillover from synaptic release (Chen et al., 2001; Makaritsis et al., 2000) but also to alter glucose and insulin homeostasis, underscoring the correlation of these two signaling pathways (Fagerholm et al., 2004). Reports have further linked sequence variants of α_{2A} and α_{2C}ARs with the occurrence of cardiac hypertrophy in knockout mice and enhanced heart failure in human patients (Brede et al., 2002). However, the validity of presynaptic autoadrenoceptor signal regulation has been questioned (Baker et al., 1984; Kalsner, 1984; Powell et al., 2005).

4.1.6.1 Acute Agonism

Clonidine action in the periphery was expected to include specific targeting of α_2ARs, resulting in reduced NE synaptic release (Langer, 1980) and subsequent elevation of

[^{11}C]HED uptake and retention. However, pretreatment with varying doses of clonidine did not evoke the desired effect, having little impact on [^{11}C]HED retention in most peripheral tissues and in myocardium. There was a variable effect depending on dosage, however.

It has been suggested that presynaptic action of α_2ARs is best attained by administering low doses of clonidine, avoiding the postsynaptic vasoconstrictive effects and central nervous effects that can also modulate increased blood pressure and are observed at higher doses (Brede et al., 2002; Fagerholm et al., 2004; Meana et al., 1997). Indeed, the 0.05 mg/kg dose appeared to be more efficacious than higher dosage, particularly in the atria. Reduced [^{11}C]HED retention in these regions indicates either elevated synaptic NE levels or decreased NET-1 expression or activity, the opposite of our anticipated results. As the converse of our expectation is observed, alternative mechanisms may be involved in the regulation of synaptic NE.

One of these mechanisms may relate to short term regulation of the uptake-1 transporter. As previously discussed, some regulation of NET-1 appears dependent upon second messengers including cAMP and cGMP (Bryan-Lluka et al., 2001; Mandela and Ordway, 2006). As clonidine is an agonist, presynaptic second-messenger signaling may result in elevated cAMP, PKC, and subsequent phosphorylation and potential internalization of NET-1, decreasing tracer uptake. The focus of changes in the atrial tissue may reflect the morphology of αARs, which show a slightly greater density in atrial as compared to ventricular tissue (Brodde et al., 2001). This theory is supported in that only low dose elicited the reduction in [^{11}C]HED retention, suggesting that only targeted presynaptic stimulation is involved.

A further complicating factor in prejunctional αAR targeting is the cross-activity of several drugs, including clonidine, with non-adrenergic receptors, specifically the imidazoline

receptors, especially at high doses. Imidazoline receptors are centrally located and elicit hypotensive effects in the brainstem that cannot be blocked by yohimbine nor mimicked by direct NE administration (Bousquet et al., 1975). Imidazoline agonists evoke increased NE stimulation within the central nervous system, feeding onto the periphery (Meana et al., 1997). The effect of centrally augmented stimulation and locally dampened NE release is not clear. Experiments in isolated rat atria have shown that imidazoline receptor/α_2AR agonists effectively reduce the efflux of [^{3}H]NE by up to 75% (Thaina et al., 1999), but this effect has not been observed *in vivo*, suggesting that central pathways may obscure the local effect.

One or a combination of three approaches may elucidate the physiological consequences of clonidine administration on synaptic environment: i) measurement of NE concentration in both plasma and myocardium to separate the spillover from general circulation and local effect on catecholamine release; ii) administration of a more specific α_2AR agonist such as idazoxan to eliminate imidazoline cross-reactivity; and/or iii) co-administration of clonidine with yohimbine to block the α_2AR effect and delineate the non-specific imidazoline effects.

4.1.6.2 Acute Antagonism

The use of the selective α_2AR antagonist yohimbine to increase synaptic cardiac NE has been well documented (Dart et al., 1984; Du and Riemersma, 1992; Heyndrickx et al., 1984; Szemeredi et al., 1991; Zugck et al., 2003). There remains some debate as to whether prepulse inhibition actually occurs via α_2ARs. Powell and colleagues (2005) have suggested that yohimbine actually works indirectly via serotonin 1A receptors (5-HT$_{1A}$R). A selective 5HT$_{1A}$ antagonist (WAY100,635) effectively blocked yohimbine-induced elevations of synaptic NE in rats (Powell et al., 2005).

Administration of yohimbine is expected to increase synaptic NE by inhibiting negative feedback presynaptically, blocking the normal feedback signaled by endogenous NE. This would result in decreased [^{11}C]HED retention in uptake-1 specific regions. Minor changes were observed in most peripheral tissues following yohimbine treatment, but a modest, significant, and unexpected increase in tracer uptake was observed in all myocardial regions, consistent with enhanced expression of uptake-1 transporter or depleted synaptic NE. The treatment period, 15 minutes prior to [^{11}C]HED injection, was insufficient to allow for short-term regulation of NET-1 (Bryan-Lluka et al., 2001). Moreover, 1.0 mg/kg, one tenth of the dose used in this experiment, has been shown to augment plasmatic NE levels by 30% within 30 minutes of injection (Szemeredi et al., 1991)*. Isolated rat heart preparations have also displayed a 100% increase in NE overflow and a mild increase in NE outflow without a change in heart rate at low and moderate sympathetic stimulation levels following infusion of 1 μM (0.4 mg/mL) yohimbine (Dart et al., 1984). Conversely, Du and Rimersma (1992) reported that in pulse-stimulated isolated heart preparations, yohimbine actually decreased NE efflux at high stimulation frequencies, suggesting a variable effect of αAR inhibition dependent on basal signaling.

As with clonidine, complications may also derive from the inability to selectively target local effects of the αAR. Central inhibition of αARs decreases SNS stimulation, which may in turn mask the presynaptic effects of the drug (Heyndrickx et al., 1984; Kalsner, 1984).

Measurement of NE levels will be a useful step in determining the causative factor for increased cardiac [^{11}C]HED retention following yohimbine treatment. Coupled with

* Considering both the pre-tracer injection time of 15 minutes and the tracer incubation time of 30 minutes, yohimbine treatment was actually administered 45 minutes before sacrifice.

uptake-1 density determination studies using [^{3}H]nisoxetine, a clearer picture of the mechanisms involved might be obtained.

4.2 Obesity

4.2.1 Effect of Diet

It has been suggested that the development of diet-induced obesity is a direct result of high diet palatability and consequent overfeeding (Farley et al., 2003; Levin and Dunn-Meynell, 2002; Levin et al., 1987; Levin et al., 1983; Ricci and Levin, 2003). Indeed, Levin and colleagues (1983) demonstrated that organ NE turnover was altered in various tissues at different time points of feeding a condensed milk diet versus standard chow (Levin et al., 1983). NE turnover in brown adipose tissue was increased after 7 days of condensed milk diet while no change was detected in heart or other peripheral tissues; conversely, after 3 months of condensed milk diet, heart turnover of NE was reduced by 50% with no changes observed in adipose tissues or pancreata (Levin et al., 1983). Comparatively, consumption of a high sucrose diet by obesity-prone rats elicited significant changes in glucose, triglyceride and leptin levels as well as altered heart rate variability and sympathetic activity (Park et al., 2000). Our results indicate that consumption of high fat diet alone does not significantly alter cardiac, brown adipose tissue, white adipose tissue, or pancreatic uptake of [^{11}C]HED, suggesting that any change in NE levels or NET-1 density is not substantive to distinguish high fat diet fed animals from chow fed controls. Variability in tracer uptake among DIO, DR, and Sprague-Dawley normals is resultant of factors beyond simply diet composition.

Moreover, despite documented concern that fasting significantly alters NE turnover (Young et al., 1978), overnight fasting did not change tracer kinetics in tissues of interest. Some

reported tissue-specific fluctuations may be valid, as we have shown liver uptake of [^{11}C]HED was increased following overnight fasting.

4.2.2 Food Intake and Weight Gain

The lack of variation in food intake shown in this study contradicts some documented data (Levin et al., 1987; Ricci and Levin, 2003). The difference here may reflect variability in calculations. Levin and colleagues (1987) calculated food intake by kilocalories without accommodating for body weight of the rat to determine a metabolic efficiency value that varied among DIO, DR, and chow-fed animals (Levin et al., 1987). Our measurements take into account body weight, vastly different between each of the rat substrains, and an important factor in total volume of food consumption. When considering body weight as a factor, variation in food consumption is negligible. At day 49 of high fat feeding, the trend of higher food intake reverses, with DR rats consuming slightly more on average than DIO (Figure 3.8B). This timeframe corresponds with documented normalization of body weight gain in DIO and DR animals (Farley et al., 2003; Levin et al., 1987; Ricci and Levin, 2003), which may account for this intriguing reversal. Measurement of caloric intake and efficiency would be additionally useful, and the literature indicates that food intake does play an important role in altering body weight gain and adiposity. However, indications from the literature and our own analysis support the contention that factors beyond food intake are also required to confer the altered weight gain and [^{11}C]HED biodistribution characteristics onto DIO, DR, and Sprague-Dawley rats.

Weight gain profiles, as indicated, were substantially different between the two rat strains. Cumulative weight gain was comparable to previous documented tracking data (Levin et al., 1987; Park et al., 2000) and confirms the biological variability of the substrains.

Changes in SNS signaling detected by [^{11}C]HED can therefore be considered representative of the differences between obese and lean animals and not a direct result of diet, fasting, or overfeeding.

High fat diet appears to have augmented insulin levels in both control animals and DIOs, and to a lesser extent in DR (Table 3.5). Hyperinsulinemia has been reported in DIO rats (Levin and Dunn-Meynell, 2000; Levin and Dunn-Meynell, 2002; Levin et al., 1987), and may represent one factor involved in elevated SNS signaling. At longer high fat feeding time periods than our documented data (e.g. 119 days), the insulin levels of DIO rats may become more homogeneously and substantially elevated than observed in short and intermediate term rats.

4.2.3 Biodistribution of [^{11}C]HED in DIO and DR Rats

Retention of [^{11}C]HED was expected to be lower in DIO as compared to DR, owing to elevated NE levels in the former and expected lack of cogent signaling, particularly in thermogenic tissues and in the heart. Our results indicate that following two weeks of high fat diet consumption, no clear difference in SNS innervation or NE levels is present between the two substrains or in comparison with Sprague-Dawley rats fed high fat diet. This may indicate that two weeks is not a sufficient timeframe to fully develop symptoms of obesity. Importantly, blockade of uptake-1 with desipramine reduced tracer uptake to comparable levels in all cases, demonstrating that the changes in [^{11}C]HED retention observed were representative of uptake-1 specific alterations, albeit miniscule in the short term animals.

Previous reports have indicated that NE levels in DIO rats as compared to DR and chow-fed controls are vastly different following high fat diet consumption (Gao et al., 2002; Levin and Dunn-Meynell, 2000; Levin and Dunn-Meynell, 2002; Levin et al., 1983). The

timeframe for measurement of NE is highly variant in these examinations. In one study, Levin and Dunn Meynell observed elevations in urinary NE levels in the initial week of high fat diet consumption (Levin and Dunn-Meynell, 2000). Generally, measurements of NE have been made at later time points, often at 3 months following initiation of diet, at which point differences in NE concentration are more absolute (Levin et al., 1989; Levin et al., 1983). An additional intriguing factor is the alterations in levels of the SNS regulatory compounds leptin, NEFA, insulin, and glucose. At early time points on high sucrose diet, leptin and triglyceride levels were doubled and NEFA and insulin levels were only mildly elevated (Park et al., 2000). This trend is comparable to high fat diet where a marked 230% elevation of plasma leptin was observed in high fat diet fed DIOs compared to chow-fed DIO controls after only 3 days, though no changes in plasma insulin were detected within the first 14 days of high fat diet (Ricci and Levin, 2003). After 49 days of high fat diet consumption, leptin and insulin levels were three times higher in DIO than DR and triglyceride levels were doubled (Gao et al., 2002). Later time points also showed differential leptin and insulin levels, though the variability was minimal between 3 months and 49 days (Levin and Dunn-Meynell, 2000). Sustained alterations in SNS modulators may be necessary to precipitate changes in NET-1 function.

4.2.3.1 Myocardium

The lack of difference in [^{11}C]HED retention between DIO and DR hearts at 14 days following high fat diet is unsurprising. There is a mild trend in our experiments to increased [^{11}C]HED retention in DIO and decreased [^{11}C]HED retention in DR heart, focused at the ventricles. This deviation is enhanced over time. As previously discussed, the atria exhibit higher densities of NET-1 than ventricles (Pissarek et al., 2002; Shore et al., 1958), a fact that may confer greater capacity for adaptation to altered NE content. The

elevation of [^{11}C]HED retention in ventricular tissues in DIO following 17 weeks of high fat diet consumption indicates a reduction of synaptic NE or an elevation of NET-1, whereas decreased [^{11}C]HED retention in DR suggest increased synaptic NE or reduced NET-1. The effect of long-term high fat diet consumption on NE turnover in myocardium is somewhat contentious. Levin and colleagues (1983) demonstrated a significant reduction in cardiac NE turnover in rats fed a high fat diet for 3 months compared to chow-fed controls. At 22 weeks of feeding, NE turnover in DIO rats was comparable to chow fed controls while DR rats exhibited twofold greater NE turnover (Levin et al., 1987). Our data partially supports this observation, with reduced [^{11}C]HED retention in DR hearts. The increased tracer retention observed in myocardium of DIO animals was unexpected, and requires further analysis to determine comparability of both substrains to normal Sprague-Dawleys, and to delineate whether NET-1 density, synaptic NE level, or a combination of both is responsible for differential [^{11}C]HED uptake in these animal sets.

Despite elevations in plasmatic NE, the heart may be differentially regulated due to tight synaptic control. Unlike dispersed tissues such as brown adipose tissue and skeletal muscle, the majority (>80%) of NE used by the heart is synthesized within the myocardial autonomic neurons (Kopin and Gordon, 1963), potentially acting as a transient buffering system to accommodate for excess NE release. However, alterations in blood pressure and R-R intervals suggest that either SNS or pSNS signaling in the heart is *not* maintained in obesity (Landsberg, 1986; Park et al., 2000), countering the previous observation. It is conceivable that hyperglycaemia in experiments by Park and colleagues (2000) on high sucrose diet-induced obesity differentially affected electrocardiograms than what might be expected with high fat diet-induced obesity, particularly relating to the resulting hyperglycaemia which is not a characteristic of the latter group (Levin and Dunn-Meynell,

2000; Levin and Dunn-Meynell, 2002). Co-modulation of the SNS by leptin and glucose may serve to further augment NE signaling and precipitate differential effects.

The elevation of [^{11}C]HED retention in tightly regulated tissues including heart and lung suggest that an intrinsic regulatory pathway may be reducing synthesis or synaptic exposure time of NE in DIO animals. This could be initiated by α_{2A}AR at the bouton surface (Baker et al., 1984; Du and Riemersma, 1992; Starke, 2001), which has been suggested to work cooperatively with presynaptic βARs in modulating cardiac sympathetic outflow (Akers and Cassis, 2004). In tight junctional synapses, the role of presynaptic receptors may be augmented. As such, elevated NE spillover to blood observed in obesity (Dulloo, 2002; Levin and Dunn-Meynell, 2002) may drive an αAR-induced decrease in local NE synthesis, decreasing competition with [^{11}C]HED for limited reuptake sites.

4.2.3.2 Brown Adipose Tissue

Interestingly, [^{11}C]HED retention in brown adipose tissue following 17 weeks of high fat diet consumption is lower in DIO than DR, the opposite result to cardiac tracer accumulation. This result indicates differential levels of NET-1 and/or synaptic NE in these tissues.

Brown adipose tissue and skeletal muscle rely heavily on NE spillover from adrenal glands and general circulation due to more dispersed innervation and less local neurotransmitter synthesis (Esler et al., 1990). As such, plasmatic changes in NE concentration, which more closely reflect NE spillover than synaptic levels, correlate more strongly with brown adipose tissue than with heart. At 14 days, there is a slight trend to increased tracer retention in DR compared to both DIO and normal animals, a difference that becomes more pronounced at 56 days and 119 days, indicating either an increase in uptake-1 density or a decrease of synaptic NE. DR animals exhibit plasmatic NE greater than is seen in Sprague-

Dawley normals, but lower than in DIO (Levin and Dunn-Meynell, 2000; Levin and Dunn-Meynell, 2002). As such, it is unlikely that decreased competition for reuptake is responsible for the increase in [^{11}C]HED accumulation. Potentially, DR animals exhibit a more efficient uptake-1 pathway in thermogenic tissue, in order to remove excesses of NE from the synapse to prevent disproportionate downregulation and/or desensitization of βAR and maintain greater levels of NE within neurons for subsequent signaling. DIO animals exhibit even higher plasmatic NE as compared to normal SD rats (Levin and Dunn-Meynell, 2002; Levin and Dunn-Meynell, 2004), and a trend toward reduced retention of [^{11}C]HED is evident. The difference in tracer accumulation between DIO and DR may therefore reflect different levels of synaptic NE and increased competition at uptake-1 sites in DIO rats, potentially owing to an inability to recapture NE from the synapse. Further examination is warranted to elucidate the cause of this behaviour.

Postsynaptic measurements of AR density in brown adipose tissue of 2-4 month old lean and obese Zucker rats support the concept of differential signaling levels (Raasmaja and York, 1988). Raasmaja and York (1988) showed a significant increase in βAR density in obese animals as compared to lean animals, as measured *ex vivo* by [^{3}H]CGP12177 binding assays to brown adipose tissue crude membranes (25.3±3.0 vs. 14.7±0.8 fmol/mg protein). These data would imply increased tracer retention in obese brown adipose tissue as compared to lean, the opposite of our results. One problem with the binding assay is the use of [^{3}H]CGP12177, which has been shown to have variable binding affinities for different βAR subtypes, with a lower binding affinity for β_3AR, specifically 70 nM in β_3 versus 1 nM in $\beta_{1/2}$ (Mohell and Dicker, 1989). Thus, in lean animals, a higher proportion of β_3AR, the primary modulator of thermogenesis (Astrup, 2000; Begin-Heick, 1996; Robidoux et al., 2004), compared to other subtypes may result in decreased binding of

CGP12177. Labeled non-selective βAR antagonists such as pindolol or propranolol may provide a more accurate indication of postsynaptic AR densities in brown adipocytes (Kopka et al., 2003; van Waarde et al., 2004).

It has also been reported that at 22 weeks of high fat diet consumption, NE turnover in intrascapular brown adipose tissue was markedly elevated in DR as compared to DIO and controls which were quite similar (Levin et al., 1987), a circumstance that would result in decreased [^{11}C]HED retention in DR compared to DIO and controls. Measurement of organ NE turnover is an imprecise method, relying on estimation of turnover by NE synthesis inhibition (Brodie et al., 1966). Quantitative NE measurement by HPLC with and without inhibition of NE synthesis using α-*para*-methyltyrosine would be a more accurate and direct measurement, providing more reliable results. Elevated synaptic NE would evoke downregulation of postsynaptic receptors (Seo et al., 1999) and dampening of baseline activities. This result is in keeping with the theory that obesity is associated with SNS dysfunction in brown adipose tissue (Bachman et al., 2002; Dulloo, 2002; Lowell and Bachman, 2003).

4.2.3.3 Pancreas

Levin and colleagues (1987) reported decreased pancreatic NE turnover rate in DIO rats compared to DR and chow fed controls, as estimated by synthesis inhibition. It was further postulated that a decrease in sympathetic tone to this organ may be partially responsible for alterations in insulin observed in DIO rats. Our results indicate a mild but statistically insignificant reduction in [^{11}C]HED retention at 119 days on high fat diet in DR rats as compared to DIOs. No difference at earlier time points was detected. It is potentially more likely that variations in DIO and DR insulin levels resulting from increased adiposity, and the probable presence of insulin resistance developing in parallel with obesity in the

former, confers elevated NE levels in the pancreas (Bloomgarden, 2002; Cruz et al., 2005; Landsberg, 2005). Decreased SNS innervation or activity in this tissue is not expected without the presence of hyperinsulinemia and/or hyperglycaemia.

4.2.3.4 Other Peripheral Tissues

As described above (Section 4.1), tracer uptake (%ID/g*BW) in lung closely resembles that of the myocardium. Sympathetic innervation to the lung is quite dense and tightly regulated and morphologically similar to myocardial innervation (Schafers et al., 2001). Lung NE turnover has not been previously examined in DIO and DR animals. Low tissue density of lung restricts utility of [^{11}C]HED as an imaging agent.

Unclear variation in tracer retention was observed in metabolic organs, white adipose tissue, skeletal muscle, or blood. The lack of difference in [^{11}C]HED accumulation in white adipose tissue is likely due to very low tracer uptake levels and sparse NET-1 density, limiting the detection of alterations among rat strains. As previously described, skeletal muscle does not exhibit uptake-1 specific retention.

4.3 Diabetes Mellitus

4.3.1 Animal Models

Animal tracking data indicate that the type I and type II animal models used in this experiment were distinct from one another, at least at early time points, as evidenced by elevated *fasting* blood glucose levels at 14 days in type I but not type II animals (Table 3.8). Moreover, the presence of insulin in the type II diabetic animal model verifies the presence of functional β-cells (Table 3.9), further distinguishing it from the high-dose streptozocin treatment. Previous descriptions of streptozocin effects on insulin levels confirm the expected differences between the high intravenous and moderate

intraperitoneal streptozocin treatments (Srinivasan et al., 2005; Szkudelski, 2001; Zhang et al., 2003). Fasting insulin levels reflect the capacity of glyceamic regulation, reduced in hyperglycaemic animals (non-responsive to glucose) and elevated in euglycaemic animals. This result indicates that the type II diabetic rats do not develop hyperinsulinemia as expected (Haffner and Miettinen, 1997; Masuo et al., 1997; Muscelli et al., 1998). However, later stages in type II DM are associated with hyperglycaemia and reduced insulin (Quilliot et al., 2005), which may partially explain our divided animal set (i.e. responders and apparent non-responders to streptozocin). Our results indicate that high fat diet alone is capable of inducing elevated insulin levels over 8 weeks of consumption.

The success of DM induction was variable in our experiments, specifically with the type II DM model. The absence of hyperglycaemia (blood glucose concentration $\geq$11 mmol/L (Srinivasan et al., 2005; Zhang et al., 2003) in 50% of moderate dose streptozocin-treated rats is troubling, and implies a lack of true DM in these animals. In some cases, the tendency to recover normal blood sugar levels after an initial spike appears to reflect a compensatory normalization of insulin action and glycaemic control (Szkudelski, 2001). Indeed, prior applications of low-dose streptozocin to induce DM have frequently been cited as unreliable, owing to low clear induction rates, and high variability in symptoms (Zhang et al., 2003). Moreover, weight gain patterns were predictive of hyperglycaemic and disease state. The differential nature of streptozocin susceptibility may be indicative of variable metabolic regulatory capabilities in Sprague-Dawley rats. Indeed, our [^{11}C]HED biodistribution data indicates that the moderate dose streptozocin *did* exert an effect on NET-1 activity in brown adipose tissue (Section 4.3.2.2) despite a lack of hyperglycaemia.

There is additional concern that at late time points, the type II DM model developed symptoms more consistent with type I than type II DM. Indeed, blood glucose levels

continued to rise in type II DM animals over the 56 days of the experiments, but fasting levels continued to be low compared to type I models, if slightly elevated to controls. This is consistent with the progression of type II DM, wherein glycaemic regulation in the long term deteriorates over time (Newman et al., 2004; Wilkin, 2001). It is the author's opinion that the type II DM model used in these experiments was successful in addressing the specific aims of this project. Further analysis of blood markers including leptin, NEFAs, and triglycerides will provide more insight on presence or absence of true type II DM in moderate-dose streptozocin-treated rats without elevated blood glucose levels.

4.3.2 Biodistribution in Type I Diabetes Mellitus

Type I DM and subsequent elevations in blood glucose levels were expected to elicit diverse effects on baseline NE signaling, particularly in myocardium, brown adipose tissue, and pancreas. Our results indicate that changes to myocardium and brown adipose tissue are minimal, with very minor differences in uptake-1 specific retention of [^{11}C]HED as delineated by pre-treatment with desipramine. Pancreatic uptake was significantly reduced in type I DM rats compared to untreated controls.

4.3.2.1 Myocardium

Alterations in cardiac NE signaling have been demonstrated in type I DM both in animal models and clinically (Bell, 2003; Ding and Fowler, 2005; Kiyono et al., 2001; Pop-Busui et al., 2004; Schmid et al., 1999; Stevens et al., 1999; Turpeinen et al., 1996). PET studies in type I DM patients have demonstrated a deficit of [^{11}C]HED retention in myocardium, particularly at distal segments of the left ventricle at long time points (Pop-Busui et al., 2004; Stevens et al., 1999). Moreover, Stevens and colleagues (1999) reported that [^{11}C]HED retention indices were substantially improved in diabetic patients after three years of improved glycaemic control, whereas retention indices were further reduced if

glycaemic control was not improved over this same follow-up period. These results have been mirrored in hearts of streptozocin-induced type I DM rats 6 and 9 months following DM induction, showing marked reductions in [^{11}C]HED retention and elevations in NE content in distal and proximal left ventricle, and reduced [^{11}C]HED retention without NE fluctuation in right ventricle (Schmid et al., 1999). Scintigraphic studies with [^{123}I]MIBG have exhibited similar findings, with abnormalities of myocardial MIBG accumulation focused predominantly in the inferior portion of the left ventricle (Kiyono et al., 2001).

Some of this apparent sympathetic dysfunction has been correlated with impaired myocardial blood flow, but perfusion deficits indicated by [^{13}N]ammonia PET are not sufficient to completely explain alterations in [^{11}C]HED retention (Pop-Busui et al., 2004). Indeed, Pop-Busui and colleagues have provided hemodynamic verification of left ventricular diastolic dysfunction in type I DM patients.

The lack of myocardial tracer uptake differences in our 2 week streptozocin-induced type I DM model is not surprising, as each of the documented alterations in tracer kinetics result from chronic diabetic states, with a minimum of 6 months duration (Schmid et al., 1999). It is possible that alterations to SNS signaling in type I DM rats was not observed due to the short time course of our experiments after induction of DM. Additionally, it has been suggested that the densely innervated distal segments of the left ventricle are affected more quickly than proximal regions (Kiyono et al., 2001; Schmid et al., 1999; Stevens et al., 1999). As a result, excision of whole left ventricles in our experiments may serve to dampen the variability in SNS innervation that may be progressing in distal regions. Future experiments may require segregation of proximal and distal left ventricular tissues to further examine this phenomenon.

4.3.2.2 Brown Adipose Tissue

The lack of a significant reduction of tracer retention in brown adipose tissue indicates that regulation of the SNS in this peripheral tissue is unaffected within the short timeframe of hyperglycaemia. Examinations of type I DM effects on brown adipose tissue are scarce. Muller and colleagues (1989) reported that children with type I DM had increased thermogenic capability as compared to healthy controls, an effect that was independent of glycaemic state. As type I DM individuals tend to be lean, this observation parallels our DR data. Moreover, qualitative analysis of our high dose streptozocin-treated animals revealed increased size of intrascapular brown adipose tissue deposits, consistent with increased capacity for thermogenesis (data not shown).

4.3.2.3 Pancreas

Pancreatic tracer uptake was reduced in type I DM rats to levels comparable to desipramine-treated animals. This suggests that uptake-1 specific retention of [^{11}C]HED was entirely lost for this tissue in these rats. As the mechanism of streptozocin is to selectively acetylate and destroy pancreatic β-cells (Szkudelski, 2001), SNS innervation to these cells may be effectively lost. Myrsen and colleagues (1996) postulated that β-cells were necessary for proper islet innervation, secreting factors required for attracting nerve fibres to the pancreas. Lack of specific [^{11}C]HED uptake potentially relates to sympathetic denervation of the pancreas.

4.3.2.4 Other Peripheral Tissues

Metabolic organs exhibited marked reductions of tracer uptake following streptozocin treatment. The actions of streptozocin have residual effects on liver and kidney, and alterations of glycaemic regulation can also impact normal liver function (Szkudelski, 2001). Reductions in [^{11}C]HED retention in liver and kidney potentially relate to this

abnormality. White adipose tissue and skeletal muscle were unaffected in short term type I DM animals.

4.3.3 Biodistribution in Type II Diabetes Mellitus

Type II DM elevates blood glucose and insulin levels which concurrently potentiate elevations in plasmatic and synaptic NE (Feve et al., 1994; Morisco et al., 2005). These alterations were expected to elicit elevated baseline NE levels, downregulation or desensitization of NET-1, and subsequent reductions of [^{11}C]HED retention in myocardium, brown adipose tissue, and pancreas. Our results indicate time- and hyperglycaemia-dependent alterations in SNS activity in myocardium and no clear effect on pancreatic NE innervation. Intriguingly, a massive elevation in [^{11}C]HED retention was observed in brown adipose tissue, an effect that was independent of both duration of diabetes and glycaemic condition.

4.3.3.1 Myocardium

As discussed previously, DAN is a condition wherein myocardium and/or other organs exhibit selective autonomic denervation (Ewing et al., 1986; Stevens, 2001). While it has been diagnosed and analysed thoroughly in the type I diabetic heart, links to SNS dysfunction in type II DM are relatively unexplored. The recovery observed in type I DM patients with improved glycaemic control suggests that the process is dependent upon glucose regulation (Stevens et al., 1999), and may explain our results, wherein myocardial sympathetic dysfunction is only detected in intermediate term moderate dose streptozocin-treated, hyperglycaemic rats.

The concept of myocardial sympathetic dysinnervation* in type II DM is not unfounded. Turpeinen and colleagues (1996) compared regional MIBG uptake in myocardium of type I and type II DM patients using SPECT. Deficits in left ventricle MIBG retention were more pronounced in type II DM, and persisted when corrections for myocardial perfusion were applied. Furthermore, as documented with type I DM-induced DAN (Schmid et al., 1999; Stevens et al., 1999), the sympathetic alterations were predominantly focused in apical regions of the myocardium (Turpeinen et al., 1996). Taken together, these results indicate that SNS dysfunction occurs in cardiac tissue, regardless of denervation events, but is dependent on prolonged hyperglycaemia.

Because SNS dysfunction is absent in euglycaemic, streptozocin-treated "type II DM" animals, it is likely driven by elevated glucose levels in the myocardium. As described previously, DM is associated with altered metabolism in the heart (Taegtmeyer et al., 2002; Young et al., 2002). In hyperglycaemic conditions, insulin resistance develops, potentially due to O-linked glycosylation of specific proteins in the insulin signal transduction pathway (McClain and Crook, 1996; Young et al., 2002). As a result, NE signaling may also be adversely impacted due to cross-talk between insulin and ARs (Morisco et al., 2005). Moreover, glucose stimulation of the SNS within the heart may augment dysfunction, particularly in regions of dense innervation, such as the apex of the left ventricle. Elevated glucose may also be involved in glycosylation of NET-1 sites owing to increased free oxygen radicals, reducing responsiveness to SNS stimulation, and decreasing tracer retention (Mao et al., 2005).

---

* Dysinnervation is used to describe dysfunctional sympathetic innervation wherein some machinery of normal cell signaling is impaired. Importantly, it is distinct from denervation, in which apoptosis and necrosis destroys the neuron.

Lag time to the development of sympathetic dysfunction in myocardium suggests that this result is dependent upon long-term, sustained elevations of glucose. As such, it is likely that chronic hyperglycaemia drives a long term elevation of NE and subsequent dysinnervation of myocardium. Further, the glucose, insulin, and NE signaling abnormalities observed in this study may be important causative or compounding factors in the development of CHF in type II diabetic patients (Suskin et al., 2000; Swan et al., 1997).

4.3.3.2 Brown Adipose Tissue

Type II DM is believed to alter thermogenic activity in a similar way to obesity, with increased baseline NE levels impairing the normal NE signaling in brown adipose tissue, overstimulating the receptors and reducing tissue responsiveness to neural stimulation (Harper and Brand, 1993; Harper and Himms-Hagen, 2001). However, we observe a substantive 200% increase in [^{11}C]HED retention in this tissue, suggesting that a combination of upregulated NET-1 and depressed baseline NE is likely present in this disease state. A lesser elevation would be expected if only one of these factors was present, particularly considering pharmacologic data (Section 4.1). The result was observed in both hyperglycaemic and euglycaemic streptozocin-treated animals, suggesting that glucose is not a driving factor in this phenomenon.

Short term type II DM is associated with elevations in insulin, NEFAs, and glucose, each of which should augment NE signaling, particularly in thermogenic tissue (Bryan-Lluka et al., 2001; Feve et al., 1994; Figlewicz et al., 1993b; Gilinsky et al., 2001; Haynes et al., 1997; Kern et al., 2005; Leibowitz and Wortley, 2004; Levin and Sullivan, 1987; Levin and Sullivan, 1989; Mardon et al., 2003; Robidoux et al., 2004). As such, our results are counterintuitive. It appears that there is a differential regulation of NET-1 in brown adipose tissue resulting from either type II DM-like symptoms, regardless of glycaemic

state, or an adverse effect of streptozocin action as yet undescribed. Specific targeting of streptozocin is *via* GLUT2, a protein that is not present in brown adipose tissue (Cannon and Nedergaard, 2004), which suggests that altered SNS regulation in this tissue is not a direct result of streptozocin action, supporting an indirect and DM-driven mechanism behind the elevated [^{11}C]HED retention.

Increased innervation in a type II diabetic state may be necessary for extended control of adipose tissue glucoregulation (Lindmark et al., 2005; Romijn and Fliers, 2005). The SNS regulates glucose use by adipose and other storage tissues (Cannon and Nedergaard, 2004; Romijn and Fliers, 2005). As insulin resistance develops, the ability of the body to utilize glucose as a fuel source decreases, and liberation of NEFAs for general metabolism becomes more important. As evidenced by the heart, metabolic shift toward greater use of NEFA as a fuel is a cornerstone of DM (Taegtmeyer et al., 2002). To stimulate the lipolysis necessary for the release of NEFAs for general use, greater SNS innervation capacity is required, potentially resulting in increased density of NE boutons in adipocytes, or enhanced recovery of synaptic NE by upregulation of NET-1. Indeed, at 56 days, increases in [^{11}C]HED uptake were also observed in white adipose tissue, supporting this generalized theory.

Further analyses are required to fully understand the alterations in brown adipose tissue of moderate-dose streptozocin-treated animals, particularly with regard to the causative factor (i.e. increased NET-1 expression, decreased synaptic NE, or both) of the increased [^{11}C]HED retention (Appendix A).

4.3.3.3 Pancreas

Unlike type I DM, no decrease in uptake-1 specific tracer retention was observed in type II DM pancreata, regardless of blood glucose levels. This result suggests that neuropathy

does not occur following moderate dose streptozocin, which supports the distinctness of this condition from type I DM.

4.3.3.4 Other Peripheral Tissues

As described above, white adipose tissue exhibited increased [^{11}C]HED uptake at 56 days, suggesting that it plays a role in metabolic shift observed in type II DM (Romijn and Fliers, 2005). Changes in skeletal muscle were also detected, with a significant decrease in tracer retention in hyperglycaemic animals. This reduction is closely paralleled by lower tracer presence in blood. Moreover, hyperglycaemia has been associated with vascular abnormalities, particularly influencing the depression of NO-mediated vasodilation and augmentation of NE-mediated vasoconstriction of blood vessels (Caballero, 2005). The result is reduced myocyte blood flow, potentially reducing delivery of [^{11}C]HED to skeletal muscle for non-specific retention.

Metabolic organs show minor changes in retention, but little significance is observed. Reduced tracer retention in the liver of hyperglycaemic animals resembles high dose streptozocin treatment effects, suggesting that elevated glucose decreases liver uptake of [^{11}C]HED.

5.0 CONCLUSIONS

5.1 CONCLUSIONS

The conclusions of this project are as follows:

1) Uptake-1 specific retention of [^{11}C]HED is present in myocardium and lung, and newly reported in *brown adipose tissue* and *pancreas*. Low uptake levels are present in white adipose tissue as well.
2) Retention of [^{11}C]HED is dependent on NET-1 density and function, vesicular packaging, and is likely inversely proportional to synaptic NE levels, possibly even in the absence of long term downregulation of NET-1.
3) There is a fundamental difference in [^{11}C]HED retention between diet-induced obese, normal Sprague-Dawley, and diet resistant lean rats in myocardium, brown adipose tissue, and pancreas, indicating altered NET-1 function, density, and/or differences in synaptic NE concentration among these animals.
    a. Diet-induced obese rats exhibit a time-dependent increase in [^{11}C]HED retention in myocardium and a consistent decrease in [^{11}C]HED retention in brown adipose tissue as compared to normal Sprague-Dawley and diet resistant lean rats.
    b. Diet resistant lean rats exhibit a time-dependent decrease in [^{11}C]HED retention in myocardium and a consistent increase in [^{11}C]HED retention in brown adipose tissue as compared to normal Sprague-Dawley and diet-induced obese rats.
4) There is a fundamental difference in [^{11}C]HED retention between type I DM, type II DM, and normal Sprague-Dawley rats, indicating altered NET-1 function, density, and/or differences in synaptic NE concentration among these animals.

a. High dose streptozocin-induced type I DM animals exhibit slight depression of [^{11}C]HED retention in brown adipose tissue and complete loss of uptake-1 specific tracer retention in pancreas.

b. Type II DM animals exhibit time- and hyperglycaemia-dependent reduction in myocardial [^{11}C]HED retention and consistently increased brown adipose tissue [^{11}C]HED retention as compared to age-matched controls.

5) [^{11}C]HED and PET may provide a useful predictive diagnostic measurement in assessing cardiac health in obese and diabetic patients, and may gauge progress of therapeutic interventions in these patients.

6) Imaging of brown adipose tissue with [^{11}C]HED and PET may be possible in rats, owing to high uptake and consistent localization of deposits. Human imaging presents more challenges.

6.0 REFERENCES

Agostini D, Belin A, Amar MH, Darlas Y, Hamon M, Grollier G, Potier JC, Bouvard G. 2000. Improvement of cardiac neuronal function after carvedilol treatment in dilated cardiomyopathy: a 123I-MIBG scintigraphic study. J Nucl Med 41(5):845-851.

Akers WS, Cassis LA. 2004. Presynaptic modulation of evoked NE release contributes to sympathetic activation after pressure overload. Am J Physiol Heart Circ Physiol 286(6):H2151-2158.

al Maskati HA, Zbrozyna AW. 1989. Stimulation in prefrontal cortex area inhibits cardiovascular and motor components of the defence reaction in rats. J Auton Nerv Syst 28(2):117-125.

Allman KC, Wieland DM, Muzik O, Degrado TR, Wolfe ER, Jr., Schwaiger M. 1993. Carbon-11 hydroxyephedrine with positron emission tomography for serial assessment of cardiac adrenergic neuronal function after acute myocardial infarction in humans. J Am Coll Cardiol 22(2):368-375.

Amara SG, Pacholczyk T. 1991. Sodium-dependent neurotransmitter reuptake systems. Curr Opin Neurobiol 1(1):84-90.

Angus JA, Cocks TM. 1984. Role of endothelium in vascular responses to norepinephrine, serotonin and acetylcholine. Bibl Cardiol(38):43-52.

Angus JA, Korner PI, Jackman GP, Bobik A, Kopin IJ. 1984. Role of autoinhibitory feedback in cardiac sympathetic transmission. Clin Exp Hypertens A 6(1-2):371-385.

Apparsundaram S, Galli A, DeFelice LJ, Hartzell HC, Blakely RD. 1998. Acute regulation of norepinephrine transport: I. protein kinase C-linked muscarinic receptors influence transport capacity and transporter density in SK-N-SH cells. J Pharmacol Exp Ther 287(2):733-743.

Arch JR, Wilson S. 1996. Prospects for beta 3-adrenoceptor agonists in the treatment of obesity and diabetes. Int J Obes Relat Metab Disord 20(3):191-199.

Argyropoulos G, Harper ME. 2002. Uncoupling proteins and thermoregulation. J Appl Physiol 92(5):2187-2198.

Astrup A. 2000. Thermogenic drugs as a strategy for treatment of obesity. Endocrine 13(2):207-212.

Avendano GF, Agarwal RK, Bashey RI, Lyons MM, Soni BJ, Jyothirmayi GN, Regan TJ. 1999. Effects of glucose intolerance on myocardial function and collagen-linked glycation. Diabetes 48(7):1443-1447.

Bachman ES, Dhillon H, Zhang CY, Cinti S, Bianco AC, Kobilka BK, Lowell BB. 2002. betaAR signaling required for diet-induced thermogenesis and obesity resistance. Science 297(5582):843-845.

Backs J, Haunstetter A, Gerber SH, Metz J, Borst MM, Strasser RH, Kubler W, Haass M. 2001. The neuronal norepinephrine transporter in experimental heart failure: evidence for a posttranscriptional downregulation. J Mol Cell Cardiol 33(3):461-472.

Bailey CJ, Turner RC. 1996. Metformin. N Engl J Med 334(9):574-579.

Baker DJ, Drew GM, Hilditch A. 1984. Presynaptic alpha-adrenoceptors: do exogenous and neuronally released noradrenaline act at different sites? Br J Pharmacol 81(3):457-464.

Balon R, Pohl R, Yeragani VK, Berchou R, Gershon S. 1990. Monosodium glutamate and tranylcypromine administration in healthy subjects. J Clin Psychiatry 51(7):303-306.

Barbier J, Reland S, Ville N, Rannou-Bekono F, Wong S, Carre F. 2006. The effects of exercise training on myocardial adrenergic and muscarinic receptors. Clin Auton Res 16(1):61-65.

Barbier M, Attoub S, Galmiche JP. 2000. [Leptin: physiological aspects and implications in hepato-gastroenterology]. Gastroenterol Clin Biol 24(5):506-519.

Barinaga M. 1995. "Obese" protein slims mice. Science 269(5223):475-476.

Barinaga M. 1996. Obesity: leptin receptor weighs in. Science 271(5245):29.

Beckman ML, Bernstein EM, Quick MW. 1998. Protein kinase C regulates the interaction between a GABA transporter and syntaxin 1A. J Neurosci 18(16):6103-6112.

Begin-Heick N. 1996. Of mice and women: the beta 3-adrenergic receptor leptin and obesity. Biochem Cell Biol 74(5):615-622.

Bell DS. 2003. Diabetic cardiomyopathy. Diabetes Care 26(10):2949-2951.

Bengel FM, Ueberfuhr P, Hesse T, Schiepel N, Ziegler SI, Scholz S, Nekolla SG, Reichart B, Schwaiger M. 2002. Clinical determinants of ventricular sympathetic reinnervation after orthotopic heart transplantation. Circulation 106(7):831-835.

Bengel FM, Ueberfuhr P, Schiepel N, Nekolla SG, Reichart B, Schwaiger M. 2001. Effect of sympathetic reinnervation on cardiac performance after heart transplantation. N Engl J Med 345(10):731-738.

Benmansour S, Altamirano AV, Jones DJ, Sanchez TA, Gould GG, Pardon MC, Morilak DA, Frazer A. 2004. Regulation of the norepinephrine transporter by chronic administration of antidepressants. Biol Psychiatry 55(3):313-316.

Benthem L, Keizer K, Wiegman CH, de Boer SF, Strubbe JH, Steffens AB, Kuipers F, Scheurink AJ. 2000. Excess portal venous long-chain fatty acids induce syndrome X via HPA axis and sympathetic activation. Am J Physiol Endocrinol Metab 279(6):E1286-1293.

Berding G, Schrader CH, Peschel T, van den Hoff J, Kolbe H, Meyer GJ, Dengler R, Knapp WH. 2003. [N-methyl 11C]meta-Hydroxyephedrine positron emission tomography in Parkinson's disease and multiple system atrophy. Eur J Nucl Med Mol Imaging 30(1):127-131.

Birkenfeld AL, Schroeder C, Boschmann M, Tank J, Franke G, Luft FC, Biaggioni I, Sharma AM, Jordan J. 2002. Paradoxical effect of sibutramine on autonomic cardiovascular regulation. Circulation 106(19):2459-2465.

Blaak EE, van Baak MA, Kempen KP, Saris WH. 1993. Role of alpha- and beta-adrenoceptors in sympathetically mediated thermogenesis. Am J Physiol 264(1 Pt 1):E11-17.

Blakely RD, De Felice LJ, Hartzell HC. 1994. Molecular physiology of norepinephrine and serotonin transporters. J Exp Biol 196:263-281.

Blakely RD, Ramamoorthy S, Schroeter S, Qian Y, Apparsundaram S, Galli A, DeFelice LJ. 1998. Regulated phosphorylation and trafficking of antidepressant-sensitive serotonin transporter proteins. Biol Psychiatry 44(3):169-178.

Bloomgarden ZT. 2002. Obesity, hypertension, and insulin resistance. Diabetes Care 25(11):2088-2097.

Bobbio M, Ferrua S, Opasich C, Porcu M, Lucci D, Scherillo M, Tavazzi L, Maggioni AP. 2003. Survival and hospitalization in heart failure patients with or without diabetes treated with beta-blockers. J Card Fail 9(3):192-202.

Bonisch H, Bruss M. 1994. The noradrenaline transporter of the neuronal plasma membrane. Ann N Y Acad Sci 733:193-202.

Bonisch H, Hammermann R, Bruss M. 1998. Role of protein kinase C and second messengers in regulation of the norepinephrine transporter. Adv Pharmacol 42:183-186.

Bousquet P, Feldman J, Velly J, Bloch R. 1975. Role of the ventral surface of the brain stem in the hypotensive action of clonidine. Eur J Pharmacol 34(1):151-156.

Brede M, Wiesmann F, Jahns R, Hadamek K, Arnolt C, Neubauer S, Lohse MJ, Hein L. 2002. Feedback inhibition of catecholamine release by two different alpha2-adrenoceptor subtypes prevents progression of heart failure. Circulation 106(19):2491-2496.

Bristow MR, Anderson FL, Port JD, Skerl L, Hershberger RE, Larrabee P, O'Connell JB, Renlund DG, Volkman K, Murray J, et al. 1991. Differences in beta-adrenergic neuroeffector mechanisms in ischemic versus idiopathic dilated cardiomyopathy. Circulation 84(3):1024-1039.

Bristow MR, Ginsburg R, Minobe W, Cubicciotti RS, Sageman WS, Lurie K, Billingham ME, Harrison DC, Stinson EB. 1982. Decreased catecholamine sensitivity and beta-adrenergic-receptor density in failing human hearts. N Engl J Med 307(4):205-211.

Brodde OE. 1993. Beta-adrenoceptors in cardiac disease. Pharmacol Ther 60(3):405-430.

Brodde OE, Bruck H, Leineweber K, Seyfarth T. 2001. Presence, distribution and physiological function of adrenergic and muscarinic receptor subtypes in the human heart. Basic Res Cardiol 96(6):528-538.

Brodde OE, Michel MC. 1999. Adrenergic and muscarinic receptors in the human heart. Pharmacol Rev 51(4):651-690.

Brodie BB, Costa E, Dlabac A, Neff NH, Smookler HH. 1966. Application of steady state kinetics to the estimation of synthesis rate and turnover time of tissue catecholamines. J Pharmacol Exp Ther 154(3):493-498.

Brouri F, Hanoun N, Mediani O, Saurini F, Hamon M, Vanhoutte PM, Lechat P. 2004. Blockade of beta 1- and desensitization of beta 2-adrenoceptors reduce isoprenaline-induced cardiac fibrosis. Eur J Pharmacol 485(1-3):227-234.

Bryan-Lluka LJ, Paczkowski FA, Bonisch H. 2001. Effects of short- and long-term exposure to c-AMP and c-GMP on the noradrenaline transporter. Neuropharmacology 40(4):607-617.

Buchanan TA, Xiang AH, Peters RK, Kjos SL, Marroquin A, Goico J, Ochoa C, Tan S, Berkowitz K, Hodis HN, Azen SP. 2002. Preservation of pancreatic beta-cell function and prevention of type 2 diabetes by pharmacological treatment of insulin resistance in high-risk hispanic women. Diabetes 51(9):2796-2803.

Bulow HP, Stahl F, Lauer B, Nekolla SG, Schuler G, Schwaiger M, Bengel FM. 2003. Alterations of myocardial presynaptic sympathetic innervation in patients with multi-vessel coronary artery disease but without history of myocardial infarction. Nucl Med Commun 24(3):233-239.

Caballero AE. 2005. Metabolic and vascular abnormalities in subjects at risk for type 2 diabetes: the early start of a dangerous situation. Arch Med Res 36(3):241-249.

Calera MR, Martinez C, Liu H, Jack AK, Birnbaum MJ, Pilch PF. 1998. Insulin increases the association of Akt-2 with Glut4-containing vesicles. J Biol Chem 273(13):7201-7204.

Canning PM, Courage ML, Frizzell LM. 2004. Prevalence of overweight and obesity in a provincial population of Canadian preschool children. Cmaj 171(3):240-242.

Cannon B, Nedergaard J. 2004. Brown adipose tissue: function and physiological significance. Physiol Rev 84(1):277-359.

Cardell SL. 2006. The natural killer T lymphocyte: a player in the complex regulation of autoimmune diabetes in non-obese diabetic mice. Clin Exp Immunol 143(2):194-202.

Carnethon MR, Golden SH, Folsom AR, Haskell W, Liao D. 2003. Prospective investigation of autonomic nervous system function and the development of type 2 diabetes: the Atherosclerosis Risk In Communities study, 1987-1998. Circulation 107(17):2190-2195.

Carson RP, Diedrich A, Robertson D. 2002. Autonomic control after blockade of the norepinephrine transporter: a model of orthostatic intolerance. J Appl Physiol 93(6):2192-2198.

Cettour-Rose P, Rohner-Jeanrenaud F. 2002. The leptin-like effects of 3-d peripheral administration of a melanocortin agonist are more marked in genetically obese Zucker (fa/fa) than in lean rats. Endocrinology 143(6):2277-2283.

Chakraborty PK, Gildersleeve DL, Jewett DM, Toorongian SA, Kilbourn MR, Schwaiger M, Wieland DM. 1993. High yield synthesis of high specific activty R-(-)-[^{11}C]epinephrine for routine PET studies in humans. Nucl Med Biol 20(8):939-944.

Chen H, Higashino H, Maeda K, Zhang Z, Ohta Y, Wang Z, Su DF, Yuan WJ. 2001. Reduction of cardiac norepinephrine improves postischemic heart function in stroke-prone spontaneously hypertensive rats. J Cardiovasc Pharmacol 38(6):821-832.

Choi YH, Li C, Hartzell DL, Lin J, Della-Fera MA, Baile CA. 2003. MTII administered peripherally reduces fat without invoking apoptosis in rats. Physiol Behav 79(2):331-337.

Citrome L. 2005. Metabolic syndrome and cardiovascular disease. J Psychopharmacol 19(6 Suppl):84-93.

Clark PB, Gage HD, Brown-Proctor C, Buchheimer N, Calles-Escandon J, Mach RH, Morton KA. 2004. Neurofunctional imaging of the pancreas utilizing the cholinergic PET radioligand [18F]4-fluorobenzyltrozamicol. Eur J Nucl Med Mol Imaging 31(2):258-260.

Cohade C, Mourtzikos KA, Wahl RL. 2003. "USA-Fat": prevalence is related to ambient outdoor temperature-evaluation with 18F-FDG PET/CT. J Nucl Med 44(8):1267-1270.

Cohen RA, Tesfamariam B, Weisbrod RM, Zitnay KM. 1990. Adrenergic denervation in rabbits with diabetes mellitus. Am J Physiol 259(1 Pt 2):H55-61.

Cohn JN, Levine TB, Olivari MT, Garberg V, Lura D, Francis GS, Simon AB, Rector T. 1984. Plasma norepinephrine as a guide to prognosis in patients with chronic congestive heart failure. N Engl J Med 311(13):819-823.

Collins S, Surwit RS. 2001. The beta-adrenergic receptors and the control of adipose tissue metabolism and thermogenesis. Recent Prog Horm Res 56:309-328.

Corbett SW, Stern JS, Keesey RE. 1986. Energy expenditure in rats with diet-induced obesity. Am J Clin Nutr 44(2):173-180.

Coudray C, Charon C, Komas N, Mory G, Diot-Dupuy F, Manganiello V, Ferre P, Bazin R. 1999. Evidence for the presence of several phosphodiesterase isoforms in brown adipose tissue of Zucker rats: modulation of PDE2 by the fa gene expression. FEBS Lett 456(1):207-210.

Cruz ML, Shaibi GQ, Weigensberg MJ, Spruijt-Metz D, Ball GD, Goran MI. 2005. Pediatric obesity and insulin resistance: chronic disease risk and implications for treatment and prevention beyond body weight modification. Annu Rev Nutr 25:435-468.

Czech MP, Corvera S. 1999. Signaling mechanisms that regulate glucose transport. J Biol Chem 274(4):1865-1868.

Daneman D. 2006. Type 1 diabetes. Lancet 367(9513):847-858.

Dart AM, Dietz R, Hieronymus K, Kubler W, Mayer E, Schomig A, Strasser R. 1984. Effects of alpha- and beta-adrenoceptor blockade on the neurally evoked overflow of endogenous noradrenaline from the rat isolated heart. Br J Pharmacol 81(3):475-478.

DaSilva JN, Lourenco CM, Meyer JH, Hussey D, Potter WZ, Houle S. 2002. Imaging cAMP-specific phosphodiesterase-4 in human brain with (*R*)-[^{11}C]rolipram and positron emission tomography. Eur J Nucl Med Mol Imaging 29(12):1680-1683.

DaSilva JN, Lourenco CM, Wilson AA, Houle S. 2001. Syntheses of the phosphodiesterase-4 inhibitors [^{11}C]Ro 20-1724, *R*-, *R/S*- and *S*-[^{11}C]rolipram. J Label Compd Radiopharm 44(5):373-384.

Deedwania PC, Fonseca VA. 2005. Diabetes, prediabetes, and cardiovascular risk: shifting the paradigm. Am J Med 118(9):939-947.

deGrado TR, Hutchins G, SA T, DM W, M S. 1993. Myocardial Kinetics of Carbon-11-Meta-Hydroxyephedrine: Retention Mechanisms and Effects of Norepinephrine. J Nucl Med 34(8):1287-1293.

DeGrado TR, Hutchins GD, Toorongian SA, Wieland DM, Schwaiger M. 1993. Myocardial kinetics of carbon-11-meta-hydroxyephedrine: retention mechanisms and effects of norepinephrine. J Nucl Med 34(8):1287-1293.

Deken SL, Wang D, Quick MW. 2003. Plasma membrane GABA transporters reside on distinct vesicles and undergo rapid regulated recycling. J Neurosci 23(5):1563-1568.

Del Rosario RB, Jung Y-W, Caraher J, Chakraborty PK, Wieland DM. 1996. Synthesis and Preliminary Evaluation of [^{11}C]-(-)-Phenylephrine as a Functional Heart Neuronal PET Agent. Nucl Med Biol 23:611-616.

Delaney CA, Dunger A, Di Matteo M, Cunningham JM, Green MH, Green IC. 1995. Comparison of inhibition of glucose-stimulated insulin secretion in rat islets of Langerhans by streptozotocin and methyl and ethyl nitrosoureas and methanesulphonates. Lack of correlation with nitric oxide-releasing or O6-alkylating ability. Biochem Pharmacol 50(12):2015-2020.

Delforge J, Mesangeau D, Dolle F, Merlet P, Loc'h C, Bottlaender M, Trebossen R, Syrota A. 2002. In vivo quantification and parametric images of the cardiac beta-adrenergic receptor density. J Nucl Med 43(2):215-226.

Depre C, Davies PJ, Taegtmeyer H. 1999a. Transcriptional adaptation of the heart to mechanical unloading. Am J Cardiol 83(12A):58H-63H.

Depre C, Rider MH, Hue L. 1998. Mechanisms of control of heart glycolysis. Eur J Biochem 258(2):277-290.

Depre C, Vanoverschelde JL, Taegtmeyer H. 1999b. Glucose for the heart. Circulation 99(4):578-588.

Ding YS, Fowler J. 2005. New-generation radiotracers for nAChR and NET. Nucl Med Biol 32(7):707-718.

Doze P, Elsinga PH, van Waarde A, Pieterman RM, Pruim J, Vaalburg W, Willemsen AT. 2002. Quantification of beta-adrenoceptor density in the human heart with (S)-[11C]CGP 12388 and a tracer kinetic model. Eur J Nucl Med Mol Imaging 29(3):295-304.

Du XJ, Riemersma RA. 1992. Effects of presynaptic alpha-adrenoceptors and neuronal reuptake on noradrenaline overflow and cardiac response. Eur J Pharmacol 211(2):221-226.

Dulloo AG. 2002. Biomedicine. A sympathetic defense against obesity. Science 297(5582):780-781.

Eisenhofer G, Rundquist B, Aneman A, Friberg P, Dakak N, Kopin IJ, Jacobs MC, Lenders JW. 1995. Regional release and removal of catecholamines and extraneuronal metabolism to metanephrines. J Clin Endocrinol Metab 80(10):3009-3017.

Eisenhofer G, Smolich JJ, Esler MD. 1992. Disposition of endogenous adrenaline compared to noradrenaline released by cardiac sympathetic nerves in the anaesthetized dog. Naunyn Schmiedebergs Arch Pharmacol 345(2):160-171.

Elder DA, Prigeon RL, Wadwa RP, Dolan LM, D'Alessio DA. 2005. {beta}-cell Function, Insulin Sensitivity and Glucose Tolerance in Obese Diabetic and Nondiabetic Adolescents and Young Adults. J Clin Endocrinol Metab.

Elsner M, Guldbakke B, Tiedge M, Munday R, Lenzen S. 2000. Relative importance of transport and alkylation for pancreatic beta-cell toxicity of streptozotocin. Diabetologia 43(12):1528-1533.

Enevoldsen LH, Stallknecht B, Fluckey JD, Galbo H. 2000. Effect of exercise training on in vivo lipolysis in intra-abdominal adipose tissue in rats. Am J Physiol Endocrinol Metab 279(3):E585-592.

Esler M. 1993. Clinical application of noradrenaline spillover methodology: delineation of regional human sympathetic nervous responses. Pharmacol Toxicol 73(5):243-253.

Esler M, Jennings G, Lambert G, Meredith I, Horne M, Eisenhofer G. 1990. Overflow of catecholamine neurotransmitters to the circulation: source, fate, and functions. Physiol Rev 70(4):963-985.

Esler M, Rumantir M, Wiesner G, Kaye D, Hastings J, Lambert G. 2001. Sympathetic nervous system and insulin resistance: from obesity to diabetes. Am J Hypertens 14(11 Pt 2):304S-309S.

Ewing DJ, Bellavere F, Espi F, McKibben BM, Buchanan KD, Riemersma RA, Clarke BF. 1986. Correlation of cardiovascular and neuroendocrine tests of autonomic function in diabetes. Metabolism 35(4):349-353.

Ewing DJ, Campbell IW, Clarke BF. 1980a. Assessment of cardiovascular effects in diabetic autonomic neuropathy and prognostic implications. Ann Intern Med 92(2 Pt 2):308-311.

Ewing DJ, Campbell IW, Clarke BF. 1980b. The natural history of diabetic autonomic neuropathy. Q J Med 49(193):95-108.

Fagerholm V, Gronroos T, Marjamaki P, Viljanen T, Scheinin M, Haaparanta M. 2004. Altered glucose homeostasis in alpha2A-adrenoceptor knockout mice. Eur J Pharmacol 505(1-3):243-252.

Farley C, Cook JA, Spar BD, Austin TM, Kowalski TJ. 2003. Meal pattern analysis of diet-induced obesity in susceptible and resistant rats. Obes Res 11(7):845-851.

Feve B, Elhadri K, Quignard-Boulange A, Pairault J. 1994. Transcriptional down-regulation by insulin of the beta 3-adrenergic receptor expression in 3T3-F442A adipocytes: a mechanism for repressing the cAMP signaling pathway. Proc Natl Acad Sci U S A 91(12):5677-5681.

Feve B, Emorine LJ, Lasnier F, Blin N, Baude B, Nahmias C, Strosberg AD, Pairault J. 1991. Atypical beta-adrenergic receptor in 3T3-F442A adipocytes. Pharmacological and molecular relationship with the human beta 3-adrenergic receptor. J Biol Chem 266(30):20329-20336.

Figlewicz DP, Bentson K, Ocrant I. 1993a. The effect of insulin on norepinephrine uptake by PC12 cells. Brain Res Bull 32(4):425-431.

Figlewicz DP, Szot P, Israel PA, Payne C, Dorsa DM. 1993b. Insulin reduces norepinephrine transporter mRNA in vivo in rat locus coeruleus. Brain Res 602(1):161-164.

Finn RD, Schlyer DJ. 2002. Production of Radionuclides for PET. In: Wahl RL, editor. Principles and Practice of Positron Emission Tomography. Philadelphia, PA: Lippincott Williams & Wilkins. p. 1-15.

Flegal KM, Williamson DF, Pamuk ER, Rosenberg HM. 2004. Estimating deaths attributable to obesity in the United States. Am J Public Health 94(9):1486-1489.

Foley KF, Van Dort ME, Sievert MK, Ruoho AE, Cozzi NV. 2002. Stereospecific inhibition of monoamine uptake transporters by meta-hydroxyephedrine isomers. J Neural Transm 109(10):1229-1240.

Fowler JS, Ding YS. 2002. Chemistry. In: Wahl RL, editor. Principles and Practice of Positron Emission Tomography. Philadelphia, PA: Lippincott Williams & Wilkins. p. 16-47.

Fowler JS, Logan J, Wang GJ, Volkow ND, Telang F, Ding YS, Shea C, Garza V, Xu Y, Li Z, Alexoff D, Vaska P, Ferrieri R, Schlyer D, Zhu W, John Gatley S. 2004. Comparison of the binding of the irreversible monoamine oxidase tracers, [(11)C]clorgyline and [(11)C]l-deprenyl in brain and peripheral organs in humans. Nucl Med Biol 31(3):313-319.

Freeman R. 2006. Assessment of cardiovascular autonomic function. Clin Neurophysiol 117(4):716-730.

Fuller RW, Snoddy HD, Perry KW, Bernstein JR, Murphy PJ. 1981. Formation of alpha-methylnorepinephrine as a metabolite of metaraminol in guinea pigs. Biochem Pharmacol 30(20):2831-2836.

Gallego M, Setien R, Izquierdo MJ, Casis O, Casis E. 2003. Diabetes-induced biochemical changes in central and peripheral catecholaminergic systems. Physiol Res 52(6):735-741.

Ganda OP, Rossini AA, Like AA. 1976. Studies on streptozotocin diabetes. Diabetes 25(7):595-603.

Ganguly PK, Beamish RE, Dhalla KS, Innes IR, Dhalla NS. 1987. Norepinephrine storage, distribution, and release in diabetic cardiomyopathy. Am J Physiol 252(6 Pt 1):E734-739.

Ganguly PK, Dhalla KS, Innes IR, Beamish RE, Dhalla NS. 1986. Altered norepinephrine turnover and metabolism in diabetic cardiomyopathy. Circ Res 59(6):684-693.

Gao J, Ghibaudi L, van Heek M, Hwa JJ. 2002. Characterization of diet-induced obese rats that develop persistent obesity after 6 months of high-fat followed by 1 month of low-fat diet. Brain Res 936(1-2):87-90.

Garcia-Sevilla JA, Zubieta JK. 1986. Activation and desensitization of presynaptic alpha 2-adrenoceptors after inhibition of neuronal uptake by antidepressant drugs in the rat vas deferens. Br J Pharmacol 89(4):673-683.

Geerlings A, Lopez-Corcuera B, Aragon C. 2000. Characterization of the interactions between the glycine transporters GLYT1 and GLYT2 and the SNARE protein syntaxin 1A. FEBS Lett 470(1):51-54.

Giacobino JP. 1999. Effects of dietary deprivation, obesity and exercise on UCP3 mRNA levels. Int J Obes Relat Metab Disord 23 Suppl 6:S60-63.

Gilinsky MA, Faibushevish AA, Lunte CE. 2001. Determination of myocardial norepinephrine in freely moving rats using in vivo microdialysis sampling and liquid chromatography with dual-electrode amperometric detection. J Pharm Biomed Anal 24(5-6):929-935.

Giralt MT, Garcia-Sevilla JA. 1989. Acute and long-term regulation of brain alpha 2-adrenoceptors after manipulation of noradrenergic transmission in the rat. Eur J Pharmacol 164(3):455-466.

Goldstein DS, Holmes C, Frank SM, Dendi R, Cannon RO, 3rd, Sharabi Y, Esler MD, Eisenhofer G. 2002. Cardiac sympathetic dysautonomia in chronic orthostatic intolerance syndromes. Circulation 106(18):2358-2365.

Goodwin GW, Ahmad F, Doenst T, Taegtmeyer H. 1998a. Energy provision from glycogen, glucose, and fatty acids on adrenergic stimulation of isolated working rat hearts. Am J Physiol 274(4 Pt 2):H1239-1247.

Goodwin GW, Taylor CS, Taegtmeyer H. 1998b. Regulation of energy metabolism of the heart during acute increase in heart work. J Biol Chem 273(45):29530-29539.

Graefe KH, Bonisch H, Keller B. 1978. Saturation kinetics of the adrenergic neurone uptake system in the perfused rabbit heart. A new method for determination of initial rates of amine uptake. Naunyn Schmiedebergs Arch Pharmacol 302(3):263-273.

Grassi G, Dell'Oro R, Quarti-Trevano F, Scopelliti F, Seravalle G, Paleari F, Gamba PL, Mancia G. 2005. Neuroadrenergic and reflex abnormalities in patients with metabolic syndrome. Diabetologia 48(7):1359-1365.

Grassi G, Seravalle G, Colombo M, Bolla G, Cattaneo BM, Cavagnini F, Mancia G. 1998. Body weight reduction, sympathetic nerve traffic, and arterial baroreflex in obese normotensive humans. Circulation 97(20):2037-2042.

Greenshaw AJ, Nazarali AJ, Rao TS, Baker GB, Coutts RT. 1988. Chronic tranylcypromine treatment induces functional alpha 2-adrenoceptor down-regulation in rats. Eur J Pharmacol 154(1):67-72.

Haase J, Killian AM, Magnani F, Williams C. 2001. Regulation of the serotonin transporter by interacting proteins. Biochem Soc Trans 29(Pt 6):722-728.

Haenni A, Lithell H. 1994. Treatment with a beta-blocker with beta 2-agonism improves glucose and lipid metabolism in essential hypertension. Metabolism 43(4):455-461.

Haffner SM, Miettinen H. 1997. Insulin resistance implications for type II diabetes mellitus and coronary heart disease. Am J Med 103(2):152-162.

Haffner SM, Morales PA, Stern MP, Gruber MK. 1992. Lp(a) concentrations in NIDDM. Diabetes 41(10):1267-1272.

Hagstrom-Toft E, Arner P, Wahrenberg H, Wennlund A, Ungerstedt U, Bolinder J. 1993. Adrenergic regulation of human adipose tissue metabolism in situ during mental stress. J Clin Endocrinol Metab 76(2):392-398.

Haney M, Collins ED, Ward AS, Foltin RW, Fischman MW. 1999. Effect of a selective dopamine D1 agonist (ABT-431) on smoked cocaine self-administration in humans. Psychopharmacology (Berl) 143(1):102-110.

Hanft G, Gross G. 1990. The effect of reserpine, desipramine and thyroid hormone on α_{1a}- and α_{1b}-adrenoceptor binding sites: evidence for a subtype-specific regulation. Br J Clin Pharmac 30:125S-127S.

Hany TF, Gharehpapagh E, Kamel EM, Buck A, Himms-Hagen J, von Schulthess GK. 2002. Brown adipose tissue: a factor to consider in symmetrical tracer uptake in the neck and upper chest region. Eur J Nucl Med Mol Imaging 29(10):1393-1398.

Harder R, Bonisch H. 1985. Effects of monovalent ions on the transport of noradrenaline across the plasma membrane of neuronal cells (PC-12 cells). J Neurochem 45(4):1154-1162.

Harper ME, Brand MD. 1993. The quantitative contributions of mitochondrial proton leak and ATP turnover reactions to the changed respiration rates of hepatocytes from rats of different thyroid status. J Biol Chem 268(20):14850-14860.

Harper ME, Himms-Hagen J. 2001. Mitochondrial efficiency: lessons learned from transgenic mice. Biochim Biophys Acta 1504(1):159-172.

Haynes WG, Morgan DA, Walsh SA, Mark AL, Sivitz WI. 1997. Receptor-mediated regional sympathetic nerve activation by leptin. J Clin Invest 100(2):270-278.

Hebert C, Habimana A, Elie R, Reader TA. 2001. Effects of chronic antidepressant treatments on 5-HT and NA transporters in rat brain: an autoradiographic study. Neurochem Int 38(1):63-74.

Herscovitch P. 1990. Principles of positron emission tomography. In: Martin W, editor. Functional Imaging in Movement Disorders. Boca Raton: CRC Press. p. 1-46.

Hertel C, Muller P, Portenier M, Staehelin M. 1983. Determination of the desensitization of beta-adrenergic receptors by [3H]CGP-12177. Biochem J 216(3):669-674.

Heyndrickx GR, Vilaine JP, Moerman EJ, Leusen I. 1984. Role of prejunctional alpha 2-adrenergic receptors in the regulation of myocardial performance during exercise in conscious dogs. Circ Res 54(6):683-693.

Hilton J, Yokoi F, Dannals RF, Ravert HT, Szabo Z, Wong DF. 2000. Column-switching HPLC for the analysis of plasma in PET imaging studies. Nucl Med Biol 27(6):627-630.

Himms-Hagen J. 1990. Brown adipose tissue thermogenesis: interdisciplinary studies. Faseb J 4(11):2890-2898.

Hoffman BB, Lefkowitz RJ. 1995. Catecholamines, Sympathomimetic Drugs, and Adrenergic Receptor Antagonists. In: Hardman JGL, Lee E., editor. Goodman & Gilman's The Pharmacological Basis of Therapeutics. Ninth Edition ed. New York: McGraw-Hill. p. 199-248.

Holton KL, Loder MK, Melikian HE. 2005. Nonclassical, distinct endocytic signals dictate constitutive and PKC-regulated neurotransmitter transporter internalization. Nat Neurosci 8(7):881-888.

Hows ME, Lacroix L, Heidbreder C, Organ AJ, Shah AJ. 2004. High-performance liquid chromatography/tandem mass spectrometric assay for the simultaneous measurement of dopamine, norepinephrine, 5-hydroxytryptamine and cocaine in biological samples. J Neurosci Methods 138(1-2):123-132.

Huff RA, Vaughan RA, Kuhar MJ, Uhl GR. 1997. Phorbol esters increase dopamine transporter phosphorylation and decrease transport Vmax. J Neurochem 68(1):225-232.

Jacob S, Rett K, Henriksen EJ. 1998. Antihypertensive therapy and insulin sensitivity: do we have to redefine the role of beta-blocking agents? Am J Hypertens 11(10):1258-1265.

Kaiser T, Sawicki PT. 2004. Acarbose for prevention of diabetes, hypertension and cardiovascular events? A critical analysis of the STOP-NIDDM data. Diabetologia 47(3):575-580.

Kalsner S. 1984. Limitations of presynaptic theory: no support for feedback control of autonomic effectors. Fed Proc 43(5):1358-1364.

Kannel WB, Brand N, Skinner JJ, Jr., Dawber TR, McNamara PM. 1967. The relation of adiposity to blood pressure and development of hypertension. The Framingham study. Ann Intern Med 67(1):48-59.

Katsumata K, Katsumata K, Jr., Katsumata Y. 1992. Protective effect of diltiazem hydrochloride on the occurrence of alloxan- or streptozotocin-induced diabetes in rats. Horm Metab Res 24(11):508-510.

Kawai H, Mohan A, Hagen J, Dong E, Armstrong J, Stevens SY, Liang CS. 2000. Alterations in cardiac adrenergic terminal function and beta-adrenoceptor density in pacing-induced heart failure. Am J Physiol Heart Circ Physiol 278(5):H1708-1716.

Kaye DM, Wiviott SD, Kobzik L, Kelly RA, Smith TW. 1997. S-nitrosothiols inhibit neuronal norepinephrine transport. Am J Physiol 272(2 Pt 2):H875-883.

Keck PE, Jr., Carter WP, Nierenberg AA, Cooper TB, Potter WZ, Rothschild AJ. 1991. Acute cardiovascular effects of tranylcypromine: correlation with plasma drug, metabolite, norepinephrine, and MHPG levels. J Clin Psychiatry 52(6):250-254.

Keenan KP, Hoe CM, Mixson L, McCoy CL, Coleman JB, Mattson BA, Ballam GA, Gumprecht LA, Soper KA. 2005. Diabesity: a polygenic model of dietary-induced obesity from ad libitum overfeeding of sprague-dawley rats and its modulation by moderate and marked dietary restriction. Toxicol Pathol 33(6):650-674.

Keller NR, Diedrich A, Appalsamy M, Tuntrakool S, Lonce S, Finney C, Caron MG, Robertson D. 2004. Norepinephrine transporter-deficient mice exhibit excessive tachycardia and elevated blood pressure with wakefulness and activity. Circulation 110(10):1191-1196.

Kenchaiah S, Evans JC, Levy D, Wilson PW, Benjamin EJ, Larson MG, Kannel WB, Vasan RS. 2002. Obesity and the risk of heart failure. N Engl J Med 347(5):305-313.

Kern W, Peters A, Born J, Fehm HL, Schultes B. 2005. Changes in blood pressure and plasma catecholamine levels during prolonged hyperinsulinemia. Metabolism 54(3):391-396.

Kiyono Y, Iida Y, Kawashima H, Tamaki N, Nishimura H, Saji H. 2001. Regional alterations of myocardial norepinephrine transporter density in streptozotocin-induced diabetic rats: implications for heterogeneous cardiac accumulation of MIBG in diabetes. Eur J Nucl Med 28(7):894-899.

Koeppe RA. 2002. Data Analysis and Imaging Processing. In: Wahl RL, editor. Principles and Practice of Positron Emission Tomography. Philadelphia, PA: Lippincott Williams & Wilkins. p. 65-99.

Kohn AD, Takeuchi F, Roth RA. 1996. Akt, a pleckstrin homology domain containing kinase, is activated primarily by phosphorylation. J Biol Chem 271(36):21920-21926.

Kopin IJ, Gordon EK. 1963. Origin of Norepinephrine in the Heart. Nature 199:1289.

Kopka K, Wagner S, Riemann B, Law MP, Puke C, Luthra SK, Pike VW, Wichter T, Schmitz W, Schober O, Schafers M. 2003. Design of new beta1-selective adrenoceptor ligands as potential radioligands for in vivo imaging. Bioorg Med Chem 11(16):3513-3527.

Kostis JB, Sanders M. 2005. The association of heart failure with insulin resistance and the development of type 2 diabetes. Am J Hypertens 18(5 Pt 1):731-737.

Kroncke KD, Fehsel K, Sommer A, Rodriguez ML, Kolb-Bachofen V. 1995. Nitric oxide generation during cellular metabolization of the diabetogenic N-methyl-N-nitroso-urea streptozotozin contributes to islet cell DNA damage. Biol Chem Hoppe Seyler 376(3):179-185.

LaBuda CJ, Fuchs PN. 2002. Catecholamine depletion by reserpine blocks the anxiolytic actions of ethanol in the rat. Alcohol 26(1):55-59.

Lafontan M, Berlan M. 1993. Fat cell adrenergic receptors and the control of white and brown fat cell function. J Lipid Res 34(7):1057-1091.

Landsberg L. 1986. Diet, obesity and hypertension: an hypothesis involving insulin, the sympathetic nervous system, and adaptive thermogenesis. Q J Med 61(236):1081-1090.

Landsberg L. 2005. Insulin resistance and the metabolic syndrome. Diabetologia 48(7):1244-1246.

Langer O, Valette H, Dolle F, Halldin C, Loc'h C, Fuseau C, Coulon C, Ottaviani M, Bottlaender M, Maziere B, Crouzel C. 2000. High specific radioactivity (1R,2S)-4-[(18)F]fluorometaraminol: a PET radiotracer for mapping sympathetic nerves of the heart. Nucl Med Biol 27(3):233-238.

Langer SZ. 1980. Presynaptic regulation of the release of catecholamines. Pharmacol Rev 32(4):337-362.

Law MP, Osman S, Davenport RJ, Cunningham VJ, Pike VW, Camici PG. 1997. Biodistribution and metabolism of [N-methyl-11C]m-hydroxyephedrine in the rat. Nucl Med Biol 24(5):417-424.

Leibowitz SF, Wortley KE. 2004. Hypothalamic control of energy balance: different peptides, different functions. Peptides 25(3):473-504.

Levin BE, Dunn-Meynell AA. 2000. Defense of body weight against chronic caloric restriction in obesity-prone and -resistant rats. Am J Physiol Regul Integr Comp Physiol 278(1):R231-237.

Levin BE, Dunn-Meynell AA. 2002. Defense of body weight depends on dietary composition and palatability in rats with diet-induced obesity. Am J Physiol Regul Integr Comp Physiol 282(1):R46-54.

Levin BE, Dunn-Meynell AA. 2004. Chronic exercise lowers the defended body weight gain and adiposity in diet-induced obese rats. Am J Physiol Regul Integr Comp Physiol 286(4):R771-778.

Levin BE, Hogan S, Sullivan AC. 1989. Initiation and perpetuation of obesity and obesity resistance in rats. Am J Physiol 256(3 Pt 2):R766-771.

Levin BE, Keesey RE. 1998. Defense of differing body weight set points in diet-induced obese and resistant rats. Am J Physiol 274(2 Pt 2):R412-419.

Levin BE, Sullivan AC. 1987. Glucose-induced norepinephrine levels and obesity resistance. Am J Physiol 253(3 Pt 2):R475-481.

Levin BE, Sullivan AC. 1989. Glucose-induced sympathetic activation in obesity-prone and resistant rats. Int J Obes 13(2):235-246.

Levin BE, Triscari J, Hogan S, Sullivan AC. 1987. Resistance to diet-induced obesity: food intake, pancreatic sympathetic tone, and insulin. Am J Physiol 252(3 Pt 2):R471-478.

Levin BE, Triscari J, Sullivan AC. 1983. Altered sympathetic activity during development of diet-induced obesity in rat. Am J Physiol 244(3):R347-355.

Levine TB, Francis GS, Goldsmith SR, Simon AB, Cohn JN. 1982. Activity of the sympathetic nervous system and renin-angiotensin system assessed by plasma hormone levels and their relation to hemodynamic abnormalities in congestive heart failure. Am J Cardiol 49(7):1659-1666.

Liang CS, Himura Y, Kashiki M, Stevens SY. 2002. Differential pre- and postsynaptic effects of desipramine on cardiac sympathetic nerve terminals in RHF. Am J Physiol Heart Circ Physiol 283(5):H1863-1872.

Liao D, Cai J, Barnes RW, Tyroler HA, Rautaharju P, Holme I, Heiss G. 1996. Association of cardiac autonomic function and the development of hypertension: the ARIC study. Am J Hypertens 9(12 Pt 1):1147-1156.

Liatis S, Tentolouris N, Katsilambros N. 2004. Cardiac autonomic nervous system activity in obesity. Pediatr Endocrinol Rev 1 Suppl 3:476-483.

Lindmark S, Lonn L, Wiklund U, Tufvesson M, Olsson T, Eriksson JW. 2005. Dysregulation of the autonomic nervous system can be a link between visceral adiposity and insulin resistance. Obes Res 13(4):717-728.

Link JM, Stratton JR, Levy W, Poole JE, Shoner SC, Stuetzle W, Caldwell JH. 2003. PET measures of pre- and postsynaptic cardiac beta adrenergic function. Nucl Med Biol 30(8):795-803.

Link JM, Synovec RE, Krohn KA, Caldwell JH. 1997. High speed liquid chromatography of phenylethanolamines for the kinetic analysis of [11C]-meta-hydroxyephedrine and metabolites in plasma. J Chromatogr B Biomed Sci Appl 693(1):31-41.

Loder MK, Melikian HE. 2003. The dopamine transporter constitutively internalizes and recycles in a protein kinase C-regulated manner in stably transfected PC12 cell lines. J Biol Chem 278(24):22168-22174.

Lourenco CM, DaSilva JN, Warsh JJ, Wilson AA, Houle S. 1999a. Imaging of cAMP-specific phosphodiesterase-IV: comparison of [^{11}C]rolipram and [^{11}C]Ro 20-1724 in rats. Synapse 31(1):41-50.

Lourenco CM, DaSilva JN, Wilson AA, Houle S. 1999b. Metabolism of the phosphodiesterase-4 inhibitor R-[11C]rolipram in rat plasma and brain. J Label Compd Radiopharm 42:S663-S665.

Lourenco CM, Houle S, Wilson AA, DaSilva JN. 2001. Characterization of (*R*)-[^{11}C]rolipram for PET imaging of phosphodiesterase-4: in vivo binding, metabolism, and dosimetry studies in rats. Nucl Med Biol 28(4):347-358.

Lourenco CM, Kenk M, Beanlands RS, DaSilva JN. 2006. Increasing synaptic noradrenaline, serotonin and histamine enhances in vivo binding of phosphodiesterase-4 inhibitor (R)-[11C]rolipram in rat brain, lung and heart. Life Sci 79(4):356-364.

Lowe MC, Reichenbach DD, Horita A. 1975. Extraneuronal monoamine oxidase in rat heart: biochemical characterization and electron microscopic localization. J Pharmacol Exp Ther 194(3):522-536.

Lowell BB, Bachman ES. 2003. Beta-Adrenergic receptors, diet-induced thermogenesis, and obesity. J Biol Chem 278(32):29385-29388.

Mager DE, Wan R, Brown M, Cheng A, Wareski P, Abernethy DR, Mattson MP. 2006. Caloric restriction and intermittent fasting alter spectral measures of heart rate and blood pressure variability in rats. Faseb J 20(6):631-637.

Makaritsis KP, Johns C, Gavras I, Gavras H. 2000. Role of alpha(2)-adrenergic receptor subtypes in the acute hypertensive response to hypertonic saline infusion in anephric mice. Hypertension 35(2):609-613.

Malizia AL, Melichar JK, Rhodes CG, Haida A, Reynolds AH, Jones T, Nutt DJ. 2000. Desipramine binding to noradrenaline reuptake sites in cardiac sympathetic neurons in man in vivo. Eur J Pharmacol 391(3):263-267.

Mandela P, Ordway GA. 2006. The norepinephrine transporter and its regulation. J Neurochem 97(2):310-333.

Mao W, Iwai C, Qin F, Liang CS. 2005. Norepinephrine induces endoplasmic reticulum stress and downregulation of norepinephrine transporter density in PC12 cells via oxidative stress. Am J Physiol Heart Circ Physiol 288(5):H2381-2389.

Marangou AG, Alford FP, Ward G, Liskaser F, Aitken PM, Weber KM, Boston RC, Best JD. 1988. Hormonal effects of norepinephrine on acute glucose disposal in humans: a minimal model analysis. Metabolism 37(9):885-891.

Mardon K, Montagne O, Elbaz N, Malek Z, Syrota A, Dubois-Rande JL, Meignan M, Merlet P. 2003. Uptake-1 carrier downregulates in parallel with the beta-adrenergic receptor desensitization in rat hearts chronically exposed to high levels of circulating norepinephrine: implications for cardiac neuroimaging in human cardiomyopathies. J Nucl Med 44(9):1459-1466.

Martinez-Merlos MT, Angeles-Castellanos M, Diaz-Munoz M, Aguilar-Roblero R, Mendoza J, Escobar C. 2004. Dissociation between adipose tissue signals, behavior and the food-entrained oscillator. J Endocrinol 181(1):53-63.

Masuo K, Katsuya T, Fu Y, Rakugi H, Ogihara T, Tuck ML. 2005. Beta2-adrenoceptor polymorphisms relate to insulin resistance and sympathetic overactivity as early markers of metabolic disease in nonobese, normotensive individuals. Am J Hypertens 18(7):1009-1014.

Masuo K, Mikami H, Ogihara T, Tuck ML. 1997. Sympathetic nerve hyperactivity precedes hyperinsulinemia and blood pressure elevation in a young, nonobese Japanese population. Am J Hypertens 10(1):77-83.

Matthias A, Ohlson KB, Fredriksson JM, Jacobsson A, Nedergaard J, Cannon B. 2000. Thermogenic responses in brown fat cells are fully UCP1-dependent. UCP2 or UCP3 do not substitute for UCP1 in adrenergically or fatty scid-induced thermogenesis. J Biol Chem 275(33):25073-25081.

McClain DA, Crook ED. 1996. Hexosamines and insulin resistance. Diabetes 45(8):1003-1009.

Meana JJ, Herrera-Marschitz M, Goiny M, Silveira R. 1997. Modulation of catecholamine release by alpha 2-adrenoceptors and I1-imidazoline receptors in rat brain. Brain Res 744:216.

Merlet P, Benvenuti C, Moyse D, Pouillart F, Dubois-Rande JL, Duval AM, Loisance D, Castaigne A, Syrota A. 1999. Prognostic value of MIBG imaging in idiopathic dilated cardiomyopathy. J Nucl Med 40(6):917-923.

Mohell N, Dicker A. 1989. The beta-adrenergic radioligand [3H]CGP-12177, generally classified as an antagonist, is a thermogenic agonist in brown adipose tissue. Biochem J 261(2):401-405.

Mokdad AH, Bowman BA, Ford ES, Vinicor F, Marks JS, Koplan JP. 2001. The continuing epidemics of obesity and diabetes in the United States. Jama 286(10):1195-1200.

Molon-Noblot S, Keenan KP, Coleman JB, Hoe CM, Laroque P. 2001. The effects of ad libitum overfeeding and moderate and marked dietary restriction on age-related spontaneous pancreatic islet pathology in Sprague-Dawley rats. Toxicol Pathol 29(3):353-362.

Morgan NG, Cable HC, Newcombe NR, Williams GT. 1994. Treatment of cultured pancreatic B-cells with streptozotocin induces cell death by apoptosis. Biosci Rep 14(5):243-250.

Morisco C, Condorelli G, Trimarco V, Bellis A, Marrone C, Sadoshima J, Trimarco B. 2005. Akt mediates the cross-talk between beta-adrenergic and insulin receptors in neonatal cardiomyocytes. Circ Res 96(2):180-188.

Muller FU, Boknik P, Horst A, Knapp J, Linck B, Schmitz W, Vahlensieck U, Walter A. 1995. In vivo isoproterenol treatment leads to downregulation of the mRNA encoding the cAMP response element binding protein in the rat heart. Biochem Biophys Res Commun 215(3):1043-1049.

Muller MJ, von zur Muhlen A, Lautz HU, Schmidt FW, Daiber M, Hurter P. 1989. Energy expenditure in children with type I diabetes: evidence for increased thermogenesis. Bmj 299(6697):487-491.

Muscelli E, Emdin M, Natali A, Pratali L, Camastra S, Gastaldelli A, Baldi S, Carpeggiani C, Ferrannini E. 1998. Autonomic and hemodynamic responses to insulin in lean and obese humans. J Clin Endocrinol Metab 83(6):2084-2090.

Myrsen U, Keymeulen B, Pipeleers DG, Sundler F. 1996. Beta cells are important for islet innervation: evidence from purified rat islet-cell grafts. Diabetologia 39(1):54-59.

Någren K, Halldin C, Swahn C-G, Suhara T, Farde L. 1996. [^{11}C]Metaraminol, a false neurotransmitter: Preparation, metabolite studies and positron emission tomography examination in monkey. Nuclear Medicine & Biology 23:221-227.

Newman S, Steed L, Mulligan K. 2004. Self-management interventions for chronic illness. Lancet 364(9444):1523-1537.

Niijima A. 1986. Neural control of blood glucose level. Jpn J Physiol 36(5):827-841.

Nitzsche EU, Choi Y, Killion D, Hoh CK, Hawkins RA, Rosenthal JT, Buxton DB, Huang SC, Phelps ME, Schelbert HR. 1993. Quantification and parametric imaging of renal cortical blood flow in vivo based on Patlak graphical analysis. Kidney Int 44(5):985-996.

Noble MD, Liddle RA. 2005. Neurohormonal control of exocrine pancreatic secretion. Curr Opin Gastroenterol 21(5):531-537.

Norton GR, Candy G, Woodiwiss AJ. 1996. Aminoguanidine prevents the decreased myocardial compliance produced by streptozotocin-induced diabetes mellitus in rats. Circulation 93(10):1905-1912.

Novak I. 1998. beta-Adrenergic regulation of ion transport in pancreatic ducts: patch-clamp study of isolated rat pancreatic ducts. Gastroenterology 115(3):714-721.

Nup C, Rosenberg P, Linke H, Tordik P. 2001. Quantitation of catecholamines in inflamed human dental pulp by high-performance liquid chromatography. J Endod 27(2):73-75.

O'Brien CP. 1995. Drug Addiction and Drug Abuse. In: Hardman JG, Limbird LE, editors. Goodman & Gilman's The Pharmacological Basis of Therapeutics. New York, NY: McGraw-Hill.

O'Brien IA, McFadden JP, Corrall RJ. 1991. The influence of autonomic neuropathy on mortality in insulin-dependent diabetes. Q J Med 79(290):495-502.

Odaka K, von Scheidt W, Ziegler SI, Ueberfuhr P, Nekolla SG, Reichart B, Bengel FM, Schwaiger M. 2001. Reappearance of cardiac presynaptic sympathetic nerve terminals in the transplanted heart: correlation between PET using (11)C-hydroxyephedrine and invasively measured norepinephrine release. J Nucl Med 42(7):1011-1016.

O'Rahilly S, Yeo GS, Farooqi IS. 2004. Melanocortin receptors weigh in. Nat Med 10(4):351-352.

Pacak K, Armando I, Komoly S, Fukuhara K, Weise VK, Holmes C, Kopin IJ, Goldstein DS. 1992. Hypercortisolemia inhibits yohimbine-induced release of norepinephrine in the posterolateral hypothalamus of conscious rats. Endocrinol 131:1369-1376.

Pacholczyk T, Blakely RD, Amara SG. 1991. Expression cloning of a cocaine- and antidepressant-sensitive human noradrenaline transporter. Nature 350(6316):350-354.

Paczkowski FA, Bryan-Lluka LJ. 2004. Role of proline residues in the expression and function of the human noradrenaline transporter. J Neurochem 88(1):203-211.

Pao CS, Benovic JL. 2002. Phosphorylation-independent desensitization of G protein-coupled receptors? Sci STKE 2002(153):PE42.

Paolisso G, De Riu S, Marrazzo G, Verza M, Varricchio M, D'Onofrio F. 1991. Insulin resistance and hyperinsulinemia in patients with chronic congestive heart failure. Metabolism 40(9):972-977.

Park SY, Lee YJ, Kim YW, Kim HJ, Doh KO, Lee MK, Kim JY, Lee SK. 2000. Change in activity of the sympathetic nervous system in diet-induced obese rats. J Korean Med Sci 15(6):635-640.

Pessin JE, Saltiel AR. 2000. Signaling pathways in insulin action: molecular targets of insulin resistance. J Clin Invest 106(2):165-169.

Pissarek M, Ermert J, Oesterreich G, Bier D, Coenen HH. 2002. Relative uptake, metabolism, and beta-receptor binding of (1R,2S)-4-(18)F-fluorometaraminol and (123)I-MIBG in normotensive and spontaneously hypertensive rats. J Nucl Med 43(3):366-373.

Poirier P, Giles TD, Bray GA, Hong Y, Stern JS, Pi-Sunyer FX, Eckel RH. 2006. Obesity and cardiovascular disease: pathophysiology, evaluation, and effect of weight loss. Arterioscler Thromb Vasc Biol 26(5):968-976.

Pop-Busui R, Kirkwood I, Schmid H, Marinescu V, Schroeder J, Larkin D, Yamada E, Raffel DM, Stevens MJ. 2004. Sympathetic dysfunction in type 1 diabetes: association with impaired myocardial blood flow reserve and diastolic dysfunction. J Am Coll Cardiol 44(12):2368-2374.

Portha B, Picon L, Rosselin G. 1979. Chemical diabetes in the adult rat as the spontaneous evolution of neonatal diabetes. Diabetologia 17(6):371-377.

Powell SB, Palomo J, Carasso BS, Bakshi VP, Geyer MA. 2005. Yohimbine disrupts prepulse inhibition in rats via action at 5-HT1A receptors, not alpha2-adrenoceptors. Psychopharmacology (Berl) 180(3):491-500.

Quilliot D, Zannad F, Ziegler O. 2005. Impaired response of cardiac autonomic nervous system to glucose load in severe obesity. Metabolism 54(7):966-974.

Raasch W, Dominiak P, Ziegler A, Dendorfer A. 2004. Reduction of vascular noradrenaline sensitivity by AT1 antagonists depends on functional sympathetic innervation. Hypertension 44(3):346-351.

Raasmaja A, York DA. 1988. Alpha 1- and beta-adrenergic receptors in brown adipose tissue of lean (Fa/?) and obese (fa/fa) Zucker rats. Effects of cold-acclimation, sucrose feeding and adrenalectomy. Biochem J 249(3):831-838.

Raffel D, Wieland D. 2001a. Assessment of cardiac sympathetic nerve integrity with positron emission tomography. Nucl Med Biol 28:541-559.

Raffel DM, Corbett JR, del Rosario RB, Gildersleeve DL, Chiao PC, Schwaiger M, Wieland DM. 1996. Clinical evaluation of carbon-11-phenylephrine: MAO-sensitive marker of cardiac sympathetic neurons. J Nucl Med 37(12):1923-1931.

Raffel DM, Jung YW, Gildersleeve DL, Chen W. ^{11}C-Phenethylguanidines: A novel class of radiotracers for quntitative PET studies of cardiac sympathetic innervation.; 2005; Toronto, ON, Canada.

Randle PJ, Garland PB, Hales CN, Newsholme EA. 1963. The glucose fatty-acid cycle. Its role in insulin sensitivity and the metabolic disturbances of diabetes mellitus. Lancet 1:785-789.

Rawlow A, Fleig H, Kurahashi K, Trendelenburg U. 1980. The neuronal and extraneuronal uptake and deamination of 3H-(-)-phenylephrine in the perfused rat heart. Naunyn Schmiedebergs Arch Pharmacol 314(3):237-247.

Reaven GM. 2005. Insulin resistance, the insulin resistance syndrome, and cardiovascular disease. Panminerva Med 47(4):201-210.

Reaven GM, Chen YD. 1988. Role of abnormal free fatty acid metabolism in the development of non-insulin-dependent diabetes mellitus. Am J Med 85(5A):106-112.

Reaven GM, Hollenbeck C, Jeng CY, Wu MS, Chen YD. 1988. Measurement of plasma glucose, free fatty acid, lactate, and insulin for 24 h in patients with NIDDM. Diabetes 37(8):1020-1024.

Ren J. 2004. Leptin and hyperleptinemia - from friend to foe for cardiovascular function. J Endocrinol 181(1):1-10.

Reynisdottir S, Wahrenberg H, Carlstrom K, Rossner S, Arner P. 1994. Catecholamine resistance in fat cells of women with upper-body obesity due to decreased expression of beta 2-adrenoceptors. Diabetologia 37(4):428-435.

Ricci MR, Levin BE. 2003. Ontogeny of diet-induced obesity in selectively bred Sprague-Dawley rats. Am J Physiol Regul Integr Comp Physiol 285(3):R610-618.

Richards RJ, Porter JR, Svec F. 2000. Serum leptin, lipids, free fatty acids, and fat pads in long-term dehydroepiandrosterone-treated Zucker rats. Proc Soc Exp Biol Med 223(3):258-262.

Rizk N, Dunbar JC. 2004. Insulin-mediated increase in sympathetic nerve activity is attenuated by C-peptide in diabetic rats. Exp Biol Med (Maywood) 229(1):80-84.

Robidoux J, Martin TL, Collins S. 2004. Beta-Adrenergic Receptors and Regulation of Energy Expenditure: A Family Affair. Annu Rev Pharmacol Toxicol 44:297-323.

Rocchini AP, Yang JQ, Gokee A. 2004. Hypertension and insulin resistance are not directly related in obese dogs. Hypertension 43(5):1011-1016.

Romijn JA, Fliers E. 2005. Sympathetic and parasympathetic innervation of adipose tissue: metabolic implications. Curr Opin Clin Nutr Metab Care 8(4):440-444.

Rosenberg DE, Jabbour SA, Goldstein BJ. 2005. Insulin resistance, diabetes and cardiovascular risk: approaches to treatment. Diabetes Obes Metab 7(6):642-653.

Rosenspire KC, Haka MS, Van Dort ME, Jewett DM, Gildersleeve DL, Schwaiger M, Wieland DM. 1990. Synthesis and preliminary Evaluation of Carbon-11-Meta-Hydroxyephedrine: A False Transmitter Agent for Heart Neuronal Imaging. J Nucl Med 31(8):1328-1334.

Sakai N, Sasaki K, Nakashita M, Honda S, Ikegaki N, Saito N. 1997. Modulation of serotonin transporter activity by a protein kinase C activator and an inhibitor of type 1 and 2A serine/threonine phosphatases. J Neurochem 68(6):2618-2624.

Sanchez A, Toledo-Pinto EA, Menezes ML, Pereira OC. 2004. A simple high-performance liquid chromatography assay for on-line determination of catecholamines in adrenal gland by direct injection on an ISRP column. Pharmacol Res 50(5):481-485.

Sartor G, Schersten B, Carlstrom S, Melander A, Norden A, Persson G. 1980. Ten-year follow-up of subjects with impaired glucose tolerance: prevention of diabetes by tolbutamide and diet regulation. Diabetes 29(1):41-49.

Sasaki N, Uchida E, Niiyama M, Yoshida T, Saito M. 1998. Anti-obesity effects of selective agonists to the beta 3-adrenergic receptor in dogs. II. Recruitment of thermogenic brown adipocytes and reduction of adiposity after chronic treatment with a beta 3-adrenergic agonist. J Vet Med Sci 60(4):465-469.

Satoh H, Nguyen MT, Trujillo M, Imamura T, Usui I, Scherer PE, Olefsky JM. 2005. Adenovirus-mediated adiponectin expression augments skeletal muscle insulin sensitivity in male Wistar rats. Diabetes 54(5):1304-1313.

Satoh N, Ogawa Y, Katsuura G, Numata Y, Tsuji T, Hayase M, Ebihara K, Masuzaki H, Hosoda K, Yoshimasa Y, Nakao K. 1999. Sympathetic activation of leptin via the ventromedial hypothalamus: leptin-induced increase in catecholamine secretion. Diabetes 48(9):1787-1793.

Sawant SP, Dnyanmote AV, Shankar K, Limaye PB, Latendresse JR, Mehendale HM. 2004. Potentiation of carbon tetrachloride hepatotoxicity and lethality in type 2 diabetic rats. J Pharmacol Exp Ther 308(2):694-704.

Schafers M, Dutka D, Rhodes CG, Lammertsma AA, Hermansen F, Schober O, Camici PG. 1998. Myocardial presynaptic and postsynaptic autonomic dysfunction in hypertrophic cardiomyopathy. Circ Res 82(1):57-62.

Schafers MA, Wichter T, Schafers KP, Rahman S, Rhodes CG, Lammertsma AA, Lerch H, Knickmeier M, Hermansen F, Schober O, Camici PG, Breithardt G. 2001. Pulmonary beta adrenoceptor density in arrhythmogenic right ventricular cardiomyopathy and idiopathic tachycardia. Basic Res Cardiol 96(1):91-97.

Schmid H, Forman LA, Cao X, Sherman PS, Stevens MJ. 1999. Heterogeneous cardiac sympathetic denervation and decreased myocardial nerve growth factor in streptozotocin-induced diabetic rats: implications for cardiac sympathetic dysinnervation complicating diabetes. Diabetes 48(3):603-608.

Schnell O, Muhr D, Weiss M, Kirsch CM, Haslbeck M, Tatsch K, Standl E. 1997. Three-year follow-up on scintigraphically assessed cardiac sympathetic denervation in patients with long-term insulin-dependent (type I) diabetes mellitus. J Diabetes Complications 11(5):307-313.

Schwaiger M, Kalff V, Rosenspire K, Haka MS, Molina E, Hutchins GD, Deeb M, Wolfe E, Jr., Wieland DM. 1990. Noninvasive evaluation of sympathetic nervous system in human heart by positron emission tomography. Circ 82(2):457-464.

Sedvall G. 1991. PET scanning as a tool in clinical psychopharmacology. Triangle 30(1/2):11-20.

Seo DO, Shin CY, Lee CJ, Dailey JW, Reith ME, Jobe PC, Ko KH. 1999. Effect of alterations in extracellular norepinephrine on adrenoceptors: a microdialysis study in freely moving rats. Eur J Pharmacol 365(1):39-46.

Sharma AM, Pischon T, Hardt S, Kunz I, Luft FC. 2001. Hypothesis: Beta-adrenergic receptor blockers and weight gain: A systematic analysis. Hypertension 37(2):250-254.

Shekelle PG, Rich MW, Morton SC, Atkinson CS, Tu W, Maglione M, Rhodes S, Barrett M, Fonarow GC, Greenberg B, Heidenreich PA, Knabel T, Konstam MA, Steimle A, Warner Stevenson L. 2003. Efficacy of angiotensin-converting enzyme inhibitors and beta-blockers in the management of left ventricular systolic dysfunction according to race, gender, and diabetic status: a meta-analysis of major clinical trials. J Am Coll Cardiol 41(9):1529-1538.

Shore PA, Cohn VH, Jr., Highman B, Maling HM. 1958. Distribution of norepinephrine in the heart. Nature 181(4612):848-849.

Shulkin BL, Wieland DM, Schwaiger M, Thompson NW, Francis IR, Haka MS, Rosenspire KC, Shapiro B, Sisson JC, Kuhl DE. 1992. PET scanning with hydroxyephedrine: an approach to the localization of pheochromocytoma. J Nucl Med 33(6):1125-1131.

Sisson JC, Frager MS, Valk TW, Gross MD, Swanson DP, Wieland DM, Tobes MC, Beierwaltes WH, Thompson NW. 1981. Scintigraphic localization of pheochromocytoma. N Engl J Med 305(1):12-17.

Srinivasan K, Viswanad B, Asrat L, Kaul CL, Ramarao P. 2005. Combination of high-fat diet-fed and low-dose streptozotocin-treated rat: a model for type 2 diabetes and pharmacological screening. Pharmacol Res 52(4):313-320.

Staehelin M, Hertel C. 1983. [3H]CGP-12177, a beta-adrenergic ligand suitable for measuring cell surface receptors. J Recept Res 3(1-2):35-43.

Staehelin M, Simons P, Jaeggi K, Wigger N. 1983. CGP-12177. A hydrophilic beta-adrenergic receptor radioligand reveals high affinity binding of agonists to intact cells. J Biol Chem 258(6):3496-3502.

Stanley WC, Lopaschuk GD, McCormack JG. 1997. Regulation of energy substrate metabolism in the diabetic heart. Cardiovasc Res 34(1):25-33.

Starke K. 2001. Presynaptic autoreceptors in the third decade: focus on alpha2-adrenoceptors. J Neurochem 78(4):685-693.

Starling EH, Lovatt Evans C. 1914. The respiratory exchanges of the heart in the diabetic animal. J Physiol (Lond) 49:67-88.

Steinberg GR, Dyck DJ. 2000. Development of leptin resistance in rat soleus muscle in response to high-fat diets. Am J Physiol Endocrinol Metab 279(6):E1374-1382.

Stevens MJ. 2001. New imaging techniques for cardiovascular autonomic neuropathy: a window on the heart. Diabetes Technol Ther 3(1):9-22.

Stevens MJ, Raffel DM, Allman KC, Dayanikli F, Ficaro E, Sandford T, Wieland DM, Pfeifer MA, Schwaiger M. 1998. Cardiac sympathetic dysinnervation in diabetes: implications for enhanced cardiovascular risk. Circulation 98(10):961-968.

Stevens MJ, Raffel DM, Allman KC, Schwaiger M, Wieland DM. 1999. Regression and progression of cardiac sympathetic dysinnervation complicating diabetes: an assessment by C-11 hydroxyephedrine and positron emission tomography. Metabolism 48(1):92-101.

Stumvoll M, Goldstein BJ, van Haeften TW. 2005. Type 2 diabetes: principles of pathogenesis and therapy. Lancet 365(9467):1333-1346.

Sung U, Apparsundaram S, Galli A, Kahlig KM, Savchenko V, Schroeter S, Quick MW, Blakely RD. 2003. A regulated interaction of syntaxin 1A with the antidepressant-sensitive norepinephrine transporter establishes catecholamine clearance capacity. J Neurosci 23(5):1697-1709.

Suskin N, McKelvie RS, Burns RJ, Latini R, Pericak D, Probstfield J, Rouleau JL, Sigouin C, Solymoss CB, Tsuyuki R, White M, Yusuf S. 2000. Glucose and insulin abnormalities relate to functional capacity in patients with congestive heart failure. Eur Heart J 21(16):1368-1375.

Swan JW, Anker SD, Walton C, Godsland IF, Clark AL, Leyva F, Stevenson JC, Coats AJ. 1997. Insulin resistance in chronic heart failure: relation to severity and etiology of heart failure. J Am Coll Cardiol 30(2):527-532.

Swan JW, Walton C, Godsland IF, Clark AL, Coats AJ, Oliver MF. 1994. Insulin resistance in chronic heart failure. Eur Heart J 15(11):1528-1532.

Swanson LW, Sawchenko PE, Lind RW, Rho JH. 1987. The CRH motoneuron: differential peptide regulation in neurons with possible synaptic, paracrine, and endocrine outputs. Ann N Y Acad Sci 512:12-23.

Sweet IR, Cook DL, Lernmark A, Greenbaum CJ, Krohn KA. 2004. Non-invasive imaging of beta cell mass: a quantitative analysis. Diabetes Technol Ther 6(5):652-659.

Sydow K, Daiber A, Oelze M, Chen Z, August M, Wendt M, Ullrich V, Mulsch A, Schulz E, Keaney JF, Jr., Stamler JS, Munzel T. 2004. Central role of mitochondrial aldehyde dehydrogenase and reactive oxygen species in nitroglycerin tolerance and cross-tolerance. J Clin Invest 113(3):482-489.

Szemeredi K, Komoly S, Kopin IJ, Bagdy G, Keiser HR, Goldstein DS. 1991. Simultaneous measurement of plasma and brain extracellular fluid concentrations of catechols after yohimbine administration in rats. Brain Res 542(1):8-14.

Szkudelski T. 2001. The mechanism of alloxan and streptozotocin action in B cells of the rat pancreas. Physiol Res 50(6):537-546.

Taegtmeyer H, Hems R, Krebs HA. 1980. Utilization of energy-providing substrates in the isolated working rat heart. Biochem J 186(3):701-711.

Taegtmeyer H, McNulty P, Young ME. 2002. Adaptation and maladaptation of the heart in diabetes: Part I: general concepts. Circulation 105(14):1727-1733.

Takahashi M, Terwilliger R, Lane C, Mezes PS, Conti M, Duman RS. 1999. Chronic antidepressant administration increases the expression of cAMP-specific phosphodiesterase 4A and 4B isoforms. J Neurosci 19(2):610-618.

Takatsu H, Nishida H, Matsuo H, Watanabe S, Nagashima K, Wada H, Noda T, Nishigaki K, Fujiwara H. 2000. Cardiac sympathetic denervation from the early stage of Parkinson's disease: clinical and experimental studies with radiolabeled MIBG. J Nucl Med 41(1):71-77.

Talman WT, Kelkar P. 1993. Neural control of the heart. Central and peripheral. Neurol Clin 11(2):239-256.

Tatsumi M, Engles JM, Ishimori T, Nicely O, Cohade C, Wahl RL. 2004. Intense (18)F-FDG Uptake in Brown Fat Can Be Reduced Pharmacologically. J Nucl Med 45(7):1189-1193.

Tejani-Butt SM, Brunswick DJ, Frazer A. 1990. [3H]nisoxetine: a new radioligand for norepinephrine uptake sites in brain. Eur J Pharmacol 191(2):239-243.

Thaina P, Nott MW, Rand MJ. 1999. Effects of some imidazolidine alpha2-adrenoceptor agonists in rat isolated atria. J Auton Pharmacol 19(3):185-191.

Thompson CJ. 2002. Instrumentation. In: Wahl RL, editor. Principles and Practice of Positron Emission Tomography. Philadelphia, PA: Lippincott Williams & Wilkins. p. 48-64.

Tooke JE. 1995. Microvascular function in human diabetes. A physiological perspective. Diabetes 44(7):721-726.

Torres GE, Gainetdinov RR, Caron MG. 2003. Plasma membrane monoamine transporters: structure, regulation and function. Nat Rev Neurosci 4(1):13-25.

Trampal C, Engler H, Juhlin C, Bergstrom M, Langstrom B. 2004. Pheochromocytomas: detection with 11C hydroxyephedrine PET. Radiology 230(2):423-428.

Trendelenburg U. 1991. The TiPS lecture: functional aspects of the neuronal uptake of noradrenaline. Trends Pharmacol Sci 12(9):334-337.

Tsai EB, Sherry NA, Palmer JP, Herold KC. 2006. The rise and fall of insulin secretion in type 1 diabetes mellitus. Diabetologia 49(2):261-270.

Tschop M, Heiman ML. 2001. Rodent obesity models: an overview. Exp Clin Endocrinol Diabetes 109(6):307-319.

Tseng H, Link J, Stratton J, Caldwell J. 2001. Cardiac receptor physiology and its application to clinical imaging: Present and future. J Nucl Cardiol 8(3):390-409.

Tuomilehto J, Lindstrom J, Eriksson JG, Valle TT, Hamalainen H, Ilanne-Parikka P, Keinanen-Kiukaanniemi S, Laakso M, Louheranta A, Rastas M, Salminen V, Uusitupa M. 2001. Prevention of type 2 diabetes mellitus by changes in lifestyle among subjects with impaired glucose tolerance. N Engl J Med 344(18):1343-1350.

Turpeinen AK, Vanninen E, Kuikka JT, Uusitupa MI. 1996. Demonstration of regional sympathetic denervation of the heart in diabetes. Comparison between patients with NIDDM and IDDM. Diabetes Care 19(10):1083-1090.

U.S. Department of Health and Human Services. 2001. The Surgeon General's call to action to prevent and decrease overweight and obesity. Rockville, MD: U.S. Department of Health and Human Services, Public Health Service, Office of the Surgeon General. 60 p.

Uberfuhr P, Frey AW, Ziegler S, Reichart B, Schwaiger M. 2000. Sympathetic reinnervation of sinus node and left ventricle after heart transplantation in humans: regional differences assessed by heart rate variability and positron emission tomography. J Heart Lung Transplant 19(4):317-323.

Uchida J, Kiuchi Y, Ohno M, Yura A, Oguchi K. 1998. Ca(2+)-dependent enhancement of [3H]noradrenaline uptake in PC12 cells through calmodulin-dependent kinases. Brain Res 809(2):155-164.

Ungerer M, Bohm M, Elce JS, Erdmann E, Lohse MJ. 1993. Altered expression of beta-adrenergic receptor kinase and beta 1-adrenergic receptors in the failing human heart. Circulation 87(2):454-463.

Ungerer M, Hartmann F, Karoglan M, Chlistalla A, Ziegler S, Richardt G, Overbeck M, Meisner H, Schomig A, Schwaiger M. 1998. Regional in vivo and in vitro characterization of autonomic innervation in cardiomyopathic human heart. Circulation 97(2):174-180.

Ungerer M, Weig HJ, Kubert S, Overbeck M, Bengel F, Schomig A, Schwaiger M. 2000. Regional pre- and postsynaptic sympathetic system in the failing human heart--regulation of beta ARK-1. Eur J Heart Fail 2(1):23-31.

Urano Y, Sakurai T, Ueda H, Ogasawara J, Takei M, Izawa T. 2004. Desensitization of the inhibitory effect of norepinephrine on insulin secretion from pancreatic islets of exercise-trained rats. Metabolism 53(11):1424-1432.

van Dijk G. 2001. The role of leptin in the regulation of energy balance and adiposity. J Neuroendocrinol 13(10):913-921.

Van Dort ME, Tluczek L. 2000. Synthesis and Carbon-11 Labeling of the Stereoisomers of meta-Hydroxyephedrine (HED) and meta-Hydroxypseudoephedrine (HPED). Journal of Labelled Compounds and Radiopharmaceuticals 43:603-612.

van Gurp PJ, Rongen GA, Lenders JW, Al Nabawy AK, Timmers HJ, Tack CJ. 2005. Sustained hyperglycaemia increases muscle blood flow but does not affect sympathetic activity in resting humans. Eur J Appl Physiol 93(5-6):648-654.

van Waarde A, Meeder JG, Blanksma PK, Bouwer J, Visser GM, Elsinga PH, Paans AM, Vaalburg W, Lie KI. 1992. Suitability of CGP-12177 and CGP-26505 for quantitative imaging of beta-adrenoceptors. Int J Rad Appl Instrum B 19(7):711-718.

Van Waarde A, Meeder JG, Blanksma PK, Brodde O-E, Visser GM, Elsinga PH, Paans AMJ, Vaalburg W, Lie KI. 1992. Uptake of radioligands by rat heart and lung in vivo:CGP 12177 does and CGP 26505 does not reflect binding to ß-adrenoceptors. Eur J Pharmacol 222:107-112.

van Waarde A, Vaalburg W, Doze P, Bosker FJ, Elsinga PH. 2004. PET imaging of beta-adrenoceptors in human brain: a realistic goal or a mirage? Curr Pharm Des 10(13):1519-1536.

Vaughan RA. 2004. Phosphorylation and regulation of psychostimulant-sensitive neurotransmitter transporters. J Pharmacol Exp Ther 310(1):1-7.

Vaughan RA, Huff RA, Uhl GR, Kuhar MJ. 1997. Protein kinase C-mediated phosphorylation and functional regulation of dopamine transporters in striatal synaptosomes. J Biol Chem 272(24):15541-15546.

Vervoort G, Wetzels JF, Lutterman JA, van Doorn LG, Berden JH, Smits P. 1999. Elevated skeletal muscle blood flow in noncomplicated type 1 diabetes mellitus: role of nitric oxide and sympathetic tone. Hypertension 34(5):1080-1085.

Wang Y, Fice DS, Yeung PK. 1999. A simple high-performance liquid chromatography assay for simultaneous determination of plasma norepinephrine, epinephrine, dopamine and 3,4-dihydroxyphenyl acetic acid. J Pharm Biomed Anal 21(3):519-525.

Wieland DM, Brown LE, Rogers WL, Worthington KC, Wu JL, Clinthorne NH, Otto CA, Swanson DP, Beierwaltes WH. 1981a. Myocardial imaging with a radioiodinated norepinephrine storage analog. J Nucl Med 22(1):22-31.

Wieland DM, Brown LE, Tobes MC, Rogers WL, Marsh DD, Mangner TJ, Swanson DP, Beierwaltes WH. 1981b. Imaging the primate adrenal medulla with [123I] and [131I] meta-iodobenzylguanidine: concise communication. J Nucl Med 22(4):358-364.

Wieland DM, Rosenspire KC, Hutchins GD, Van Dort M, Rothley JM, Mislankar SG, Lee HT, Massin CC, Gildersleeve DL, Sherman PS, et al. 1990. Neuronal mapping of the heart with 6-[18F]fluorometaraminol. J Med Chem 33(3):956-964.

Wilkin TJ. 2001. The accelerator hypothesis: weight gain as the missing link between Type I and Type II diabetes. Diabetologia 44(7):914-922.

Xu F, Gainetdinov RR, Wetsel WC, Jones SR, Bohn LM, Miller GW, Wang YM, Caron MG. 2000. Mice lacking the norepinephrine transporter are supersensitive to psychostimulants. Nat Neurosci 3(5):465-471.

Yasar SA, Tulassay T, Madacsy L, Korner A, Szucs L, Nagy I, Szabo A, Miltenyi M. 1994. Sympathetic-adrenergic activity and acid-base regulation under acute physical stress in type I (insulin-dependent) diabetic children. Horm Res 42(3):110-115.

Yoshitake T, Yoshitake S, Fujino K, Nohta H, Yamaguchi M, Kehr J. 2004. High-sensitive liquid chromatographic method for determination of neuronal release of serotonin, noradrenaline and dopamine monitored by microdialysis in the rat prefrontal cortex. J Neurosci Methods 140(1-2):163-168.

Yoshitomi H, Yamazaki K, Abe S, Tanaka I. 1998. Differential regulation of mouse uncoupling proteins among brown adipose tissue, white adipose tissue, and skeletal muscle in chronic beta 3 adrenergic receptor agonist treatment. Biochem Biophys Res Commun 253(1):85-91.

Young JB, Mullen D, Landsberg L. 1978. Caloric restriction lowers blood pressure in the spontaneously hypertensive rat. Metabolism 27(12):1711-1714.

Young ME, McNulty P, Taegtmeyer H. 2002. Adaptation and maladaptation of the heart in diabetes: Part II: potential mechanisms. Circulation 105(15):1861-1870.

Zhang F, Ye C, Li G, Ding W, Zhou W, Zhu H, Chen G, Luo T, Guang M, Liu Y, Zhang D, Zheng S, Yang J, Gu Y, Xie X, Luo M. 2003. The rat model of type 2 diabetic mellitus and its glycometabolism characters. Exp Anim 52(5):401-407.

Zugck C, Lossnitzer D, Backs J, Kristen A, Kinscherf R, Haass M. 2003. Increased cardiac norepinephrine release in spontaneously hypertensive rats: role of presynaptic alpha-2A adrenoceptors. J Hypertens 21(7):1363-1369.

APPENDICES

APPENDIX A

FUTURE DIRECTIONS

A.1 PHARMACOLOGY

Our results with tranylcypromine indicate that [^{11}C]HED retention is inversely proportional to synaptic NE levels, as elevation of endogenous catecholamines via inhibition of MAO dose-dependently decreases tracer accumulation. To confirm our results, we need to measure synaptic NE levels in tranylcypromine treated animals to determine the correlation between NE concentration and [^{11}C]HED retention. We are in the progress of developing a novel procedure for separation and quantification of NE from tissue and plasma (Appendix B). Additionally, measurement of NET-1 density using [^{3}H]nisoxetine and autoradiography will allow us to discern whether acute changes in activity of the uptake-1 transporter is responsible for decreased [^{11}C]HED retention in these treatments. Autoradiography is a well established protocol, and will allow for quantifiable measurement of NET-1 densities. If NE levels alone are altered in these acute treatments, we will have shown for the first time dependence of [^{11}C]HED kinetics on synaptic NE concentrations, even in the absence of long term downregulation of NET-1,the predictive value of which is very enticing.

The combination of these procedures will prove useful in examining both obese and diabetic animal models as well, elucidating the determining factor in altered [^{11}C]HED retention in these animals. In each case, measurements of NE and NET-1 will be taken in myocardium (left ventricle, septum, atria), brown adipose tissue, and pancreas.

A.2 Repeated Experiments

Studies are ongoing to increase sample sizes in 56 and 119 day DIO and DR as well as 56 day type II DM rats. Statistical significance is close in particular tissues of interest, most notably brown adipose tissue in obese and lean animals. At 119 days, DIO and DR animals will also be pretreated with desipramine to delineate uptake-1 specific retention in these animals and confirm no change as seen at other time points. Sprague-Dawley controls at 119 days are also in preparation for Biodistribution studies. As seen at other time points, we expect tracer uptake in these animals to be intermediate to DIO and DR, suggesting altered SNS signalling *in both* obese and lean rats. Experiments are scheduled for August (inetermediate term) and October (long term) 2006.

A.3 Metabolite Analysis

The presence of radiolabeled metabolites represents a considerable obstacle for many imaging agents, as delineation of specific binding or retention and kinetic analysis is rendered considerably more difficult. Previous studies have reported a lack of radiolabeled metabolites of [^{11}C]HED in myocardium, but six clear metabolites in liver and plasma (Law et al., 1997; Link et al., 1997; Rosenspire et al., 1990). It is important to confirm that labeled metabolites are not present in brown adipose tissue or pancreas. The elevated non-specific retention in these tissues as compared to myocardium may be partially due to the presence of labelled metabolites.

Column-switch HPLC (Hilton et al., 2000) has been used in our laboratory for such analyses of (*R*)-[^{11}C]rolipram, and will be applied for the analysis of [^{11}C]HED metabolites (Figure A.1). The procedure uses two pumps (Waters) moving two distinct solvents through both an analytical column (Phenomenex) and a capture cartridge packed with a

selcted sorbent (Waters Oasis). Briefly, the sample* is injected onto a flow-through capture column that selectively traps unchanged tracer and related metabolites. In the case of [^{11}C]HED, this is a sorbent with some cation-exchange properties. After elution of plasma proteins and other macromolecules, flow is reversed through the capture column, introducing a new solvent that elutes the bound tracer and metabolites and deposits them onto an analytical column for separation. The method allows for trapping of unchanged [^{11}C]HED and column chromatographic separation of hydrophilic and lipophilic metabolites using a reverse phase analytical column. Precise conditions for ideal trapping and elution of [^{11}C]HED are under development, as standard cation exchange sorbents do not release the compound as a bolus on solvent switch. Radiation (BioScan) and ultraviolet (UV) absorbance detection (Waters) allow for quantification of metabolites using the integration software PeakSimple 3.29.

A4 Small Animal Imaging

The arrival and subsequent characterization of the Small Animal PET Camera (LabPET™, Advance Molecular Imaging, Sherbrooke, QC) has provided the opportunity for future *in vivo* imaging studies in these same animal models. Briefly, injection of [^{11}C]HED will be followed by a dynamic PET scan of myocardium, allowing for visualization of differences in uptake parameters between animals. A primary benefit of dynamic small animal imaging is the opportunity to perform full kinetic analyses and serial scans in individual animals, measuring myocardial tracer retention at baseline (arrival), 2 weeks on high fat diet, 8 weeks on high fat diet, 16 weeks on high fat diet, etc. Comparisons within

* plasma or ultra-centrifuged tissue homogenate supernatant, acidified or alkaline as necessary

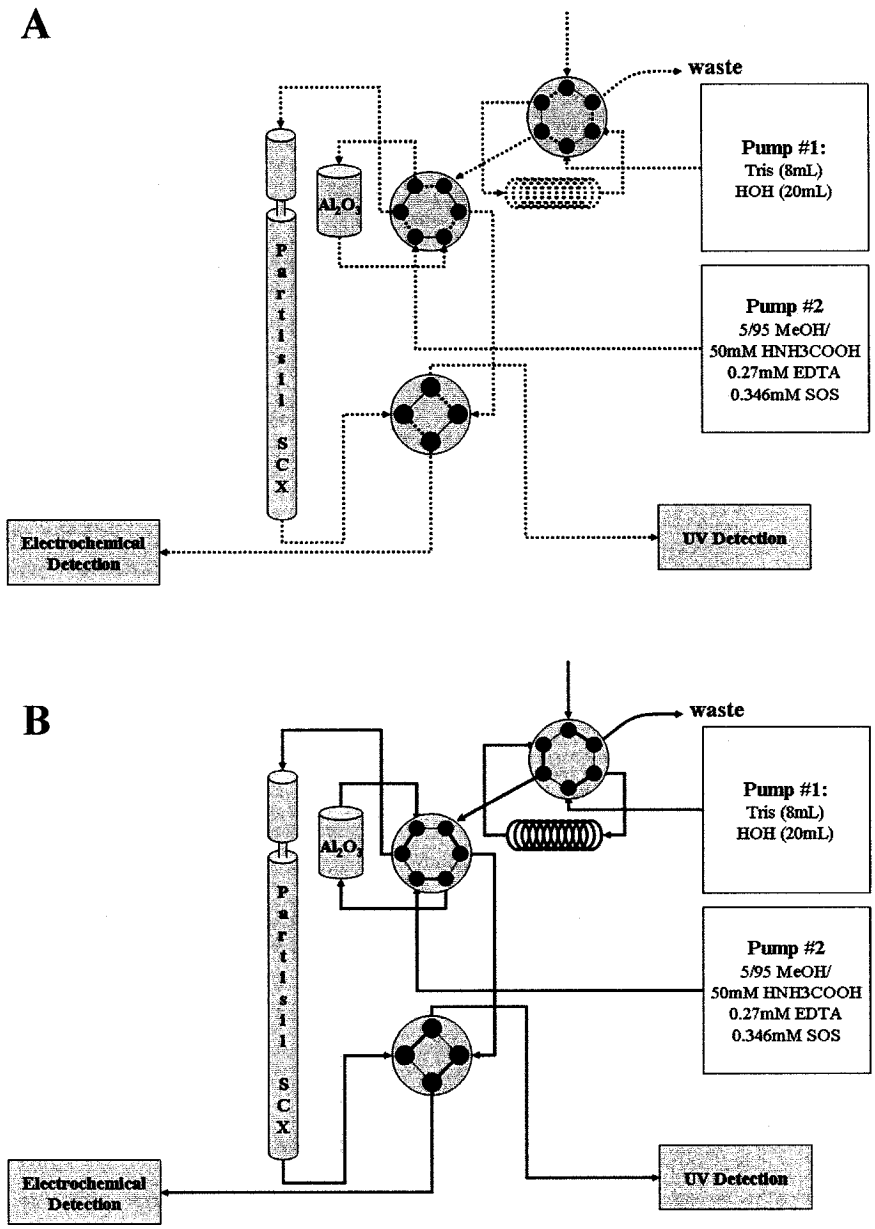

Figure A.1: Column switch methodology, as it applies to norepinephrine separation. Briefly, two pumps are connected through two valves. Initial injection into the injection port deposits the analyte within a stationary loop, supplied by pump # 1 (A). On switching this valve, the flow (2 mL/min) forces the analyte out of the loop and onto the capture column (Al_2O_3). Flow (1 mL/min) is maintained through the analytical column (SCX) by Pump #2 initially (A). Upon switch (B), pump # 2 backflushes the Al_2O_3 trapped compounds onto the SCX column. The eluent is analysed by either UV Absorbanc and radiation detection or electrochemical detection. Signals are integrated using Peak Simple software.

individual animals are more meaningful than among groups sacrificed a variable time points.

The Small Animal PET camera also affords the opportunity for feasibility studies in imaging of brown adipose tissue and pancreas. As discussed above (Section 1.6.3), serial administration of [^{11}C]HED and [^{18}F]FDG may allow for delineation of brown adipose tissue deposits without the use of CT. Pancreatic imaging against liver and gastrointestinal uptake will also be assessed.

A5 Human Imaging

The National Cardiac PET Centre began recruitment for a clinical PET pilot study in June 2006 examining alterations in both myocardial [^{11}C]HED and [^{11}C]acetate retention in *young obese males* suffering from sleep apnea and young, non-obese males without sleep apnea. If our results with DIO animals reflect the obese condition, we expect elevated [^{11}C]HED retention indices in myocardium of obese sleep apnea patients as compared to their age matched controls. Coordination with the National Cardiac PET Centre will allow for interesting comparisons of basic and clinical results, and coordination on future PET studies in this field.

APPENDIX B

SIMPLE AND RAPID HIGH PERFORMANC LIQUID CHROMATOGRAPHIC EXTRACTION, SEPARATION, AND QUANTIFICATION OF SYNAPTIC AND PLASMATIC NOREPINEPHRINE

B.1 ESTABLISHED PROTOCOLS, LIMITATIONS

The established HPLC protocol for extraction and quantification of plasma catecholamines has been used routinely since the early 1980s (Ganguly et al., 1987; Ganguly et al., 1986; Gilinsky et al., 2001; Hows et al., 2004; Nup et al., 2001; Sanchez et al., 2004; Wang et al., 1999; Yoshitake et al., 2004). Briefly, activated acidic aluminum oxide (Al_2O_3), a solution of trishydroxymethyl aminomethane (Tris base) and EDTA, and the analyte sample are placed in a microcentrifuge tube. Serial centrifugation (2000 rpm) and distilled water rinses precede an extraction step using strong acid (HCl, perchloric acid $HClO_4$, or concentrated formic acid HCOOH). The strong acid extract is injected onto an analytical column for separation and quantified by electrochemical detection (ECD).

This method, while strongly entrenched, does not preclude itself from improvement. The primary obstacles in the procedure are the inherent errors of multiple rinse and extraction steps without solid pellet formation and the strain on the column caused by an inability to fully remove large macromolecules from the analyte sample. Indeed, recovery of NE has been reported at 75-80% (Wang et al., 1999). Moreover, the procedure is time consuming, owing to multiple extractions steps. We sought to improve on this established protocol in terms of speed, simplicity, and accuracy by applying column switch techniques.

B.2 Apparatus

As described above (Appendix A.3), column switch involves two pumps (Waters 510), two solvents, and two columns (Figure A.1). Several analytical columns were tested for ability to separate catecholamines reliably. Standard samples of NE and Epi (5 ng/mL to 0.5 mg/mL) were prepared in 0.1 M HCOOH to enhance chemical stability. High doses were injected for initial characterization such that UV absorbance detection (Waters 486) was used. Solvent fronts, NE, and Epi peaks were isolated by repeat injections of NE alone, Epi alone, NE/Epi, and blank HCOOH.

B.2.1 Selection of Analytical Column

The Synergi Hydro Reversed Phase C-18 column (Phenomenex, 250 x 4.60 mm, 10 μm particle size) elution times were 2.1-2.5 and 3.2 minutes for solvent front and NE respectively. The proximity of the solvent front to NE rendered this column less desirable for ECD. Separation could not be improved in this case, as the solvent used was 100% aqueous phase potassium phosphate buffer (KH_2PO_4).

The Partisil 10 SCX Cation Exchange Reversed Phase column (Phenomenex, 250 x 4.60 mm, 10 μm particle size) elution times were 3.3-3.5, 6.8, and 8.9 minutes for solvent front, NE, and Epi, respectively (Figure A.2). Solvent for this column was 5/95 methanol (MeOH) / 0.1 M HNH_3COOH, buffered to pH 2.8 with HCOOH. Changing percentage of organic phase had minimal impact on retention times. The SCX column was selected for further analysis.

B.2.2 Selection of Capture Sorbent

The effectiveness of several capture sorbents were tested using column switch and collection of untrapped fractions to determine the efficiency of trapping. Tested sorbents

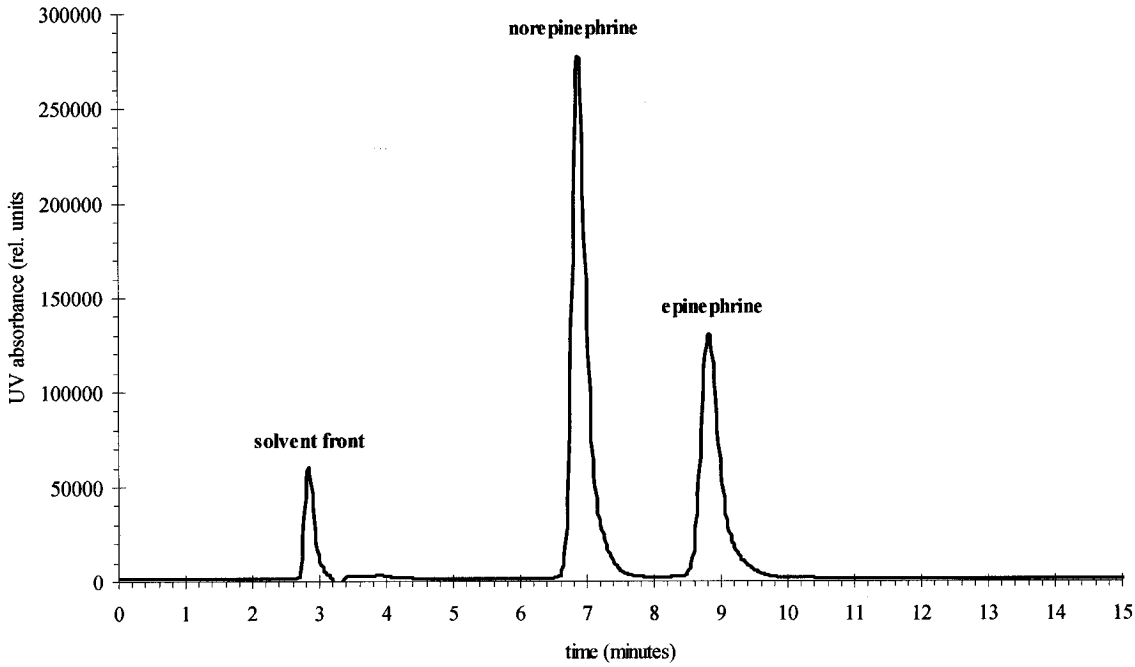

Figure A.2: HPLC separation of norepinephrine (5 μg) and epinephrine (5 μg) standards on Partisil SCX cation exchange reversed phase analytical column. Injections were directly applied to the column in 5/95 MeOH / 0.1 M HNH_3COOH, pH 2.85 at 1 mL/min. UV absorbance detection was integrated with PeakSimple 3.29.

included: hydrophilic lipophilic balanced reversed phase (HLB, Waters Oasis), mixed-mode anion exchange reversed phase (MAX, Waters Oasis), mixed-mode cation exchange reversed phase (MCX, Waters Oasis), and Al_2O_3 (acidic WA4, Sigma-Aldrich). Sorbents were packed into capture cartridges (Mandel Alltech), approximately 35 mg per column.

Trapping of NE was ineffective using HLB or MAX, with the vast majority of NE eluted directly from the capture column. Retention was better in MCX, but was complicated by the inability to effectively strip the trapped compounds from the sorbent in a single bolus onto the analytical column. Conversely, sharp, reproducible peaks were obtained using Al_2O_3 packing in the capture cartridge, indicating efficient elution of catecholamines from the resin.

Effecitve retention is dependent upon both wash-in solvent and effective rinsing. Retention of NE on Al_2O_3 matrix requires an alkaline wash-in comprised of Tris base and EDTA buffered to a pH of 8.6.

B.2.3 Detection

Detection of catecholamines at physiological levels requires greater sensitivity than is afforded by standard UV absorbance detection. Conductance detection was also ineffective at detecting physiological concentrations of NE (0.05-0.5 ng/mL). As such, a flow-through cell electrochemical detector (Waters 464 Pulsed ECD) was purchased and used for this purpose.

Standard curve generation bypassing the capture column indicated high sensitivity and a detection limit of 0.01 ng injected NE (Figure A.3). Consistency and maintenance of sensitivity has been problematic, and methods to obtain more stable, reproducible standard values are being investigated.

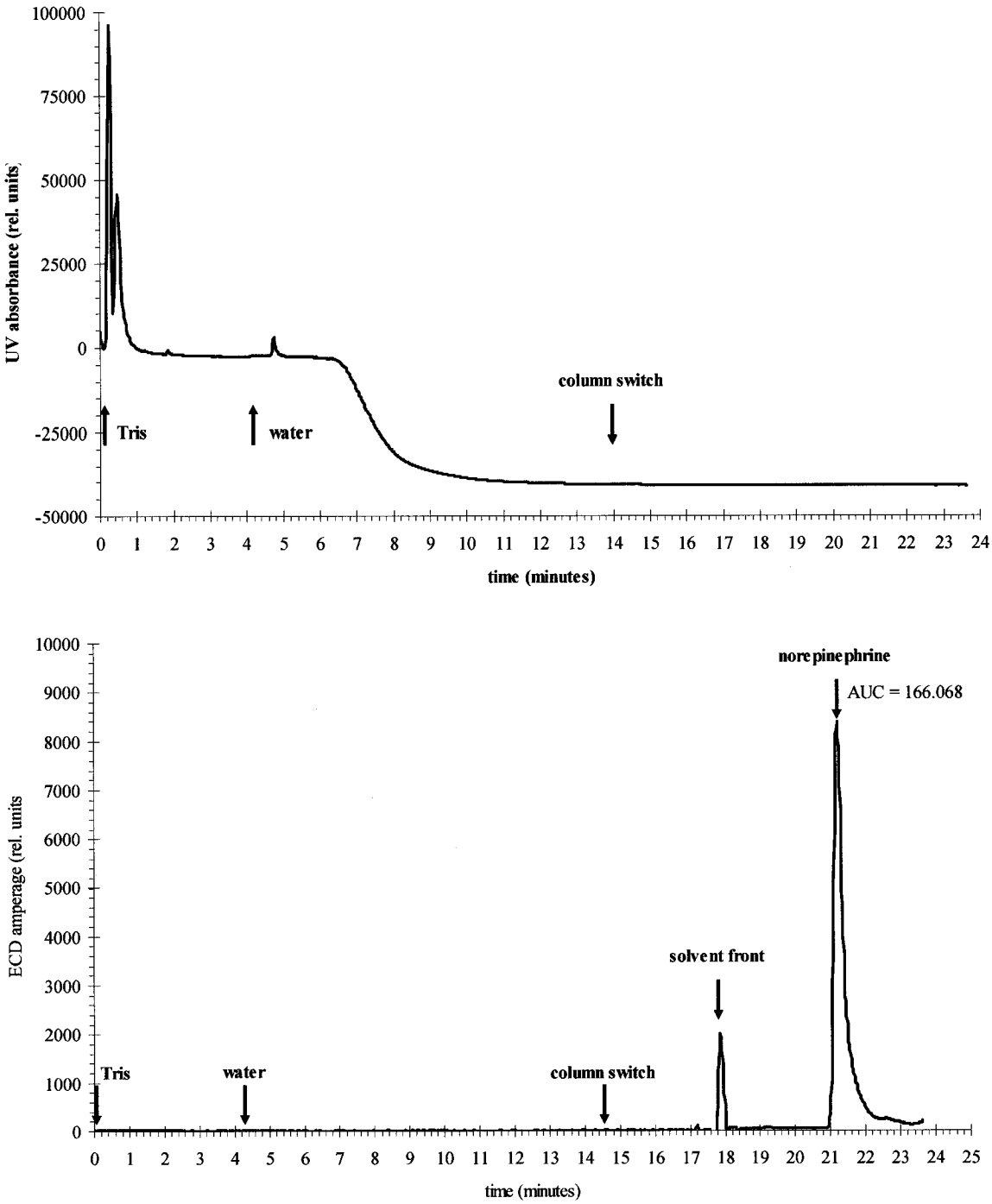

Figure A.3: Column switch extraction and quantification of NE (5 μg) from standard sample . Panel **A** shows UV detection of flow through the Al_2O_3 capture cartridge. Solvent switches are indicated. Panel **B** displays electrochemical detection of SCX analytical column efflux. Retention time of NE is indicated. Signals are integrated and converted to relative units by PeakSimple 3.29.

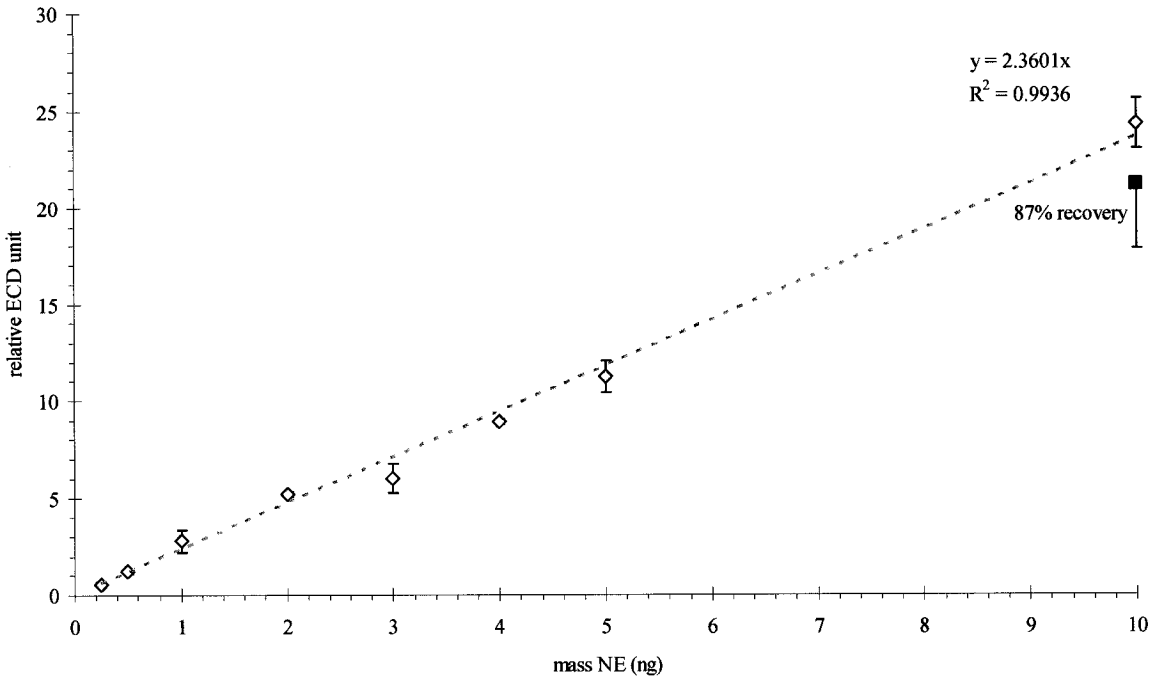

Figure A.4: Standard curve for NE electrochemical detection. NE was separated on an SCX analytical column in serial dilutions (0.01 to 10 ng). Solvent was 5/95 MeOH / 0.1 M HNH_3COOH, pH 2.85 at 1 mL/min. Recovery of 10 ng samples using full column switch methodology is indicated (solid square).

B.2.4 Final Protocol

Analyte is injected at 2 mL/min in Tris/EDTA buffer and allowed to adhere to the Al_2O_3 capture sorbent over 4 minutes (8 mL). Solvent is switched to deionized water for 10 minutes (20 mL) to remove trace amounts of Tris which are damaging to the ECD working electrode. Flow is then reversed, flushing the contents of the capture column onto the Partisil SCX analytical column at 1 mL/min with 5/95 MeOH / 0.1M HNH_3COOH, pH 2.85. Catecholamine elution is detected using ECD and integrated by PeakSimple 3.29. Areas under the curve are proportional to injected masses.

Early results indicate recovery potential of up to 95%, though sensitivity complications remain a problem at present. A sample extraction from dog plasma is shown in Figure A.4. Continued characterization will simplify the protocol and refine the efficiency, accuracy, and rapidity of the existing HPLC protocols.

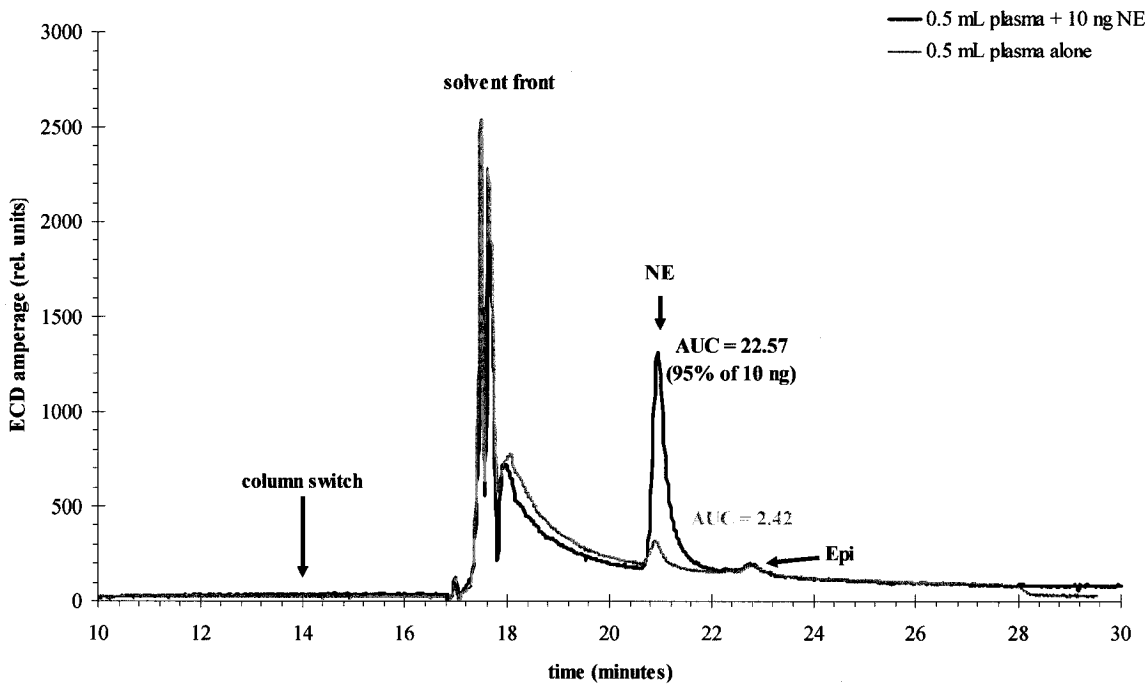

Figure A.5: Column switch extraction and quantification of NE from 0.5 mL plasma samples. Trapping was carried out on Al_2O_3 capture cartridge, with 8 mL Tris pH 8.6 and 20 mL water rinse. Separation was completed on SCX analytical column, 1 mL/min 5/95 MeOH / 0.1 M HNH_3COOH, pH 2.85. Electrochemical detection is shown, with column switch indicated. Signals were integrated using PeakSimple 3.29. The first sample was spiked with 10 ng of NE standard, while the second was injected alone. Retention times for NE and Epi are indicated.